THE AMERICAN MINERALOGIST

JOURNAL OF THE MINERALOGICAL SOCIETY OF AMERICA

Vol. 12 APRIL, 1927 No. 4

CRYSTALLOGRAPHY OF AZURITE FROM TSUMEB, SOUTHWEST AFRICA, AND THE AXIAL RATIO OF AZURITE

CHARLES PALACHE AND LYMAN W. LEWIS.

CONTENTS

Explanation of Plates and Figures

Frontispiece.

A. Three azurite crystals from Tsumeb, in parallel position, altering to malachite. The concentric, radiating structure of the invading malachite fibers is well shown. The reproduction is natural size.

B. A large pseudomorph of malachite after azurite from Bisbee partially covered by a second generation of sub-parallel crystals of azurite. The later azurite is oriented parallel to the malachite pseudomorph. Natural size.

Explanation of Figures.

Figure 1. Azurite. Projections, in normal position, of crystal of type 1.

Figure 2, Pl. I. Azurite of type 1. Mag. 5 diam.

Figure 3. Orthographic and clinographic projections of azurite crystal, transitional between 1 and 2, due to the equal development of prism and front pinacoid.

Figure 4, Pl. I. Azurite transitional between types 1 and 2.

Figure 5, Pl. I. Crystal transitional between types 2 and 3. Mag. 2 diam.

Figure 6, Pl. I. Azurite of type 3. Mag. 5 diam.

Figure 7, Pl. II. Pseudo-rhombohedral aspect of one modification of type 4. Mag. 5 diam.

Figure 8, Pl. II. Simple modification dominated by base and unit prism.

Figure 9, Pl. II. Azurite of pyramidal habit. Mag. 5 diam.

Figure 10. Orthographic projection of a crystal of type 5.

Figure 11. Orthographic projection of a crystal of type 5 with important development of clinodomes and negative pyramids.

Figure 12, Pl. II. Azurite of type 6. Mag. 4 diam.

Figure 13, Pl. III. Azurite of type 7 with few forms. Mag. 5 diam.

Figure 14, Pl. III. Doubly terminated crystal of type 7. Mag. 10 diam.

Figure 15, Pl. III. Crystal of type 7 with complex terminations. Mag. 2 diam.

Figure 16, Pl. III. Crystal of type 7 dominated by the unit prism in the truncation.

Figure 17. Type 7. Orthographic projection on the side pinacoid, and clinographic projection in normal position, of crystal of azurite.

Figure 18. Type 7. Orthographic projection, on the side pinacoid, of azurite crystal, shown in figure 16.

Figure 19. Type 8. Orthographic projection, on the side pinacoid, of crystal shown in figure 20.

Figure 20, Pl. IV. Doubly terminated crystal of type 8 showing the prominent development of σ (101), m (110), c (001), and the clinodome zone.

Figure 21, Pl. IV. Simple representative of type 8 showing the typical striated appearance of the negative orthodome zone. Also the important development of λ ($\bar{2}$.18.3). Mag. 5 diam.

Figure 22, Pl. IV. Crystal tabular parallel to c (001) and μ ($\bar{1}$05), truncated by m (110). Mag. 5 diam.

Figure 23. Orthographic projection, on the side pinacoid, of a crystal of type 9, with m (110) the dominant truncation.

Figure 24. Orthographic projection, on the side pinacoid, of a crystal of type 9, with λ (2.18.3) the dominant truncation.

Figure 25. Type 10. Orthographic projection, on the side pinacoid, and clinographic projection in normal position, of azurite crystal. This habit is very common in the collection, and includes the most perfect crystallographic material.

Figure 26, Pl. IV. Photograph illustrating the terminations of azurite shown in figure 25.

Figure 27. Type 10. Orthographic projection, on the side pinacoid, of a crystal of type 10. The modification is very striking where the flat pyramid λ (2.18.3) forms the only important truncation.

Figure 28. Type 11. Orthographic and clinographic projections of a crystal of type 11. The symmetry of the ring of forms surrounding the base is not exaggerated.

Figure 29, Pl. IV. Crystal of type 12. It is interesting to compare this illustration with figures 5, 6 and 9 to note the change of habit resulting from variation in the relative development of *m* (110), *h* (221) *c* (001) and the clinodome zone.

Figure 30. Type 11. Orthographic and clinographic projections. The clinographic projection is turned 20° from the *b* axis to show more clearly the grouping of the faces at this end of the crystal.

Figure 31, Pl. V. Specimen containing unaltered azurite and completely malachitized azurite in contact.

Figure 32, Pl. V. Large azurite crystal of type 8 with bayldonite.

Figure 33. Orthographic and clinographic projections of a malachite pseudomorph of type 10 partially surrounded by a later azurite crystal of the same type in parallel position.

Figure 34, Pl. VI. Azurite altering to malachite.

Figure 35, Pl. VI. Pseudomorph group of malachite after azurite. The crystals are perfectly sharp, and the azurite forms can be positively identified. The color is lighter than many of the pseudomorphs, and on the velvety, apple-green faces the radiating structure is very conspicuous.

Figure 36, Pl. VII. Large pseudomorph of malachite after azurite. The sheaf-like structure of the malachite is well shown.

Figure 37, Pl. VII. Malachite pseudomorph after azurite. All the fibers on the front pinacoid radiate from one center. On the prism face there are many centers of radiation.

Figure 38. Orthographic projection, on the side pinacoid of an azurite crystal from Laurium, Greece, showing the new forms.

Figure 39. Clinographic projection and orthographic projection on the side pinacoid of azurite from Bisbee, Arizona, of the type shown on the pseudomorph in the color plate.

Figure 40. Gnomonic projection, on *b* (010), of all reported forms for azurite. In the negative orthodome zone no letter has been assigned to forms reported without one, but may be readily identified from the tables where the forms are listed in order of decreasing ϕ.

- ○ New azurite forms.
- ● Azurite forms commonly observed on Tsumeb specimens.
- • Other reported forms.

SUMMARY

It has repeatedly been asserted that the elements determined by Schrauf for azurite from Chessy, France, and used as the basis of calculated angles by Dana, Goldschmidt, and Groth are not in harmony with later measurements on specimens from other localities.

In the belief that the lack of agreement between measured and calculated angles was due to inferior crystals available for measurement by Schrauf, the present study was undertaken. New elements and angles have been calculated from measurements of many excellent crystals which furnish values more nearly in accord with observed angles. The material studied was chiefly a suite of minerals secured at the Tsumeb mine in 1922 by the senior author while a member of the Shaler Memorial Expedition to S. W. Africa. In this collection were over 1500 specimens containing crystallized azurite, or malachite pseudomorphs after azurite. Of this number 170 hand specimens of the most perfect or interesting types were chosen for careful study. Most of these were covered with brilliant, transparent azurite crystals well suited for crystallographic measurement.

METHODS

All the measurements were made on a Goldschmidt two-circle goniometer. Of the 28 crystals measured from Tsumeb, 15 were perfect enough to be used in the calculations, and had from 25 to 38 faces each. These were elongated parallel to the *b* axis and were measured with the orthodome zone parallel to the axis of the vertical circle. This allowed measurement of all the faces, (usually two of each form), of singly terminated crystals with one mounting. Only single, strong signals, observable with low magnification were considered of sufficient perfection to be used in computing the averages. The following table gives the weighted average, measured angles, in side pinacoid position, of the important faces.

A projection was made on the clinopinacoid, *b*(010), the symbols for this position were determined graphically, and the elements

AZURITE ANGLE-TABLE MEASURED ON (010) USED IN CALCULATING ELEMENTS

Letter	Miller Symbol* 001	Miller Symbol* 010	Variation of ϕ ϕ to ϕ		Average ϕ	Variation of ρ ρ to ρ		Average ρ	Number of measurements used.
c	(001)	(100)	87°33′	87°37′	87°35′	89°57′	90°02′	90°00′	14
θ	(101)	(110)	$\bar{4}5$ 07	$\bar{4}5$ 14	$\bar{4}5$ 11	89 57	90 01	"	8
v	(201)	(120)	$\bar{2}6$ 06	$\bar{2}6$ 35	$\bar{2}6$ 22	89 58	90 00	"	12
η	(302)	(230)	$\bar{3}3$ 06	$\bar{3}3$ 48	$\bar{3}3$ 30	90 00	90 01	"	9
σ	(101)	(110)	42 38	42 59	42 54	90 00	90 00	"	13
w	(120)	(012)	0 00	0 00	0 00	30 15	30 20	30 18	7
m	(110)	(011)	"	"	"	49 19	49 32	49 27	13
λ	(2.18.3)	(3.2.18)	$\bar{5}7$ 04	$\bar{5}7$ 24	$\bar{5}7$ 15	12 40	12 44	12 41	10
R	(241)	(124)	$\bar{2}6$ 10	$\bar{2}6$ 20	$\bar{2}6$ 17	32 32	32 34	32 33	11
k	(221)	(122)	$\bar{2}6$ 13	$\bar{2}6$ 20	$\bar{2}6$ 17	51 54	51 58	51 56	13
h	(221)	(122)	25 19	25 26	25 23	52 50	52 58	52 52	12
s	(111)	(111)	42 54	42 57	42 55	58 55	58 58	58 57	5
P	(223)	(322)	53 48	53 58	53 52	64 31	64 39	64 34	9
γ	(121)	(112)	42 45	42 55	42 52	39 41	39 47	39 43	6
p	(021)	(102)	87 32	87 41	87 35	29 28	29 33	29 30	18
l	(023)	(302)	87 32	87 40	87 35	59 28	59 32	59 30	19
f	(011)	(101)	87 32	87 36	87 34	48 30	48 34	48 32	11

* $pqr(001) = rpq(010)$.

were then calculated according to the accepted practice.[1] From the averaged measured angles given in the above table the elements calculated on a representative number of faces is shown below:

[1] Charles Palache, *Am. Mineral.*, Vol. 5, No. 10, p. 177. The following formulas were used in the calculation and transformation:

$$x = \sin\phi \tan\rho = pp_0 \sin\mu$$

$$y = \cos\phi \tan\rho = qq_0 + pp_0 \cos\mu$$

$$\tan\mu = \frac{pp_0 \sin\mu}{pp_0 \cos\mu} = \frac{x}{y - pp_0}$$

$$p_0(001) = \frac{q_0}{p_0}(010), \qquad q_0(001) = \frac{1}{p_0}(010)$$

$$a = \frac{q_0}{p_0 \sin\mu} \qquad c = \frac{q_0}{\sin\mu}$$

Letter	Goldschmidt Symbol (010)	ϕ	ρ	pp_0''	p_0''	qq_0''	q_0''
R	$\bar{\frac{1}{4}}$ $\frac{1}{2}$	$\bar{26}°$ 17′	32° 33′	.2829	1.1316	.5840	1.1680
k	$\bar{\frac{1}{2}}$ 1	$\bar{26}$ 17	51 56	.5659	1.1318	1.1688	1.1688
h	$\frac{1}{2}$ 1	25 23	52 52	.5666	1.1332	1.1692	1.1692
s	1	42 55	58 57	1.1320	1.1320	1.1689	1.1689
P	$\frac{3}{2}$ 1	53 52	64 34	1.7000	1.1322	1.1683	1.1683
p	$\frac{1}{2}$ 0	87 35	29 30	.5653	1.1306		
l	$\frac{3}{2}$ 0	87 35	59 30	1.6961	1.1307		
f	1 0	87 35	48 32	1.1306	1.1306		

μ(measured) = 87°35′. Average $p_0'' = 1.1316$. Average $q_0'' = 1.1687$. The measured value of μ was confirmed by calculation. Transformation to the normal position followed. (See footnote preceding).

$p_0 = 1.0326$. $q_0 = 0.8836$. $a = 0.8565$. $c = 0.8844$. $\beta = 87°35'$.

THE AXIAL RATIO OF AZURITE

Anderson[2] has pointed out the unsettled question regarding the values to be assigned to the elements of azurite. He publishes the following table to show "that Schrauf's elements, though correct no doubt for the azurite of Chessy, are not the best for crystals from other localities—."

Author	Locality	a	c	β
Schrauf	Chessy	.85012	.88054	87° 36′
Lacroix	"	.8469	.8789	87 39
Gonnard	"	.8477	.8792	.. ..
Farrington	Arizona	.85676	.88603	87 36 36″
Cohen	Broken Hill	.85608	.88585	87 38
Manasse	Calabonna	.85755	.88803	87 41
Anderson	Mineral Hill	.85721	.88581	87 34
To this list may be added:				
Toborffy	Tsumeb			87 38
Thomson	"	.8549	.8853	87 34
Aminoff	Bisbee	.8561	.8842	87 35
"	Broken Hill	.8563	.8850	87 41
Smith*	" "	.8565	.8850	87 36
Palache**	Bisbee, Broken Hill, Kelly, N. M.	.8568	.8841	87 36
Palache & Lewis	Tsumeb	.8564	.8844	87 35

* Unpublished notes.

** Weighted average from the three localities—unpublished notes.

[2] C. Anderson, *Jour. Proc. Roy. Soc. N. S. Wales*, Vol. LI.

This table shows that the Chessy values are materially smaller for both a and c than corresponding values derived from later studies, and that the elements presented in this paper are intermediate between the highest and lowest derived from other localities. This small difference in the elements is magnified to significant discrepancies in the calculated angles as illustrated in a comparison of the values for the unit prism:

$m \wedge m = 81° 06'$ Calculated from our elements.
$m \wedge m = 80° 41'$ Calculated from Schrauf's elements.

$\Delta = 0° 25'$

It was considered more desirable to base a new angle table on the elements derived from our study of the excellent Tsumeb crystals than on an average for all reported elements. Measurements subsequently made on crystals from other localities show very close agreement with our calculated angles, and indicate that the choice was justified. The confirmatory measurements are presented later in this paper.

The following angle table for all reported forms is based on the new elements. In the calculations Goldschmidt's formulas and system of checks were used, and the arrangement follows the system used in the Winkeltabellen.

AZURITE ANGLE TABLE FOR MEASUREMENTS ON THE BASE-(001)

$a=0.8565$	$\log a = 9.93273$	$\log a_0 = 9.98608$
$c=0.8844$	$\log c = 9.94665$	$\log b_0 = 0.05335$
$\mu = 180°-\beta = 87°\ 35'$	$\log h = \log \sin \mu = 9.99961$	$\log e = \log \cos \mu = 8.62497$
$\log p_0 = 0.01396$	$a_0 = 0.9684$	$p_0 = 1.0326$
$\log q_0 = 9.94627$	$b_0 = 1.1307$	$q_0 = 0.8836$
$\log \frac{q_0}{p_0} = 0.06769$	$h = 0.9998$	$e = 0.0422$

Number	Letter	Miller Symbol (001)	ϕ	ρ	ξ_0	η_0	ξ	η	x'	y'	d'
1	c	001	90°00′	2°25′	2°25′	0°00′	2°25′	0°00′		0	
2	b	010	0 00	90 00	0 00	90 00	0 00	90 00	0	∞	∞
3	a	100	90 00	"	90 00	0 00	90 00	0 00	∞	0	"
4	u	310	74 05	"	"	90 00	74 05	15 55		∞	"
5	g	210	66 50	"	"	90 00	66 50	23 10		"	"
6	i	320	60 18	"	"	"	60 18	29 42		"	"
7	m	110	49 27	"	"	"	49 27	40 33		"	"
8	w	120	30 18	"	"	"	30 18	59 42		"	"
9	e	0.1.10	25 31	5 36	2 25	5 03	2 24	5 03	0.0422	0.0884	0.0980
10	C	018	20 54	6 45	2 25	6 19	2 24	6 18	0.0422	0.1106	0.1183
11	G	016	15 59	8 43	"	8 23	2 23	8 22	"	0.1474	0.1533
12	Λ	015	13 25	10 18	"	10 02	2 23	10 01	"	0.1769	0.1818
13	S	014	10 48	12 41	"	12 28	2 22	12 27	"	0.2211	0.2251
14		027	7 33	17 47	"	17 59	2 18	17 38	"	0.3181	0.3209
15	q	025	6 47	19 36	"	19 29	2 17	19 28	"	0.3538	0.3563
16	E	012	5 27	23 57	"	23 51	2 13	23 50	"	0.4422	0.4442
17	l	023	4 05	30 35	"	30 32	2 05	30 30	"	0.6033	0.5911
18	$\Re$	034	3 38	33 37	"	33 34	2 01	33 32	"	0.6610	0.6647
19	j	045	3 25	34 05	"	35 17	2 00	35 52	"	0.7075	0.6769
20	f	011	2 44	41 31	"	41 29	1 49	41 27	"	0.8844	0.8854
21		076	2 20	45 55	"	45 54	1 41	45 53	"	1.0318	1.0327
22	K	032	1 49	53 00	"	53 00	1 27	52 58	"	1.3266	1.3273
23	p	021	1 22	60 32	"	60 31	1 11	60 30	"	1.7688	1.7693
24	L	031	0 55	69 21	"	69 21	0 51	69 19	"	2.6532	2.6536
25	Ω	301	90 00	72 21	72 21	0 00	72 21	0 00	3.1428	0	3.1428
26	ϕ	201	90 00	64 38	64 38	0 00	64 38	0 00	2.1093	"	2.1093

Number	Letter	Miller Symbol (001)	ϕ	ρ	ξ_0	η_0	ξ	η	x'	y'	d'
27		905	90°00′	62°17′	62°17′	0°00′	62°17′	0°00′	1.9026	0	1.9026
28	σ	101	"	47 06	47 06	"	47 06	"	1.0758	"	1.0758
29	Φ	203	"	36 11	36 11	"	36 11	"	0.7313	"	0.7313
30	ζ	102	"	29 13	29 13	"	29 13	"	0.5590	"	0.5590
31	τ	307	"	25 53	25 53	"	25 53	"	0.4852	"	0.4852
32		205	"	24 30	24 30	"	24 30	"	0.4556	"	0.4556
33	M	104	"	16 44	16 44	"	16 44	"	0.3006	"	0.3006
34	r	$\bar{1}08$	$\bar{9}0$ 00	4 58	$\bar{4}$ 58	0 00	$\bar{4}$ 58	0 00	$\bar{0}$.0870	0	0.0870
35		$\bar{1}07$	"	6 01	$\bar{6}$ 01	"	$\bar{6}$ 01	"	$\bar{0}$.1054	"	0.1054
36		$\bar{1}06$	"	7 24	$\bar{7}$ 24	"	$\bar{7}$ 24	"	$\bar{0}$.1300	"	0.1300
37		$\bar{2}$.0.11	"	8 17	$\bar{8}$ 17	"	$\bar{8}$ 17	"	$\bar{0}$.1456	"	0.1456
38	μ	105	"	9 21	$\bar{9}$ 21	"	$\bar{9}$ 21	"	$\bar{0}$.1645	"	0.1645
39		$\bar{4}$.0.19	"	9 57	$\bar{9}$ 57	"	$\bar{9}$ 57	"	$\bar{0}$.1754	"	0.1754
40		3.0.14	"	10 10	$\bar{1}$0 10	"	$\bar{1}$0 10	"	$\bar{0}$.1793	"	0.1793
41	D	$\bar{1}04$	"	12 12	$\bar{1}$2 12	"	$\bar{1}$2 12	"	$\bar{0}$.2162	"	0.2162
42	F	$\bar{2}07$	"	14 12	$\bar{1}$4 12	"	$\bar{1}$4 12	"	$\bar{0}$.2531	"	0.2531
43		3.0.10	"	15 00	$\bar{1}$5 00	"	$\bar{1}$5 00	"	$\bar{0}$.2678	"	0.2678
44		4.0.13	"	16 01	$\bar{1}$6 01	"	$\bar{1}$6 01	"	$\bar{0}$.2758	"	0.2758
45	A	$\bar{1}03$	"	16 49	$\bar{1}$6 49	"	$\bar{1}$6 49	"	$\bar{0}$.3023	"	0.3023
46		$\bar{4}$.0.11	"	18 27	$\bar{1}$8 27	"	$\bar{1}$8 27	"	$\bar{0}$.3336	"	0.3336
47	J	$\bar{2}05$	"	20 22	$\bar{2}$0 22	"	$\bar{2}$0 22	"	$\bar{0}$.3712	"	0.3712
48	n	$\bar{1}02$	"	25 23	$\bar{2}$5 23	"	$\bar{2}$5 23	"	$\bar{0}$.4745	"	0.4745
49		$\bar{2}03$	"	32 54	$\bar{3}$2 54	"	$\bar{3}$2 54	"	$\bar{0}$.6468	"	0.6468
50	N	$\bar{5}07$	"	34 50	$\bar{3}$4 50	"	$\bar{3}$4 50	"	$\bar{0}$.6959	"	0.6959
51	T	$\bar{4}05$	"	38 07	$\bar{3}$8 07	"	$\bar{3}$8 07	"	$\bar{0}$.7846	"	0.7846
52		$\bar{1}\bar{1}$.0.13	"	39 46	$\bar{3}$9 46	"	$\bar{3}$9 46	"	$\bar{0}$.8322	"	0.8322
53	θ	$\bar{1}01$	"	44 45	$\bar{4}$4 45	"	$\bar{4}$4 45	"	$\bar{0}$.9913	"	0.9913
54	$\mathfrak{P}$	$\bar{9}08$	"	48 15	$\bar{4}$8 15	"	$\bar{4}$8 15	"	$\bar{1}$.1203	"	1.1203
55	W	$\bar{6}05$	"	50 09	$\bar{5}$0 09	"	$\bar{5}$0 09	"	$\bar{1}$.1970	"	1.1970
56	B	$\bar{5}04$	"	51 16	$\bar{5}$1 16	"	$\bar{5}$1 06	"	$\bar{1}$.2470	"	1.2470
57	κ	$\bar{4}03$	"	53 11	$\bar{5}$3 11	"	$\bar{5}$3 11	"	$\bar{1}$.3358	"	1.3358
58	η	$\bar{3}02$	"	56 24	$\bar{5}$6 24	"	$\bar{5}$6 24	"	$\bar{1}$.5045	"	1.5045
59		$\bar{5}03$	"	59 15	$\bar{5}$9 15	"	$\bar{5}$9 15	"	$\bar{1}$.6803	"	1.6803
60	$\mathfrak{F}$	$\bar{7}04$	"	60 29	$\bar{6}$0 29	"	$\bar{6}$0 29	"	$\bar{1}$.7664	"	1.7664
61		$\bar{1}\bar{5}$.0.8	"	62 11	$\bar{6}$2 11	"	$\bar{6}$2 11	"	$\bar{1}$.8956	"	1.8956
62	v	$\bar{2}01$	"	63 43	$\bar{6}$3 43	"	$\bar{6}$3 43	"	$\bar{2}$.0249	"	2.0249
63	$\mathfrak{M}$	$\bar{1}\bar{3}$.0.6	"	65 32	$\bar{6}$5 32	"	$\bar{6}$5 32	"	$\bar{2}$.1980	"	2.1980
64	$\mathfrak{X}$	$\bar{7}03$	"	67 07	67 07	"	67 07	"	$\bar{2}$.3694	"	2.3694
65		$\bar{1}\bar{9}$.0.8	"	67 30	$\bar{6}$7 30	"	$\bar{6}$7 30	"	$\bar{2}$.4128	"	2.4128
66	ψ	$\bar{3}01$	"	71 54	$\bar{7}$1 54	"	$\bar{7}$1 54	"	$\bar{3}$.0585	"	3.0585
67		$\bar{7}02$	"	74 23	$\bar{7}$4 23	"	$\bar{7}$4 23	"	$\bar{3}$.5751	"	3.5751
68	h	221	50 01	70 02	64 38	60 31	46 04	37 09	2.1091	1.7682	2.7526
69	s	111	50 35	54 19	47 05	41 29	38 46	31 03	1.0757	0.8844	1.3925

Number	Letter	Miller Symbol (001)	ϕ	ρ	ξ_0	η_0	ξ	η	x'	y'	d'
70	P	223	51°07′	43°12′	36°10′	30°32′	32°12′	25°27′	0.7313	0.5896	0.9394
71	$\mathfrak{p}$	112	51 39	35 28	29 12	23 51	27 05	21 06	0.5590	0.4422	0.7128
72	t	$\bar{2}25$	$\bar{4}6$ 22	27 09	$\bar{2}0$ 21	19 29	$\bar{1}9$ 17	17 55	$\bar{0}$.3711	0.3538	0.5127
73	Q	$\bar{1}12$	$\bar{4}6$ 53	32 54	$\bar{2}5$ 17	23 51	$\bar{2}3$ 22	21 48	$\bar{0}$.4724	0.4422	0.6471
74	z	$\bar{4}47$	$\bar{4}7$ 16	36 45	$\bar{2}8$ 44	26 49	$\bar{2}6$ 04	23 57	$\bar{0}$.5484	0.5054	0.7465
75	u	$\bar{2}23$	$\bar{4}7$ 39	41 11	$\bar{3}2$ 54	30 31	$\bar{2}9$ 08	26 20	$\bar{0}$.6468	0.5896	0.8752
76	x	$\bar{1}11$	$\bar{4}8$ 16	53 02	$\bar{4}4$ 45	41 29	$\bar{3}6$ 36	32 08	$\bar{0}$.9913	0.8844	1.3284
77	k	$\bar{2}21$	$\bar{4}8$ 52	69 36	$\bar{6}3$ 43	60 31	$\bar{4}4$ 54	38 04	$\bar{2}$.0242	1.7682	2.6822
78	π	$\bar{4}41$	$\bar{4}9$ 20	79 32	$\bar{7}6$ 15	74 13	$\bar{4}7$ 58	39 56	$\bar{4}$.1763	3.5376	5.4370
79	$\mathfrak{C}$	$\bar{7}71$	$\bar{4}9$ 17	83 59	$\bar{8}2$ 05	80 49	$\bar{4}8$ 55	40 27	7.1926	6.1910	9.4903
80	$\mathfrak{q}$	212	67 39	49 19	47 05	23 51	26 16	16 45	0 1076	0.4422	1.1631
81	γ	121	31 18	64 14	47 05	60 28	27 53	50 18	1.0757	1.7682	2.0710
82	Σ	$\bar{2}32$	$\bar{3}6$ 46	58 53	$\bar{4}4$ 45	52 59	$\bar{3}0$ 49	43 18	$\bar{0}$.9913	1.3264	1.6947
83	ν	$\bar{3}53$	$\bar{3}3$ 56	60 37	$\bar{4}4$ 45	55 50	$\bar{2}9$ 02	46 18	$\bar{0}$.9913	1.4735	1.7758
84	α	$\bar{1}21$	$\bar{2}9$ 16	63 45	$\bar{4}4$ 45	60 31	$\bar{2}6$ 00	51 29	$\bar{0}$.9913	1.7682	2.0277
85	$\mathfrak{w}$	525	70 23	46 25	44 45	19 29	43 02	14 05	0.9913	0.3537	1.0509
86	$\mathfrak{e}$	131	20 29	70 33	44 45	69 21	19 16	62 03	0.9913	2.6533	2.8324
87	$\mathfrak{r}$	122	32 18	46 18	29 12	41 30	31 28	31 26	0.5590	0.8844	1.0463
88		$\bar{3}22$	$\bar{5}9$ 37	60 14	$\bar{5}6$ 27	41 29	$\bar{4}8$ 29	26 03	$\bar{1}$.5081	0.8844	1.7482
89	$\mathfrak{y}$	$\bar{2}11$	$\bar{6}6$ 24	65 39	$\bar{6}3$ 43	41 29	$\bar{5}6$ 35	21 24	$\bar{2}$.0242	0.8844	2.2096
90	z	$\bar{4}11$	$\bar{7}7$ 46	76 32	$\bar{7}6$ 14	41 29	$\bar{7}1$ 52	11 54	$\bar{4}$.0816	0.8844	4.1764
91	ω	241	30 48	76 21	64 38	74 13	29 50	56 35	2.1091	3.5380	4.1193
92	$\mathfrak{t}$	$\bar{6}83$	$\bar{4}0$ 39	72 10	$\bar{6}3$ 43	67 01	$\bar{3}8$ 19	46 14	$\bar{2}$.0242	2.3580	3.1083
93	R	$\bar{2}41$	$\bar{2}9$ 47	76 13	$\bar{6}3$ 43	74 13	$\bar{2}8$ 54	57 27	$\bar{2}$.0242	3.5380	4.0764
94	t	$\bar{2}61$	$\bar{2}0$ 53	80 02	$\bar{6}3$ 43	79 20	$\bar{2}0$ 33	66 57	$\bar{2}$.0242	5.3065	5.6796
95	τ	$\bar{4}72$	$\bar{3}3$ 11	74 52	$\bar{6}3$ 43	72 06	$\bar{3}1$ 54	53 53	$\bar{2}$.0248	3.0955	3.6989
96	$\mathfrak{h}$	$\bar{2}.10.1$	$\bar{1}3$ 25	83 43	$\bar{6}4$ 38	83 33	$\bar{1}3$ 01	75 13	$\bar{2}$.1093	8.8443	9.0922
97	ξ	321	60 38	74 30	72 21	60 31	57 07	28 34	3.1428	1.7682	2.6061
98	G	$\bar{3}21$	$\bar{5}9$ 57	74 12	$\bar{7}1$ 53	60 31	$\bar{5}6$ 24	28 48	$\bar{3}$.0583	1.7682	3.5333
99	$\mathfrak{u}$	$\bar{3}51$	$\bar{3}4$ 40	79 28	$\bar{7}1$ 54	77 15	$\bar{3}4$ 00	53 57	$\bar{3}$.0584	4.4221	5.3767
100	$\mathfrak{i}$	$\bar{6}81$	$\bar{4}1$ 02	83 55	$\bar{8}0$ 47	82 47	$\bar{4}0$ 46	48 35	$\bar{6}$.1589	7.0754	9.3806
101	$\mathfrak{d}$	$\bar{4}.10.1$	$\bar{2}4$ 50	84 08	$\bar{7}6$ 16	83 33	$\bar{2}4$ 41	64 32	$\bar{4}$.0919	8.8443	9.7450
102	$\mathfrak{f}$	6.10.1	35 13	84 43	80 54	83 33	35 03	54 26	6.2434	8.8443	10.8260
103	K	$\bar{1}2.10.5$	$\bar{5}4$ 03	71 38	$\bar{6}7$ 42	60 31	$\bar{5}0$ 12	35 52	$\bar{2}$.4382	1.7682	3.0123
104	J	132	22 51	55 13	29 12	53 00	18 36	49 11	0.5590	1.3266	1.4396
105	χ	1.11.2	6 33	78 28	29 12	78 23	6 25	76 45	0.5590	4.8642	4.8961
106	i	$\bar{1}$.10.2	$\bar{6}$ 07	77 20	$\bar{2}5$ 23	77 15	$\bar{5}$ 59	75 57	$\bar{0}$.4745	4.4221	4.4474
107	β	$\bar{3}62$	$\bar{2}9$ 37	71 52	$\bar{5}6$ 27	69 21	$\bar{2}8$ 01	55 42	$\bar{1}$.5080	2.6532	0.3052
108	T	4.12.3	21 52	75 18	54 52	74 13	21 07	63 51	1.4203	3.5377	3.8122
109	ρ	$\bar{1}34$	$\bar{1}8$ 17	34 35	$\bar{1}2$ 12	33 12	$\bar{1}0$ 15	32 36	$\bar{0}$.2161	0.6545	0.6892
110	$\mathfrak{b}$	$\bar{5}28$	$\bar{6}9$ 53	32 44	$\bar{3}1$ 07	12 28	$\bar{3}0$ 31	10 43	$\bar{0}$.6037	0.2211	0.6429
111	S	$\bar{1}25$	$\bar{2}4$ 53	21 19	$\bar{9}$ 19	19 27	$\bar{8}$ 48	19 15	$\bar{0}$.1641	0.3538	0.3900
112	λ	$\bar{2}.18.3$	$\bar{6}$ 57	79 24	$\bar{3}2$ 54	79 20	$\bar{6}$ 50	77 21	$\bar{0}$.6468	5.3064	5.3451

Number	Letter	Miller Symbol (001)	ϕ	ρ	ξ_0	η_0	ξ	η	x'	y'	d'
113	δ	243	31°42′	54°11′	36°03′	49°42′	25°13′	47°38′	0.7279	1.1789	1.3855
114	d	$\bar{2}43$	$\bar{2}8$ 45	53 22	$\bar{3}2$ 54	49 42	$\bar{2}2$ 42	44 43	$\bar{0}$.6468	1.1789	1.3447
115	Δ	$\bar{2}.10.3$	$\bar{1}2$ 23	71 40	$\bar{3}2$ 54	71 16	$\bar{1}1$ 44	68 00	$\bar{0}$.6468	2.9478	3.0179
116	ϑ	9.12.8	42 15	60 50	50 18	53 00	35 57	40 16	1.2049	1.3266	1.7919
117	e	$\bar{2}45$	$\bar{2}7$ 41	38 38	$\bar{2}0$ 22	35 17	$\bar{1}6$ 52	33 34	$\bar{0}$.3712	0.7075	0.7990
118	H	4.10.7	26 36	54 43	32 20	51 38	21 26	46 52	0.6328	1.2634	1.4131
119	o	685	42 11	62 22	52 03	54 45	36 30	41 02	1.2825	1.4151	1.9097
120	g	283	17 13	67 57	36 40	67 01	15 56	62 17	0.7312	2.3585	2.4693
121	Φ	$\bar{2}73$	$\bar{1}7$ 24	65 11	$\bar{3}2$ 54	64 09	$\bar{1}5$ 45	60 40	$\bar{0}$.6468	2.0637	2.1627
122	j	$\bar{4}76$	$\bar{3}2$ 05	50 36	$\bar{3}2$ 54	45 54	$\bar{2}4$ 14	40 54	$\bar{0}$.6468	1.0319	1.2178
123	f	153	14 42	56 44	21 09	55 51	12 15	53 58	0.3867	1.4741	1.5240
124	l	$\bar{7}43$	$\bar{6}3$ 32	69 18	$\bar{6}7$ 07	49 42	$\bar{5}6$ 50	24 38	$\bar{2}$.3694	1.1793	2.6465
125	ȝ	287	18 28	46 49	18 39	45 18	13 21	43 46	0.3375	1.0108	1.0657
126	r	$\bar{5}73$	$\bar{3}9$ 09	69 24	$\bar{5}9$ 14	64 09	$\bar{3}6$ 14	46 33	$\bar{1}$.6803	2.0637	2.6613
127	ℭ	245	32 58	40 09	24 39	35 17	20 32	32 45	0.4589	0.7075	0.8434
128	𝔘	564	45 10	62 01	53 09	52 59	38 46	38 31	1.3341	1.3266	1.8814
129	𝔇	453	43 56	63 58	54 51	55 51	38 34	40 19	1.4203	1.4741	2.0468
130	n	231	38 29	73 34	64 38	69 20	36 39	48 40	2.1093	2.6533	3.3896

As azurite is commonly enlongated parallel to the b axis, it is often desirable to measure crystals with the orthodome zone prismatic. The following table gives the calculated angles for this position. The numbering and arrangement follows the first table to lessen confusion between the two positions.

The transformation of angles and symbols is effected by use of the relationship:

$$\phi\ (010) = 90 - \xi_0(001)$$
$$\rho\ (010) = 90 - \eta(001)$$
$$pqr\ (001) = rpq(010)$$

AZURITE ANGLE TABLE FOR MEASUREMENTS ON THE SIDE PINACOID-(010)

$p_0''=1.1316$	$q_0''=1.1687$	$\mu=87°\ 35'$

Number	Letter	Miller Symbol (010)	Miller Symbol (001)	ϕ	ρ
1	*c*	100	001	87° 35′	90° 00′
2	*b*	001	010	0 00	0 00
3	*a*	010	100	0 00	90 00
4	*u*	031	310	0 00	74 05
5	*g*	021	210	0 00	66 50
6	*i*	032	320	0 00	60 18
7	*m*	011	110	0 00	49 27
8	*w*	012	120	0 00	30 18
9	*e*	10.0.1	0.1.10	87 35	84 57
10	*C*	801	018	"	83 42
11	*G*	601	016	"	81 38
12	Λ	501	015	"	79 59
13	*S*	401	014	"	77 33
14		702	027	"	72 22
15	*q*	502	025	"	70 32
16	*E*	201	012	"	66 10
17	*l*	302	023	"	59 30
18	ℜ	403	034	"	56 28
19	*j*	504	045	"	54 08
20	*f*	101	011	"	48 33
21		607	076	"	44 07
22	*K*	203	032	"	37 02
23	*p*	102	021	"	29 30
24	*L*	103	031	"	20 41
25	Ω	130	301	17 39	90 00
26	*φ*	120	201	25 22	"
27		590	905	27 43	"
28	*σ*	110	101	42 54	"
29	ℌ	320	203	53 49	"
30	*ζ*	210	102	60 47	"
31	*τ*	730	307	64 07	"
32		520	205	65 30	"
33	*M*	410	104	73 16	"
34	*r*	$\bar{8}10$	$\bar{1}08$	$\bar{8}5$ 02	"
35		$\bar{7}10$	$\bar{1}07$	$\bar{8}3$ 59	"
36		$\bar{6}10$	$\bar{1}06$	$\bar{8}2$ 36	"
37		$\bar{1}\bar{1}.2.0$	$\bar{2}.0.11$	$\bar{8}1$ 43	"
33	*μ*	$\bar{5}10$	$\bar{1}05$	$\bar{8}0$ 39	"
89		$\bar{1}\bar{9}.4.0.$	$\bar{4}.0.19$	$\bar{8}0$ 03	"

Number	Letter	Miller Symbol	Miller Symbol	ϕ	σ
40		$\bar{1}4.3.0$	$\bar{3}.0.14$	$\bar{7}9°$ 50′	90° 00′
41	*D*	$\bar{4}10$	$\bar{1}04$	$\bar{7}7$ 48	"
42	*F*	$\bar{7}20$	$\bar{2}07$	$\bar{7}5$ 48	"
43		$\bar{1}0.3.0.$	$\bar{3}.0.10$	$\bar{7}5$ 00	"
44		$\bar{1}3.4.0$	$\bar{4}.0.13$	$\bar{7}3$ 59	"
45	*A*	$\bar{3}10$	$\bar{1}03$	$\bar{7}3$ 11	"
46		$\bar{1}1.4.0$	$\bar{4}.0.11$	$\bar{7}1$ 33	"
47	*J*	$\bar{5}20$	$\bar{2}05$	$\bar{6}9$ 38	"
48	*n*	$\bar{2}10$	$\bar{1}02$	$\bar{6}4$ 37	"
49		$\bar{3}20$	$\bar{2}03$	$\bar{5}7$ 06	"
50	*N*	$\bar{7}50$	$\bar{5}07$	$\bar{5}5$ 10	"
51	*T*	$\bar{5}40$	$\bar{4}05$	$\bar{5}1$ 53	"
52		$\bar{1}3.11.0$	$\bar{1}1.0.13$	$\bar{5}0$ 14	"
53	θ	$\bar{1}10$	$\bar{1}01$	$\bar{4}5$ 15	"
54	$\mathfrak{P}$	$\bar{8}90$	$\bar{9}08$	$\bar{4}1$ 45	"
55	*W*	$\bar{6}50$	$\bar{6}05$	$\bar{3}9$ 51	"
56	*B*	$\bar{4}50$	$\bar{5}04$	$\bar{3}8$ 44	"
57	κ	$\bar{3}40$	$\bar{4}03$	$\bar{3}6$ 49	"
58	η	$\bar{2}30$	$\bar{3}02$	$\bar{3}3$ 36	"
59		$\bar{3}50$	$\bar{5}03$	$\bar{3}0$ 45	"
60	$\mathfrak{F}$	$\bar{4}70$	$\bar{7}04$	$\bar{2}9$ 31	"
61		$\bar{8}.15.0$	$\bar{1}5.0.8$	$\bar{2}7$ 49	"
62	v	$\bar{1}20$	$\bar{2}01$	$\bar{2}6$ 17	"
63	$\mathfrak{M}$	$\bar{6};13;0$	$\bar{1}3;0;6$	$\bar{2}4$ 28	"
64	$\mathfrak{X}$	$\bar{3}70$	$\bar{7}03$	$\bar{2}2$ 53	"
65		$\bar{8}.19.0$	$\bar{1}9.0.8$	$\bar{2}2$ 30	"
66	ψ	$\bar{1}30$	$\bar{3}01$	$\bar{1}8$ 06	"
67		$\bar{2}70$	$\bar{7}02$	$\bar{1}5$ 37	"
68	*h*	122	221	25 22	52 51
69	*s*	111	111	42 55	58 57
70	*P*	322	223	53 50	64 33
71	$\mathfrak{y}$	211	112	60 48	68 54
72	*i*	$\bar{5}22$	$\bar{2}25$	$\bar{6}9$ 39	72 05
73	*Q*	$\bar{2}11$	$\bar{1}12$	$\bar{6}4$ 43	68 12
74	*z*	$\bar{7}44$	$\bar{4}47$	$\bar{6}1$ 16	66 03
75	*u*	$\bar{3}22$	$\bar{2}23$	$\bar{5}7°$ 06′	$\bar{6}3°$ 40′
76	*x*	$\bar{1}11$	$\bar{1}11$	$\bar{4}5$ 15	57 52
77	*k*	$\bar{1}22$	$\bar{2}21$	$\bar{2}6$ 17	51 56
78	π	$\bar{1}44$	$\bar{4}41$	$\bar{1}3$ 45	50 04
79	$\mathfrak{S}$	$\bar{1}77$	$\bar{7}71$	$\bar{7}$ 55	49 33
80	q	221	212	42 55	73 15
81	γ	112	121	42 55	39 42
82	Σ	$\bar{2}23$	$\bar{2}32$	$\bar{4}5$ 15	46 42
83	ν	$\bar{3}35$	$\bar{3}53$	"	43 42
84	α	$\bar{1}12$	$\bar{1}21$	"	38 31

Number	Letter	Miller Symbol (010)	Miller Symbol (001)	ϕ	ρ
85	w	$\bar{3}52$	$\bar{3}25$	$\overline{45}°$ 15′	75° 55′
86	e	$\bar{1}13$	$\bar{1}31$	"	27 57
87	r	212	122	60 48	58 34
88		232	322	33 33	65 57
89	y	$\bar{1}21$	$\bar{2}11$	$\overline{26}$ 17	68 36
90	z	$\bar{1}41$	$\bar{4}11$	$\bar{1}3$ 46	78 06
91	ω	124	241	25 22	33 25
92	τ	$\bar{3}68$	$\bar{6}83$	$\overline{26}$ 17	45 46
93	*R*	$\bar{1}24$	$\bar{2}41$	"	32 33
94	*t*	$\bar{1}26$	$\bar{2}61$	"	23 03
95	t	$\bar{2}47$	$\bar{4}72$	"	36 05
96	h	$\bar{1}.2.10$	2.10.1	"	14 09
97	ξ	132	321	17 39	61 26
98	*G*	$\bar{1}32$	$\bar{3}21$	$\overline{18}$ 07	61 12
99	u	$\bar{1}35$	$\bar{3}51$	"	36 03
100	i	$\bar{1}68$	$\bar{6}81$	$\bar{9}$ 13	41 25
101	o	$\bar{1}.4.10$	$\bar{4}.10.1$	$\bar{1}3$ 44	25 28
102	f	1.6.10	6.10.1	9 06	35 34
103	*K*	$\bar{5}.12.10$	$\bar{1}2.10.5$	$\overline{22}$ 18	54 08
104	*J*	213	132	60 48	40 49
105	χ	2.1.11	1.11.2	"	13 15
106	*i*	$\bar{2}.1.10$	$\bar{1}.10.2$	$\overline{64}$ 37	14 13
107	β	$\bar{2}36$	$\bar{3}62$	$\overline{33}$ 33	34 18
108	*T*	3.4.12	4.12.3	35 08	25 09
109	ρ	$\bar{4}13$	$\bar{1}34$	$\overline{77}$ 48	57 24
110	b	$\bar{8}52$	$\bar{5}28$	$\overline{58}$ 53	79 17
111	*S*	$\bar{5}12$	$\bar{1}25$	$\overline{80}$ 41	70 45
112	λ	$\bar{3}.2.18$	$\bar{2}.18.3$	$\overline{57}$ 06	12 39
113	δ	324	243	53 57	46 22
114	*d*	$\bar{3}24$	$\bar{2}43$	$\overline{57}$ 06	45 17
115	Δ	$\bar{3}.2.10$	$\bar{2}.10.3$	"	22 00
116	b	8.9.12	9.12.8	39 42	49 44
117	*e*	$\bar{5}24$	$\bar{2}45$	$\overline{69}$ 38	56 26
118	*H*	7.4.10	4.10.7	57 40	43 08
119	*o*	568	685	37 57	48 58
120	g	328	283	53 20	27 43
121	Φ	$\bar{3}27$	$\bar{2}73$	$\overline{57}$ 06	29 20
122	j	$\bar{6}47$	$\bar{4}76$	"	49 06
123	f	315	153	58 51	36 02
124	l	$\bar{3}74$	$\bar{7}43$	$\overline{22}$ 53	65 22
125	ϑ	728	287	71 21	46 14
126	r	$\bar{3}57$	$\bar{5}73$	$\overline{30}$ 46	43 27
127	$\mathfrak{C}$	524	245	65 21	57 15
128	$\mathfrak{U}$	456	564	36 51	51 29
129	$\mathfrak{D}$	345	453	35 07	49 41
130	n	123	231	25 22	41 20

The gnomonic projecton on *b* (010), figure 40 shows the direction line of the base 2° 25′ to the right of the 90° coordinate. The positive pyramids are in the lower right hand, and upper left hand, quadrants. A crystal is brought from the normal to this position by two 90° rotations:

1. A 90° rotation from front to back—making the front pinacoid polar.
2. A second 90° rotation from right to left—bringing the side pinacoid of the *right* end of the crystal polar.

The forms which were positive in the first position will still be positive. It is important to note that if the pole of the side pinacoid of the left end of the crystal is brought to the center of the projection, the direction line of the base will be on the left of the 90° coordinate. The position of the positive and negative pyramids is also reversed, i. e. the negative forms will lie in the lower, right quadrant. Therefore, if the right end of a crystal is measured in the side pinacoid position, the ϕ of the base will be $+87°\ 35'$ and the ϕ values of the other forms will agree, in sign, with the table. If the left end is measured, the base will have a ϕ value of $-87°\ 35'$. In this case the *sign* of all the ϕ angles must be reversed to conform to the orientation used in calculating the table.

THE ANGLES OF AZURITE FROM OTHER LOCALITIES

Azurite crystals from different localities were next studied to test the new calculated angles, and to determine, if possible, any actual variation in the angles of crystals from different localities. In the following tables the average measured angles, together with the calculated angles from this paper and the Winkeltabellen, are given for comparison. The relative weight to be accorded each form depends upon the number of measurements and quality of the reflection obtained from the face. Poor reflections are usually not included and the entries under the column marked "Signal" indicate:—E-excellent, G-good, F-fair, P-poor.

Chessy, France. Three specimens from this locality were obtained for crystallographic study. Most of the crystals are of the pyramidal habit forming a sub-parallel group on malachite pseudomorphs. Six such crystals were measured, but the signals were so confused that it was impossible to use them in checking the calculations. One vug, however, contained undisturbed crystals

elongated parallel to the *b* axis, and projecting into the cavity. Four of these crystals were measured, and gave good reflections.

AZURITE FROM CHESSY, FRANCE—MEASURED ON *b*(010)

Letter	Signal	Number of faces	ϕ						ρ					
			Calculated				Measur'd		Calculated				Measur'd	
			Winkel-tabellen		This paper				Winkel-tabellen		This paper			
c	F	2	87°	36′	87°	35′	87°	39′	90°	00′	90°	00′	90°	00′
η	G	1	$\bar{33}$	28	$\bar{33}$	36	$\bar{33}$	36	"		"		"	
θ	E	1	$\bar{45}$	09	$\bar{45}$	15	$\bar{45}$	12	"		"		"	
v	G	1	$\bar{26}$	13	$\bar{26}$	17	$\bar{26}$	07	"		"		"	
a	G	1	0	00	0	00	0	06	"		"		90	08
m	G	1	0	00	0	00	0	00	49	39	49	27	49	24
h	E	1	25	18	25	22	25	27	53	02	52	51	52	50
x	G	2	$\bar{45}$	09	$\bar{45}$	15	$\bar{45}$	18	58	02	57	52	57	47
d	G	2	$\bar{57}$	01	$\bar{57}$	06	$\bar{57}$	05	45	24	45	17	45	18
R	F	2	$\bar{26}$	13	$\bar{26}$	17	$\bar{26}$	14	32	42	32	33	32	34
f	G	2	87	36	87	35	87	35	48	40	48	33	48	34
p	E	2	87	36	87	35	87	36	29	27	29	30	29	30

The measured angles consistently agree more closely with the new calculations than with the corresponding values in the Winkeltabellen. The disagreement between the elements obtained from Chessy measurements and from other localities seems to depend on the quality of material available for the early studies, rather than upon any actual variation in angles.

BISBEE, ARIZONA. A very fine collection was available for study from this locality. Nine crystals were measured. Four of the most perfect were averaged to check the axial ratio.

AZURITE FROM BISBEE ARIZONA—MEASURED ON *b*(010)

Letter	Signal	Number of faces	φ			ρ		
			Calculated		Measur'd	Calculated		Measur'd
			Winkel-tabellen	This paper		Winkel-tabellen	This paper	
c	P	5	87° 36′	87° 35′	87° 42′	90° 00′	90° 00′	90° 00′
a	F	6	0 00	0 0	0 00	"	"	"
σ	P	4	42 50	42 54	42 58	"	"	"
θ	F	4	$\overline{45}$ 09	$\overline{45}$ 15	$\overline{45}$ 21	"	"	"
m	G	7	0 00	0 00	0 02	49 39	49 27	49 31
w	G	2	0 00	0 00	0 02	30 29	30 18	30 10
l	F	6	87 36	87 35	87 57	59 37	59 30	59 21
f	G	7	"	"	87 40	48 40	48 33	48 36
p	G	7	"	"	87 38	29 27	29 30	29 31
h	F	7	25 18	25 22	25 39	53 02	52 51	52 54
s	F	4	42 50	42 55	43 03	59 06	58 57	58 55
P	F	2	53 46	53 50	54 02	64 40	64 33	64 33
γ	G	3	42 50	42 55	42 54	39 52	39 42	39 44
k	G	5	$\overline{26}$ 13	$\overline{26}$ 17	$\overline{26}$ 18	52 08	51 56	51 55
x	F	4	$\overline{45}$ 09	$\overline{45}$ 15	$\overline{45}$ 08	58 02	57 52	57 50
d	F	6	$\overline{57}$ 01	$\overline{57}$ 06	$\overline{57}$ 00	45 24	45 17	45 20
e	G	7	$\overline{69}$ 34	$\overline{69}$ 38	$\overline{69}$ 40	56 35	56 26	56 27
R	G	8	$\overline{26}$ 13	$\overline{26}$ 17	$\overline{26}$ 15	32 42	32 33	32 33
u	F	1	$\overline{57}$ 01	$\overline{57}$ 06	$\overline{56}$ 55	65 47	63 40	63 55
ρ	G	4	$\overline{77}$ 46	$\overline{77}$ 48	$\overline{77}$ 35	57 10	57 24	57 02
q	F*	4		42 55	43 03		73 15	73 23
i	P*	3		$\overline{9}$ 13	$\overline{10}$ 20		41 25	40 46
c	P*	2		$\overline{13}$ 44	$\overline{13}$ 07		25 28	24 10
ℜ	E*	1		87 35	87 33		56 28	56 35

* New forms

LAURIUM, GREECE. Two specimens with brilliant azurite projecting into the opening of a partially filled veinlet yielded crystals of exceptional brilliance. These crystals are comparable to the Tsumeb suite in perfection and the angular agreement is correspondingly close. Four crystals were measured and averaged.

AZURITE FROM LAURIUM, GREECE—MEASURED ON (010)

Letter	Signal	Number of faces	ϕ			ρ		
			Calculated		Measur'd	Calculated		Measur'd
			Winkel-tabellen	This paper		Winkel-tabellen	This paper	
c	G	6	87° 36′	87° 35′	87° 35′	90° 00′	90° 00′	90° 00′
a	E	8	00 00	0 00	0 01	90 00	90 00	89 59
σ	G	2	42 50	42 54	42 55	90 00	90 00	90 00
v	F	6	$\bar{2}6$ 13	$\bar{2}6$ 17	$\bar{2}6$ 01	"	"	"
θ	F	7	$\bar{4}5$ 09	$\bar{4}5$ 15	$\bar{4}5$ 15	"	"	"
n	P	4	$\bar{6}4$ 32	$\bar{6}4$ 37	$\bar{6}4$ 37	"	"	"
D	F	1	$\bar{7}7$ 45	$\bar{7}7$ 48	$\bar{7}7$ 35	"	"	"
ψ	F	1	$\bar{1}8$ 03	$\bar{1}8$ 06	$\bar{1}7$ 53	"	"	"
$\bar{1}1.0.13$	P	1		$\bar{5}0$ 14	$\bar{4}9$ 36	"	"	"
$\bar{4}.0.11$	P	2		$\bar{7}1$ 33	$\bar{7}1$ 37	"	"	"
A	F	1	$\bar{7}3$ 07	$\bar{7}3$ 11	$\bar{7}3$ 11	"	"	"
$\bar{4}.0.13$	P	1		$\bar{7}3$ 59	$\bar{7}4$ 00	"	"	"
m	E	6	0 00	0 00	0 01	49 39	49 27	49 26
h	E	8	25 18	25 22	25 21	53 02	52 51	52 51
k	P	2	$\bar{2}6$ 13	$\bar{2}6$ 17	$\bar{2}6$ 20	52 08	51 56	51 55
x	G	4	$\bar{4}5$ 09	$\bar{4}5$ 15	$\bar{4}5$ 21	58 02	57 52	57 53
d	G	8	$\bar{5}7$ 01	$\bar{5}7$ 06	$\bar{5}7$ 07	45 24	45 17	45 16
e	G	6	$\bar{6}9$ 34	$\bar{6}9$ 38	$\bar{6}9$ 40	56 35	56 26	56 26
ρ	F	2	$\bar{7}7$ 46	$\bar{7}7$ 48	$\bar{7}7$ 58	57 10	57 24	57 08
R	E	6	$\bar{2}6$ 13	$\bar{2}6$ 17	$\bar{2}6$ 17	32 42	32 33	32 33
P	G	2	53 46	53 50	53 50	64 40	64 33	64 33
s	E	4	42 50	42 55	42 54	59 06	58 57	58 57
l	G	6	87 36	87 35	87 33	59 37	59 30	59 30
f	F	4	"	"	87 33	48 40	48 33	48 32
p	E	6	"	"	87 34	29 27	29 30	29 30
r*	Line	1		$\bar{3}0$ 46	$\bar{3}2$ . .		43 27	43 10
f*	G	1		9 06	9 04		35 54	35 56
u*	Dim	1		$\bar{1}8$ 07	$\bar{1}7$ 39		36 03	36 15
t*	"	1		68 51	68 06		36 02	37 05
ȣ*	"			71 21	72 16		46 14	46 40

* New forms.

KELLY, NEW MEXICO. Eight crystals were measured. Each crystal had from 25 to 40 faces, and four yielded over 35 readings. Measurements of the three most perfect crystals are included in the average.

AZURITE FROM KELLY MINE, NEW MEXICO—MEASURED ON (010)

Letter	Signal	Number of faces	ϕ			ρ		
			Calculated		Measur'd	Calculated		Measur'd
			Winkel-tabellen	This paper		Winkel-tabellen	This paper	
c	F	4	87° 36′	87° 35′	87° 37′	90° 00′	90° 00′	90° 00′
a	G	3	0 00	0 00	0 00	"	"	"
σ	F	2	42 50	42 54	42 53	"	"	90 02
v	P	2	$\bar{2}6$ 13	$\bar{2}6$ 17	$\bar{2}6$ 45	"	"	90 00
η	P	2	$\bar{3}3$ 28	$\bar{3}3$ 36	$\bar{3}3$ 28	"	"	"
θ	E	4	$\bar{4}5$ 09	$\bar{4}5$ 15	$\bar{4}5$ 15	"	"	"
n	P	2	$\bar{6}4$ 32	$\bar{6}4$ 38	$\bar{6}4$ 37	"	"	"
$\bar{1}1.0.13$	F	2		$\bar{5}0$ 14	$\bar{4}9$ 32	"	"	"
α	P	1	$\bar{6}9$ 34	$\bar{6}9$ 38	$\bar{7}0$ 11	"	"	"
$\bar{3}.0.10$	F	1		$\bar{7}5$ 00	$\bar{7}5$ 06	"	"	"
$\bar{5}.0.3$	Line	1		$\bar{3}0$ 45	$\bar{3}1$ 48	"	"	"
T	P	1	$\bar{5}1$ 47	$\bar{5}1$ 53	$\bar{5}3$ 25	"	"	"
$\bar{4}.0.13$	P	1		$\bar{7}3$ 59	$\bar{7}4$ 03	"	"	"
A	F	1	$\bar{7}3$ 07	$\bar{7}3$ 11	$\bar{7}3$ 09	"	"	"
F	P	1	$\bar{7}5$ 44	$\bar{7}5$ 48	$\bar{7}6$ 02	"	"	"
m	E	6	0 00	0 00	0 01	49 39	49 27	49 26
w	E	4	0 00	0 00	0 02	30 29	30 18	30 18
l	F	3	87 36	87 35	87 39	59 37	59 30	59 31
f	F	4	"	"	87 39	48 40	48 33	48 35
p	G	5	"	"	87 33	29 27	29 30	29 32
h	E	6	25 18	25 22	25 25	53 02	52 51	52 51
s	P	3	42 50	42 55	43 08	59 06	58 57	$\bar{5}9$ 04
P	P	2	53 46	53 50	53 47	64 40	64 33	64 35
γ	G	4	42 50	42 55	43 01	39 52	39 42	39 42
ω	E	5	25 18	25 22	25 24	33 36	33 25	33 26
ρ	G	5	$\bar{7}7$ 46	$\bar{7}7$ 48	$\bar{7}7$ 43	57 10	57 24	57 02
d	G	4	$\bar{5}7$ 01	$\bar{5}7$ 06	$\bar{5}7$ 07	45 24	45 17	45 16
e	F	5	$\bar{6}9$ 34	$\bar{6}9$ 38	$\bar{6}9$ 52	56 35	56 26	56 24
R	F	3	$\bar{2}6$ 13	$\bar{2}6$ 17	$\bar{2}6$ 07	32 42	32 33	32 36
δ	G	2	53 46	53 57	53 54	46 34	46 22	46 25
u	G	1	$\bar{5}7$ 01	$\bar{5}7$ 06	$\bar{5}7$ 05	65 47	63 40	63 37
q*	G	2		42 55	42 48		73 15	73 22
f*	F	1		9 06	9 11		35 34	35 53
c*	F	3		$\bar{1}3$ 44	$\bar{1}3$ 35		25 28	25 30
m*	G	4		$\bar{4}5$ 15	$\bar{4}5$ 12		75 55	75 56
l*	P	3		$\bar{2}2$ 53	$\bar{2}2$ 50		65 22	65 15
j*	P	1		$\bar{5}7$ 06	$\bar{5}7$ 08		49 06	49 34
h*	P	1		$\bar{5}7$ 06	$\bar{5}7$ 08		29 20	30 20

* New forms.

Broken Hill, New South Wales. A single crystal, in habit and brilliance very similar to the Tsumeb crystals, was measured. Although the following table includes only the average of two faces for each form, the excellent crystallographic quality justifies its inclusion to check the calculated angles.

Azurite from Broken Hill, N. S. W.—Measured on (010)

Letter	Signal	Notices	ϕ			ρ		
			Calculated		Measur'd	Calculated		Measur'd
			Winkel-tabellen	This paper		Winkel-tabellen	This paper	
c	G	2	87° 36′	87° 35′	87° 39′	90° 00′	90° 00′	90° 00′
a	E	1	0 00	0 00	0 02	"	"	"
σ	F	2	42 50	42 54	42 50	"	"	"
ϕ	P	1	25 18	25 22	25 56	"	"	"
η	G	2	33 28	33 36	33 35	"	"	"
θ	E	2	45 09	45 15	45 11	"	"	"
m	E	2	0 00	0 00	0 03	49 39	49 27	49 26
l	G	2	87 36	87 35	87 36	59 37	59 30	59 28
f	E	2	"	"	87 37	48 40	48 33	48 31
p	E	2	"	"	87 37	29 27	29 30	29 29
h	G	2	25 18	25 22	25 23	53 02	52 51	52 49
s	G	2	42 50	42 55	42 56	59 06	58 57	58 57
γ	G	2	42 50	42 55	43 08	39 52	39 42	39 48
k	F	2	26 13	26 17	26 12	52 08	51 56	51 55
R	F	2	26 13	26 17	26 17	32 42	32 33	32 30

Copiapó, Chile. Very small, needle-like crystals are clustered as a drusy coating on a specimen from this locality. The small size of the faces necessitates the use of the high-power magnifying lens in measurement. The signals are single and definite, and although the results are not quite as accurate as measurements on larger crystals, the following table can safely be interpreted as indicating that measured angles from this locality also are in close agreement with the new calculations.

AZURITE FROM COPIAPÓ, CHILE—MEASURED ON (010)

Letter	Signal	Number of faces	ϕ			ρ		
			Calculated		Measur'd	Calculated		Measur'd
			Winkel-tabellen	This paper		Winkel-tabellen	This paper	
c	G	2	87° 36′	87° 35′	87° 26′	90° 00′	90° 00′	90° 00′
a	F	2	0 00	0 00	0 00	"	"	"
σ	Line	1	42 50	42 54	42 22	-	"	"
v	"	1	$\bar{2}6$ 13	$\bar{2}6$ 17	$\bar{2}6$ 18			
θ	F	1	$\bar{4}5$ 09	$\bar{4}5$ 15	$\bar{4}5$ 26			
l	G	2	87 36	87 35	87 21	59 37	59 30	59 29
m	G	2	0 00	0 00	0 00	49 39	49 27	49 27
h	G	2	25 18	25 22	25 13	53 02	52 51	52 52
s	F	2	42 50	42 55	43 03	59 06	58 57	58 57
P	P	1	53 46	53 50	54 09	64 40	64 33	64 46
R	G	1	$\bar{2}6$ 13	$\bar{2}6$ 17	$\bar{2}6$ 16	32 42	32 33	32 34

CONCLUSIONS CONCERNING THE AXIAL RATIO OF AZURITE

In 1891, Farrington[3] made the first crystallographic study of azurite from Arizona, and deduced the ratio: .85676:1:88603, $\beta = 87° 36' 36''$. He says: "In the position adopted by Schrauf the vertical axis is given double the length of that in our position. Taking, therefore, one-half the value which he gives to c, his axial ratio is:

$$\dot{a}:\bar{b}:c = .85012:1:.88054, \quad \beta = 87° 36'$$

It will be seen that these ratios differ but little, the values for β being almost identical, while those for $\dot{a}$ and c agree to the third decimal place. The author's value for $\dot{a}$ is supported by several very accurate measurements of the prism $m \wedge m$, which in every case showed a close approximation to the angle 81° 8′ instead of 80° 42′ as given by Schrauf. Whether this variation is to be regarded as a fundamental difference in the prismatic angle of the crystals from the separate localities or, on the other hand, as so small as to be within the limits of error in observation, I cannot say. More data are needed for deciding the question. The most satisfactory measurements that could be obtained for judging of the correctness of the value assigned to c, were those of $c \wedge p$,

[3] C. C. Farrington, *Am. J. Sc.*, Vol. **XLI**, April, 1891.

$001 \wedge 021$, and $p \wedge p$, $021 \wedge 02\bar{1}$. The measured and calculated angles compare as follows:

	Calculated		Measured	
	Farrington	Schrauf	No. 1	No. 2
$c \wedge p$ $001 \wedge 021$	60° 33′	60° 24′	60° 29′	60° 30′
$p \wedge p$ $021 \wedge 02\bar{1}$	58 56	59 12	59 1	59 6

From these it would seem that the true value of c is about a mean between that given by Schrauf and by the author. Here, again, more accurate measurements are needed."

The value of c, as derived from the Tsumeb crystals, is .8844—a mean between the value assigned by Farrington and Schrauf.

The following table is taken from Farrington's paper with the addition of a column giving our calculated values for comparison.

ANGLES ON THE ORTHOPINACOID, $a(100)$ AND $a(\bar{1}00)$—AFTER FARRINGTON

Letter	Symbol	Calculated			Crystal No. 1	Crystal No. 2	Other measurements
		Farrington	Schrauf	Palache & Lewis			
m	(110)	40° 34′	40° 21′	40° 33′	40° 34′	40° 33′	40° 30′
w	(120)	59 43	59 41	59 42			60 17
l	(023)	87 56	87 55.8	87 55		87 56	
f	(011)	88 12	88 12	88 11		88 16	
p	(021)	88 50	88 49	88 49	88 52	88 50	
σ	(101)	42 53	42 50	42 54	42 46	42 57	42 56
$Q(P)$	(223)	57 47	57 42	57 48	57 40	57 50	
h	(221)	43 56	43 45.5	43 56	43 50	43 58	
γ	(121)	62 7	61 58	62 7		62 12	
x	($\bar{1}11$)	53 22	53 15.5	53 24	53 31	53 18	
k	($\bar{2}21$)	45 5	44 55	45 6	45 19		
G	($\bar{3}21$)	33 35	33 26	33 36			33 30
K	($\bar{1}2.10.5$)	39 48	39 37	39 48			39 55
F	($\bar{2}07$)	75 45	75 44	75 48	75 56		75 47
θ	($\bar{1}01$)	45 12	45 9	45 15	45 20	45 12	
η	($\bar{3}02$)	33 30	33 27.5	33 36			33 29

The measurements do not check closely with the calculated values, but the fact that our calculated angles agree so closely with Farrington's, shows that the variation is not to be regarded as "a fundamental difference in the prismatic angle from the separate localities." It has already been shown that measurements

on sufficiently perfect azurite from Chessy agree more closely with our calculations than with Schrauf's. Our study on azurite from Bisbee, Laurium, Kelly, Broken Hill, and Copiapó indicates that the Tsumeb elements are in accord with measurements from these localities. The conclusion seems justified that the axial ratio of azurite is constant for these different localities, and that the new tables have a general, rather than local, value.

General Features of Azurite from Tsumeb

Most of the specimens selected for study had the azurite crystals implanted without mutual interference. The crystals elongated parallel to *c* are usually attached to the matrix at one end of the vertical axis. Those elongated parallel to the ortho axis are usually attached at one end of this axis. Many doubly terminated crystals are found delicately attached to the matrix or perched on needles of malachite. Symmetrical development is the rule. Small or thin crystals are transparent and of a beautiful azure blue color, while the thicker or larger ones are much darker. Prismatic development of the orthodome zone is the most common habit. These crystals usually have a wealth of forms developed with brilliant faces and sharp angles. Vicinal, etch, and line faces are rare. No twinned crystals were observed.

The larger crystals are commonly composed of parallel aggregates of several individuals. Often a malachite pseudomorph core is observed with second generation azurite in parallel or subparallel position.

The photographs reproduced in this paper were taken by Mr. E. B. Dane, Jr., a student at Harvard University. The reproduction of the colored photographs was made possible through the generosity of Mr. E. B. Dane, of Brookline, Mass. The authors welcome this opportunity to express their appreciation of the careful work necessary to obtain the detail found in the illustrations.

HABIT OF AZURITE FROM TSUMEB

In attempting to classify such a large number of crystals, the futility of strictly defining habit is apparent. The following classification is not exhaustive, but indicates the most important modifications observed.

Habit I. Elongated parallel to the *c* axis.

Type 1. Tabular parallel to *a* (100). Figure 1. Plate I, figure 2.
Dominant—*a* (100).
Prominent—*m* (110), *σ* (101).

" 2. Prismatic. Figure 3. Plate I, figures 4 and 5.
Dominant—*m* (110).

" 3. Elongated pyramidal. Plate I, figure 6.
Dominant—*h* (221), *m* (110).
Prominent—clinodome zone.

Habit II. Essentially equant parallel to *a*, *b*, and *c* axes.

Type 4. Dominant—*m* (110) and striated negative orthodome zone. Plate II, figures 7 and 8.

" 5. Dominant—*m* (110), *c* (001). Figures 10 and 11. Plate II, figure 9.

" 6. Dominant—*m* (110), *a* (100), *σ* (101), *θ* (101), *c* (001). Plate II, figure 12.

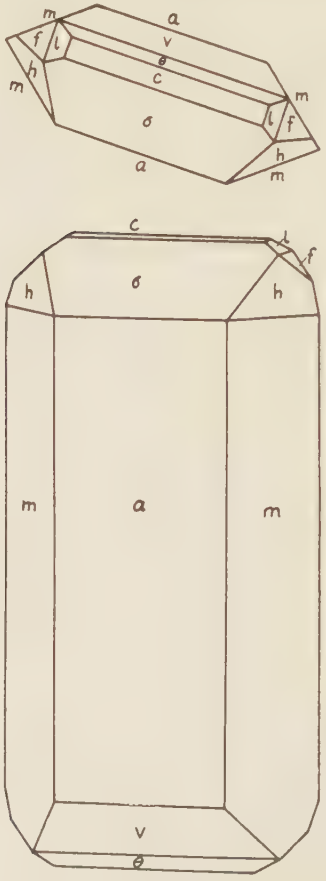

Fig. 1. Azurite. Projections, in Normal Position, of Crystal of Type 1.

Azurite of Type 1.

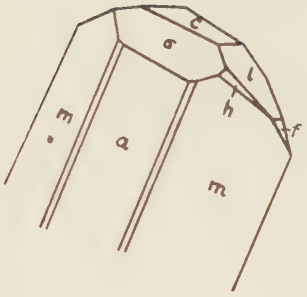

Azurite Transitional between Types 1 and 2

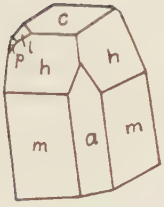

Azurite Transitional between Types 2 and 3.

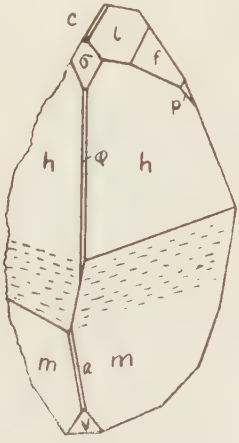

Azurite of Type 3.

PLATE I

FIG. 2

FIG. 4

FIG. 5

FIG. 6

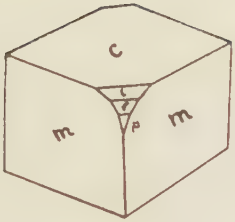

Pseudo-rhombohedral Aspect of One Modification of Type 4.

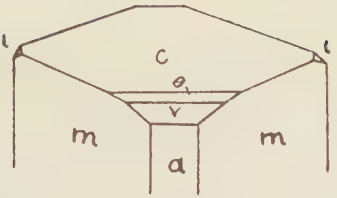

Type 4. Simple Modification Dominated by Base and Prism.

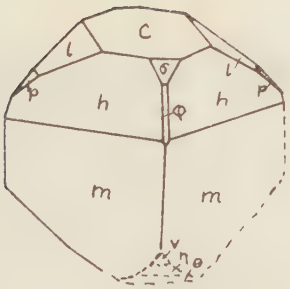

Azurite of Pyramidal Habit.

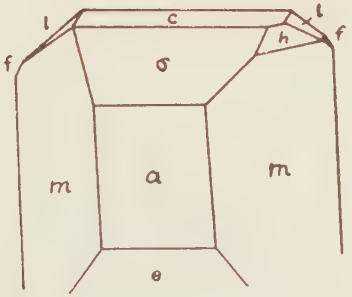

Azurite of Type 6.

FIG. 7

FIG. 8

FIG. 9

FIG. 12

Habit III. Elongated parallel to the *b* axis.

Type 7. Dominant in the orthodome zone—*a* (100). Figures 17 and 18. Plate III, figures 13, 14, 15, and 16.

" 8. Dominant in the orthodome zone—*c* (001). Figure 19. Plate IV, figures 20, 21, and 22.

" 9. Tabular parallel to striated negative orthodome zone approximating μ ($\bar{1}05$) in slope. Figures 23 and 24.

" 10. Plan of orthodome zone essentially equant. Figures 25 and 27. Plate IV, figure 26.

Habit IV. Tabular parallel to *c* (001).

Type 11. Dominant—*c* (001). Figure 28.

" 12. Dominant—*c* (001). Figure 30. Plate IV, figure 29.

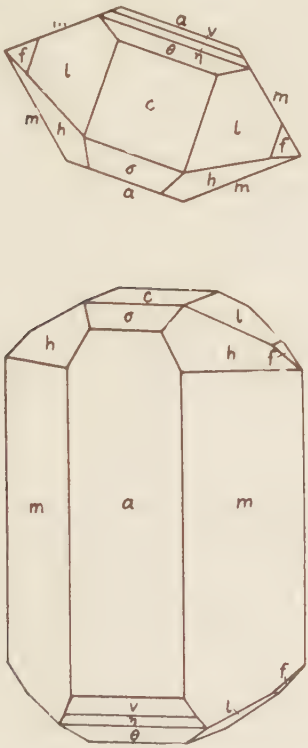

Fig. 3. Orthographic and Clinographic Projections of Azurite Crystal. Transitional between Types 1 and 2.

Habit I. Elongated parallel to the *c* axis.

Type 1. In this type the front pinacoid is dominant, and in the crystals examined *m* (110), *σ* (101), *v* ($\bar{2}01$), and *h* (221) are prominent. All the forms observed on this type are: *a* (100), *m* (110), *σ* (101), *v* ($\bar{2}01$), *θ* ($\bar{1}01$), *c* (001), *h* (221), *l* (023), *f* (011). Figure 1 shows the relative development of the forms. The crystals on specimen 87475 have a maximum size of 1.5×.8×.3 cm, and an individual crystal is illustrated in plate I, figure 2. Other specimens of this type are present in the collection, but no other forms were observed.

Type 2. The representative reproduced in plate I, figure 4, and figure 3 shows the forms: *m* (110), *a* (100), *c* (001), *σ* (101), *v* ($\bar{2}01$), *η* ($\bar{3}02$), *θ* ($\bar{1}01$), *l* (023), *f* (011), *h* (221), *s* (111). In the crystals studied, *a* (100), and *m* (110) dominate, and *c* (001), *l* (023), *σ* (101), and *θ* ($\bar{1}01$) are prominent. The crystal shown on plate I, figure 5, is transitional between types 2 and 3. The steep pyramid *h* (221) is well developed, but the truncation by the base prevents the elongation of type 3.

Type 3. The following list includes the most frequently occurring forms: *m* (110), *c* (001), *φ* (201), *σ* (101), *v* ($\bar{2}01$), *η* ($\bar{3}02$), *θ* ($\bar{1}01$), *l* (023), *f* (011), *p* (021), *h* (221). Other forms observed as small faces are: ($\bar{5}03$), *s* (111), *γ* (121), *P* (223), *k* ($\bar{2}21$), *R* ($\bar{2}41$), ($\bar{7}71$). The steep pyramid ($\bar{7}71$) has previously been reported from Tsumeb by Toborffy.[4] On one crystal measured it occurred as a line face between *R* ($\bar{2}41$) and *m* (110). The unit prism and pyramid *h* (221) are dominant, and the clinodome zone is prominent. The crystal shown on plate I, figure 6, is associated with divergent blades of malachite, and illustrates the zone of oscillation between pyramid and prism. Smaller azurite crystals less than 2 mm. in size are implanted on the malachite. Several large specimens in the collection have a steep slope due to the oscillation between *h* and *m*. Large sub-parallel aggregates are also common.

Habit II. Essentially equant parallel to the *a*, *b*, and *c* axes.

Type 4. Only five crystals of this type were observed. Plate II, figure 7, illustrates the pseudo-rhombohedral character resulting from the equal development of *m* (110) and the striated negative orthodome zone. The clinodome zone is prominent. The crystal shown on plate II, figure 8 is dominated by *m* and *c*

Type 5. Symmetrical representatives are common in the collection. The equant habit of the crystal shown on plate II, figure 9 results from the approximation of the prism angle to a right angle, and the truncation of *h* by the base. Figure 10 shows the dominance of *m* and *c* and the prominent development of *h* (221), *P* (223), *β* ($\bar{3}62$), and the clino and orthodome zones. Figure 11 shows a different modification. The following list includes the forms observed on crystals of this type: *m* (110), *a* (100), *σ* (101), *φ* (201), *θ* ($\bar{1}01$), *v* ($\bar{2}01$), *η* ($\bar{3}02$), *c* (001), *l* (023), *f* (011), *p* (021), *h* (221), *P* (223), *k* ($\bar{2}21$), *e* ($\bar{2}45$), *β* ($\bar{3}62$). Farrington describes crystals of "Pyramidal Habit" corresponding to our crystals of types 3 and 5. He says, "Aside from the one just mentioned (Chessy) and a crystal from Cornwall figured by Zippe, I have found no other figures of azurite where the pyramid *h* predominates. This habit therefore may be considered peculiar to the Arizona azurites."

[4] Toborffy, *Zeit. Kryst.*, **1913**, 52.

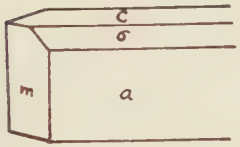

Azurite of Type 7 with Few Forms.

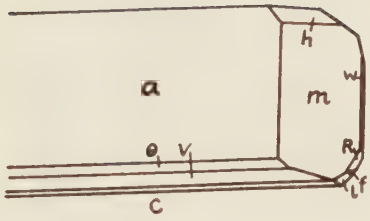

Azurite of Type 7 with Complex Terminations.

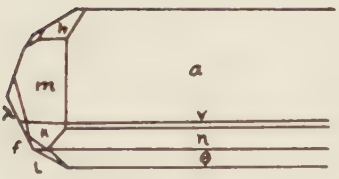

Type 7. **Terminations Dominated by Unit Prism**

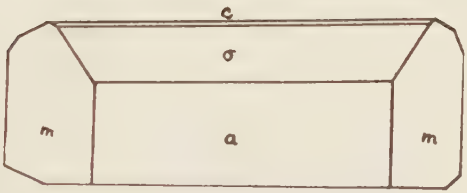

Doubly Terminated Crystal of Type 7.

FIG. 13

FIG. 15

FIG. 16

FIG. 14

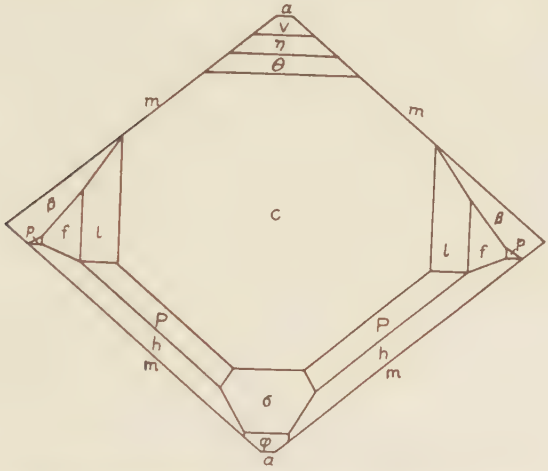

Fig. 10. Orthographic Projection of a Crystal of Type 5.

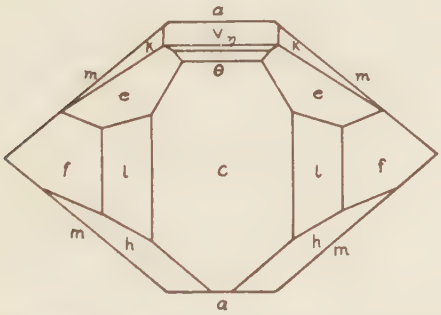

Fig. 11. Orthographic Projection of a Crystal of Type 5 with Enlarged Clinodomes and Negative Pyramids.

Type 6. Plate II, figure 12 illustrates this type in which the front pinacoid is surrounded by a ring of well developed faces. The forms a (100), m (110), σ (101), θ ($\bar{1}01$), and c (001) are dominant, and l (023), f (011), and h (221) are prominent.

Habit III. Elongated parallel to the b axis.

Type 7. These crystals are elongated parallel to the b axis and flattened parallel to the front pinacoid. Many are tabular parallel to the front pinacoid, but crystals in which it is the most prominent face in the orthodome zone are included. The collection contains many excellent representatives and plate III, figures 13, 14, 15 and 16, together with figures 17 and 18 illustrate the important modifications. The unit prism is the dominant truncation, but often the truncating forms are numerous. The forms observed are: a (100), c (001), σ (101), θ ($\bar{1}01$), v ($\bar{2}01$), η (302), m (110), w (120), l (023), f (011), p (021), h (221), P (223), R ($\bar{2}41$).

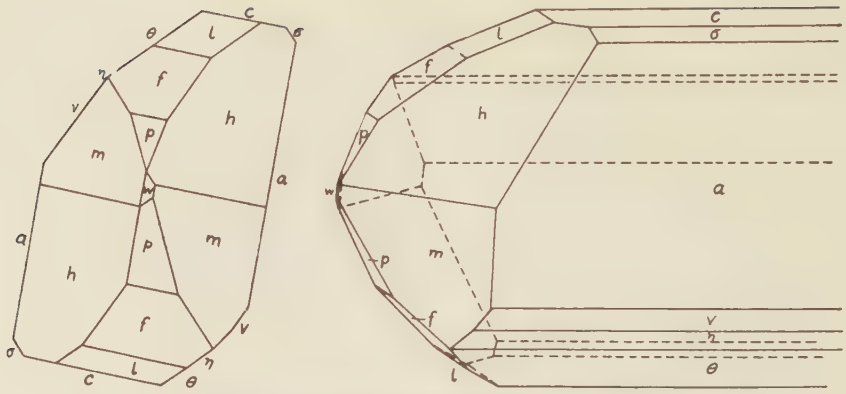

Fig. 17. Orthographic Projection on the Side Pinacoid, and Clinographic Projection in Normal Position, of Crystal of Azurite.

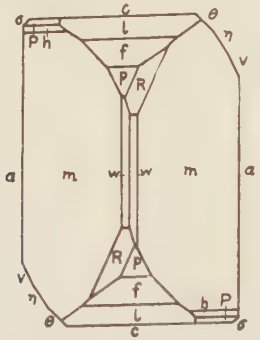

Fig. 18. Type 7. Orthographic Projection, on the Side Pinacoid, of Azurite Crystal Shown in Figure 16.

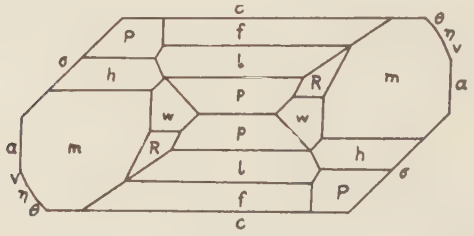

Fig. 19. Type 8. Orthographic Projection, on the Side Pinacoid, of Crystal Shown in Figure 20.

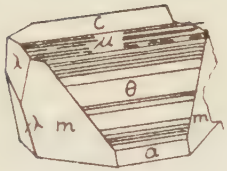

Type 8. Dominated by λ.

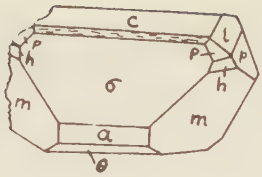

Type 8. Clinodome Dominant.

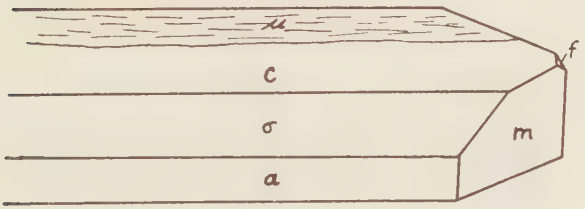

Crystal tabular parallel to c and μ.

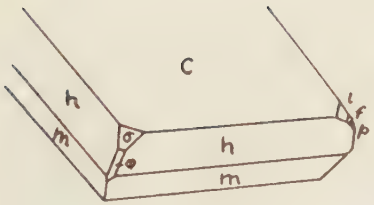

Type 12. Compare with Figs. 5, 6 and 9.

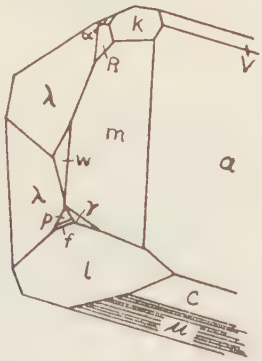

Type 10. See Figure 25.

Plate IV

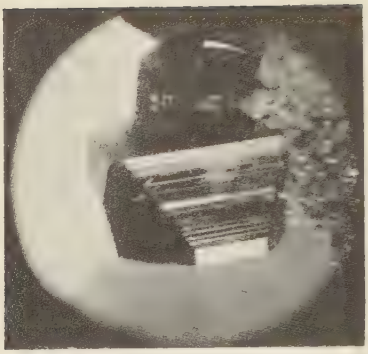

Fig. 21

Fig. 20

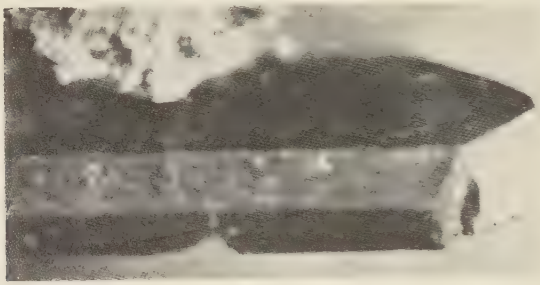

Fig. 22

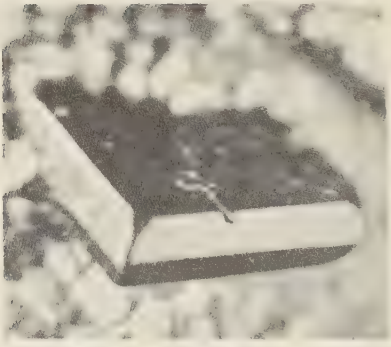

Fig. 29

Fig. 26

Type 8. The crystals are elongated parallel to the b axis with c (001) dominant in the orthodome zone. Many of the crystals are tabular parallel to the base. Figure 19 is a plan of the crystal shown on plate IV, figure 20. In this modification σ (101) and a (100) are prominent in the orthodome zone, and m (110) and the clinodome zone are the prominent truncations. Plate IV, figure 21 shows a simpler modification with m (110) and λ ($\bar{2}$.18.3) the prominent truncations. Plate IV, figure 22 illustrates a mode flattened parallel to the base and truncated by the unit prism. The following forms were observed: c (001), a (100), σ (101), θ ($\bar{1}01$), v ($2\bar{0}1$), η ($\bar{3}02$), μ ($\bar{1}05$), m (110), w (120), l (023), f (011), p (021), h (221), P (223), R ($\bar{2}41$), λ ($\bar{2}$.18.3)

Type 9. These crystals are tabular parallel to the negative striated orthodome zone. The resultant slope of this striated zone approximates μ ($\bar{1}05$) and is conspicuous for the small angle made with the base. In appearance this type is similar to the previous one, but the striations on the large face makes it easy to identify. The truncations are usually not complex and may be grouped as two modifications. One in which the unit prism is the dominant truncation and the other dominated by the flat pyramid λ ($\bar{2}$.18.3). Figure 23 illustrates a crystal with m as the dominant truncation. Figure 24 illustrates a modification in which the prism and clinodome form a frame for λ. The following forms were observed: a (100), c (001), σ (101), θ ($\bar{1}01$), v ($2\bar{0}1$), η ($\bar{3}02$), μ ($\bar{1}05$), m (110), l (023), p (021), d ($\bar{2}43$), e ($\bar{2}45$).

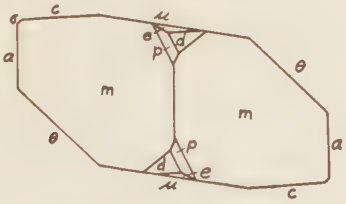

Fig. 23. Orthographic Projection, on the Side Pinacoid, of a Crystal of Type 9 with m(110) Dominant.

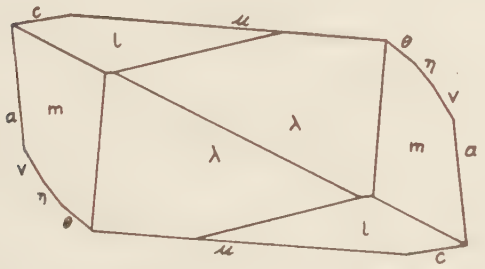

Fig. 24. Orthographic Projection, on the Side Pinacoid, of a Crystal of Type 9 with λ($\bar{2}$.18.11) Dominant.

Type 10. These crystals have a stocky appearance due to the equant plan of the orthodome zone. Figure 25 is drawn from a crystal from a large vug, and plate IV, figure 26 illustrates the terminations of another such crystal. The crystals are of desirable size for measurement, and faces unusually clean-cut and brilliant. Eight were measured and included in the average used in determining the axial ratio. Figure 25 shows the prominence of m, and λ as truncations. The zone of the three positive pyramids shown is typical and useful in orienting unmeasured crystals. The following forms were observed: a (100), c (001), σ (101), θ ($\bar{1}01$), v ($20\bar{1}$), η ($30\bar{2}$), μ ($\bar{1}05$), l (023), f (011), p (021), m (110), w (120), h (221), s (111), P (223), γ (121), k ($\bar{2}21$), R ($\bar{2}41$), α ($\bar{1}21$), λ ($\bar{2}.18.3$).

Figure 27 illustrates a modification in which the plan of the orthodome zone is similar to the one just described, but with λ as the only important termination. Crystals were observed in the collection where this pyramid was the only termination. The flat slope is very distinctive. In another modification λ is surrounded by a ring of narrow faces, as shown in figure 33. Forms observed on this mode are: a (100), c (001), σ (101), θ ($\bar{1}01$), v ($\bar{2}01$), η ($\bar{3}02$), c ($\bar{3}.0.10$), F ($\bar{2}07$), l (023), p (021), m (110), h (221), d ($\bar{2}43$), e ($\bar{2}45$).

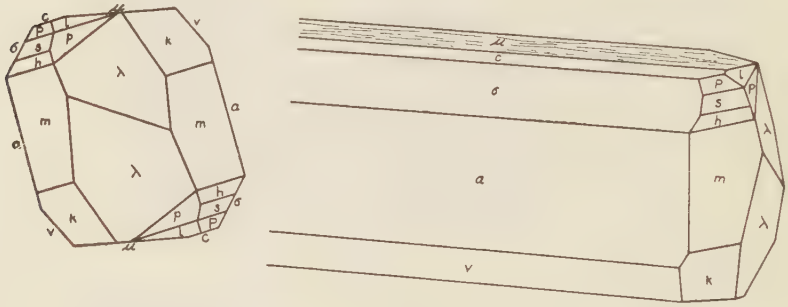

Fig. 25. Type 10. Orthographic Projection, on the Side Pinacoid, and Clinographic Projection in Normal Position, of Azurite Crystal. A very Common Habit.

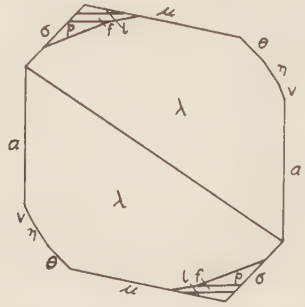

Fig. 27. Type 10. Orthographic Projection, on the Side Pinacoid, of a Crystal of Type 10.

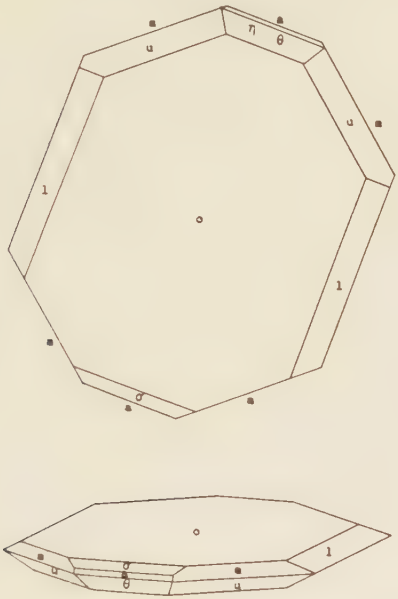

Fig. 28. Type 11. Orthographic and Clinographic Projections of a Crystal of Type 11.

Habit IV. Tabular parallel to *c* (001).

Type 11. The thin, platy crystals of this type were found on only three specimens. Figure 28 shows the development of forms. The clinodomes come to a sharp edge on the crystals from two specimens. On one the crystals have the side pinacoid present as a dull face, having more the appearance of being due to solution than to growth. This type is the only one on which the side pinacoid was observed. The equally developed ring of faces around the base is characteristic. The following forms were observed: *c* (001), *a* (100), *m* (110), *σ* (101), *θ* (Ī01), *η* (3̄02), *l* (023), *u* (2̄23), *b* (010).

Type 12. These crystals are tabular parallel to the base, and the plan is dominated by the unit prism. Plate IV, figure 29, shows one of the crystals with *c* dominant, *m* and *h* prominent, and *σ* (101), *φ* (201), *l* (023), *f* (011), *p* (021) and λ (2̄.18.3) present. Crystals with the modification illustrated in figure 30 are distinguished by the grouping of faces around the *b* axis. The forms observed are: *c* (001), *a* (100), *σ* (101), *θ* (Ī01), *η* (3̄02), *m* (110), *w* (120), *l* (023), *f* (011), *p* (021), *h* (221), *k* (2̄21), *R* (2̄41).

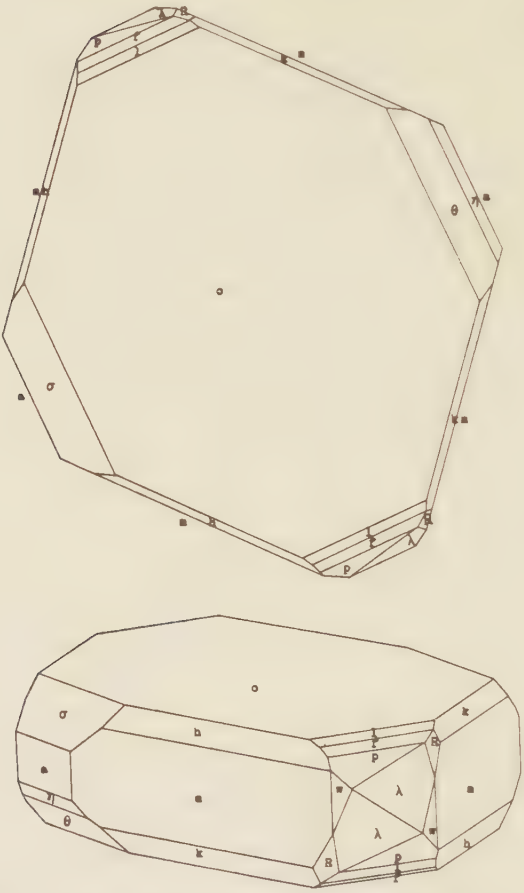

Fig. 30. Type 11. Orthographic and Clinographic Projections. The Clinographic Projection is Turned 20° from the *b* axis.

DISCUSSION OF FORMS OBSERVED ON TSUMEB AZURITE

A gnomonic projection, on the side pinacoid, of the forms observed on azurite from Tsumeb is reproduced in figure 40. The strong zonal relations are well shown. The poles of the common forms fall on important points in the network. The pyramid λ ($\bar{2}$.18.3) is an exception to this rule. The following table shows graphically the forms observed on each type together with the relative development of the form. The last column sums the number of types in which each form occurs.

COMBINATION TABLE OF AZURITE FORMS FROM TSUMEB

Letter	Symbol (001)	Symbol (010)	Habit I			Habit II			Habit III				Habit IV		No. of types in which form occurs.
			Type 1	Type 2	Type 3	Type 4	Type 5	Type 6	Type 7	Type 8	Type 9	Type 10	Type 11	Type 12	
a	(100)	(010)	x	x			–	x	x	x	x	x	–	x	10
c	(001)	(100)	–	x	–	x	x	x	x	x	x	x	x	x	12
b	(010)	(001)											–		1
m	(110)	(011)	x	x	x	x	x	x	x	x	x	x	–	x	12
w	(120)	(012)							–	–		–		–	4
σ	(101)	(110)	x	x	–		–	x	–	x	–	x	–	x	11
φ	(201)	(120)			–		–							–	13
θ	(1̄01)	(1̄10)	–	–	–		–	x	–	–	–	–	–	–	11
v	(2̄01)	(1̄20)	x	–	–		–		–	–	–	–			8
η	(3̄02)	(2̄30)		–	–		–		–	–	–	–	–	–	8
μ	(1̄05)	(5̄10)									x	x			2
f	(011)	(101)	–	–	–	–	x	–	x	x		–		–	10
l	(023)	(302)	–	x	x	–	x	–	x	x	x	–	x	–	12
p	(021)	(102)			–	–	–		x	x	–	–		–	8
h	(221)	(122)	–	–	x		x	–	–	–		–		–	9
s	(111)	(111)		–	–							–			3
P	(223)	(322)			–		–		–	–		–			5
γ	(121)	(112)			–							–			2
k	(2̄21)	(1̄22)			–		–					–		–	4
α	(1̄21)	(1̄12)										–			1
R	(2̄41)	(1̄24)			–				–	–		–		–	5
e	(2̄45)	(5̄24)					x				–				2
d	(2̄43)	(3̄24)									–				1
u	(2̄23)	(3̄22)											x		1
β	(3̄62)	(2̄36)					–								1
λ	(2̄·18·3)	(3̄·2·18)								x	x	x		x	4

Legend:
x = Form present as a well developed face.
– = " " " " small face.

The numbers in the last column in the above table give a rough idea of the importance of the different forms.

c (001) was observed on every crystal examined. In habits tabular to it the base is present as a large square or rectangular face. In other cases it is usually present as a linear face. It is always brilliant but often gives double or multiple reflections.

m (110) was invariably present—usually with large faces. The signals normally yielded were single and strong and the angular variation found was slight.

w (120) is usually present as a small face on crystals of habit III. In crystals similar to the one shown in figure 18 it forms a long narrow truncation of the unit prism. It is more often present as a small triangle as illustrated in figure 19.

a (100) is usually present, either as a broad face or a long rectangle.

b (010) was only observed on one crystal, and then as a small, dull, line face. It may be considered an exceptional occurrence on azurite from Tsumeb. The recognition of the almost universal presence of the front and absence of side pinacoid is useful in orienting crystals for measurement.

σ (101) is nearly always present, although often as a small face. The face is brilliant and yields a good reflection.

ϕ (201) is the only other positive orthodome observed, and it is not common. It occurs usually as a long narrow face truncating the edge between the faces of h (221), and narrowing to a point upon meeting a (100) or m (110). See plate II, figure 9, and plate V, figure 29.

The negative orthodomes θ ($\bar{1}01$), η ($\bar{3}02$), v ($\bar{2}01$) usually occur together and in relatively equal development. Considering all the crystals observed the unit form is the best developed. Reference to the figures shows nearly all the crystals of habit III characterized by the presence of these three faces between the front pinacoid and base. The small angle between these faces is easily recognized.

The crystals of habit III usually have a striated negative orthodome face making a small angle with the base. This zone gives a long line of signals, and the signal corresponding to the average slope is that of μ ($\bar{1}05$). In drawing the crystals the pole of this face is used to represent this zone.

The clinodomes l (023), f (011), and p (021) are present on most of the types. The three faces usually occur together. l (023) was observed on all the types, f (011) on ten, and p (021) on eight. l (023) is ordinarily the largest face of the three. p (021) is characterized by its wedge shape due to the steep slope at which it bevels the other forms. See figures 5, 6, and 9.

The three positive pyramids h (221), s (111), and P (223) form a characteristic zone with base and unit prism in crystals of type 10. See figure 25.

h (221) is present on nine of the types and largely developed in two. The most striking crystals observed are of type 3 where it dominates, resulting in an extremely elongated habit parallel to the c axis. The face is always clean-cut and sharp and gives an excellent signal.

s (111), and P (223) are usually present as rectangular faces in zone with h (221).

γ(121) is not common and occurs only as a small face. See figure 26.

k ($\bar{2}21$) was observed on crystals of four types. The face is usually small, but gives a good reflection.

λ ($\bar{2}.18.3$) is commonly developed with large brilliant faces. It occurs in only four types, but a large proportion of the crystals in the collection belong to habit III, and the importance of this form is, therefore, greater than would be indicated by the table. It commonly is the largest truncating face, and occasionally is the only one present. See figures 21, 24, 25, 26, and 30. The signal given is excellent and undoubtedly the indices are correct.

R ($\bar{2}41$) is present as a small face on crystals of five types.

e ($\bar{2}45$) was observed on only two crystals. On the crystal illustrated in figure 11 it is present as a large striated face.

The negative pyramids d ($\bar{2}43$), u ($\bar{2}23$), β($\bar{3}62$) were observed only once as small faces.

FIG. 31. Unaltered and Completely Altered Azurite in Contact.

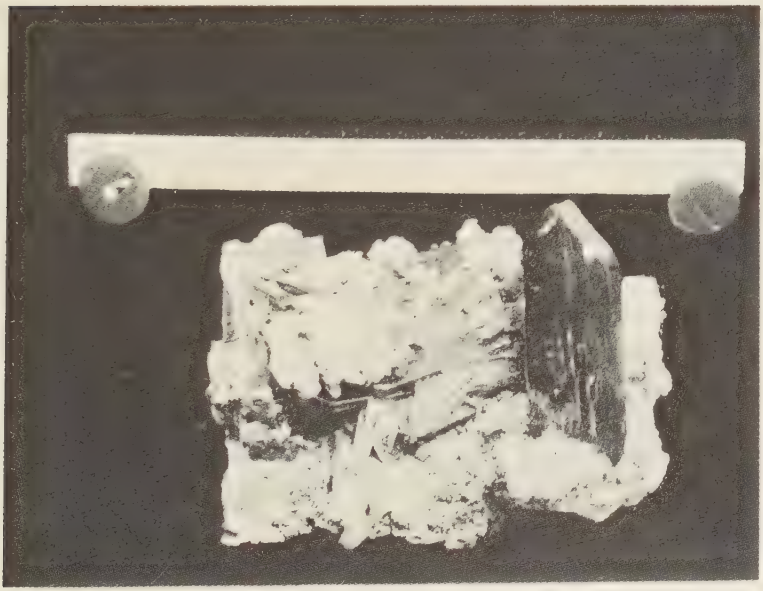

FIG. 32. Large Azurite Crystal of Type 8 with Bayldonite.

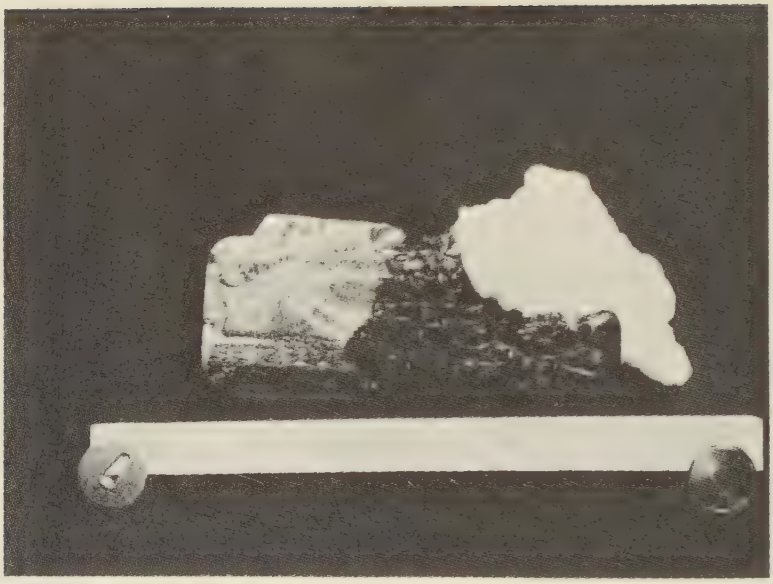

FIG. 34

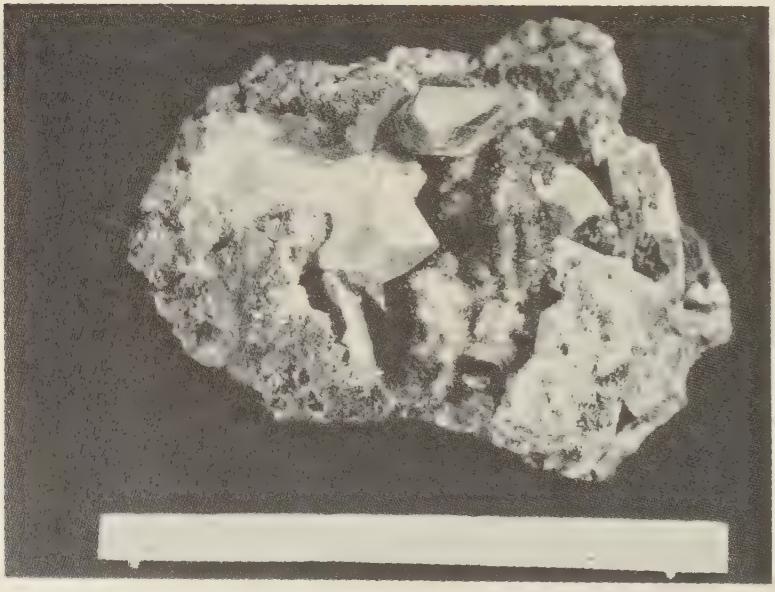

FIG. 35

Azurite Altering to Malachite

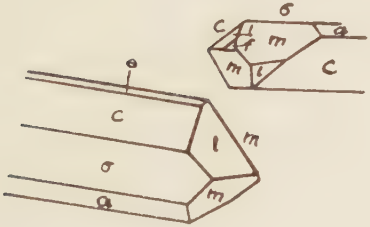

Pseudomorph Group of Malachite after Azurite.

MALACHITE PSEUDOMORPHS AFTER AZURITE

Among the very numerous specimens in the collection of malachite pseudomorphs after azurite a large part retain their original outline so perfectly that the forms can be identified with certainty. On some hand specimens a single generation of azurite crystals has been partly changed to malachite with an abrupt boundary between the fresh and altered material. This condition is illustrated in plate V, figure 31. A few crystals of azurite on the right are unaltered and show absolutely no signs even of etching. All the other crystals have been replaced by malachite. The crystals are completely interlocking where attached to the matrix, and at the contact between azurite and malachite pseudomorphs, a few crystals are partially altered. The alteration has the appearance of starting at some center and progressively attacking fresh azurite, completely converting each crystal to malachite and spreading to the next at the point of contact.

Plate VI, figure 34, illustrates a partially altered crystal. The malachite fibers radiate from one important center on the front pinacoid, and many interfering centers on the prism, giving a confused network of interwoven, splendant fibers. The front of the invading malachite is roughly concentric normal to the fibers. Several darker colored bands in the malachite may be seen surrounding the center of radiation. In this specimen the contact is uneven with many individual malachite fibers penetrating beyond the common front.

The pseudomorph group shown on plate VI, figure 35, is attached to limestone containing a network of small veinlets of azurite and malachite. The drusy surface is covered with needlelike crystals of smithsonite, stained brown at the tips. The small size of the radiating group of malachite fibers can be dimly seen, but no picture could do justice to the delicate coloring and velvety texture.

The largest pseudomorph in the collection is shown on plate VII, figure 36. Several individuals in parallel position form the complete crystal, $10\times10\times5$ cm. in size, but the prism and pinacoid faces form practically a continuous surface. Comparison with plate VII, figure 37, illustrates the coarser, sheaf-like arrangement of the fibers.

The specimen from Bisbee illustrated on the frontispiece is a large malachite pseudomorph partially covered by parallel azurite

crystals orientated to the original azurite axes. Similar examples were observed from Tsumeb. In some cases the azurite completely surrounds the malachite core. Figure 33 illustrates an example where the azurite wraps around the malachite pseudomorph without completely covering it. Apparently the pseudomorphs retain a structure adequate to control the orientation of later azurite deposited on their surface. The sequence of deposition of azurite, alteration to malachite, and later crystallization of azurite, indicates a delicate balance in the equilibrium relations.

The type of progressive alteration thus described for the figured specimens seems to be universal in the collection. A radiating fibrous or bladed structure of the invading malachite is the normal product of the change.

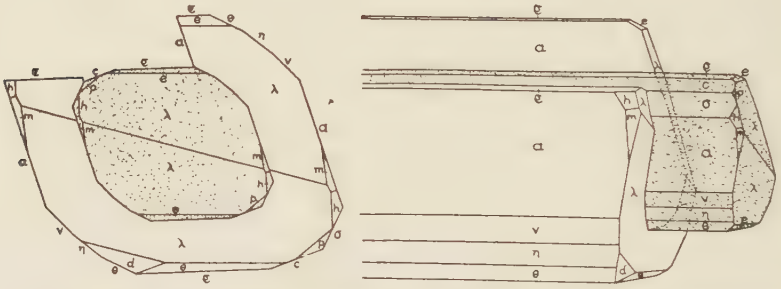

Fig. 33. Orthographic and Clinographic Projection of a Malachite Pseudomorph of Type 10 Partially Surrounded by a later Azurite Crystal in Parallel Position.

HABIT OF AZURITE FROM OTHER LOCALITIES AND FORMS OBSERVED

Azurite from Laurium, Greece

The crystals of the one specimen examined were elongated in the direction of the *b* axis, and tabular parallel to θ $(\bar{1}01)$. The habit is similar to that of crystals described by Zimányi[5] from this locality.

The following combination table shows the forms observed on the five crystals measured. (See figure 38.)

[5] K. Zimányi, *Zeit. Kryst.*, **21**, p. 86. 1882. The orthogonal projection shown in Fig. 22, Taf. V, of his paper illustrates the type observed on our crystals. This plan is reproduced in Goldschmidt's Atlas, Band V, Tafel 68, Figure 232

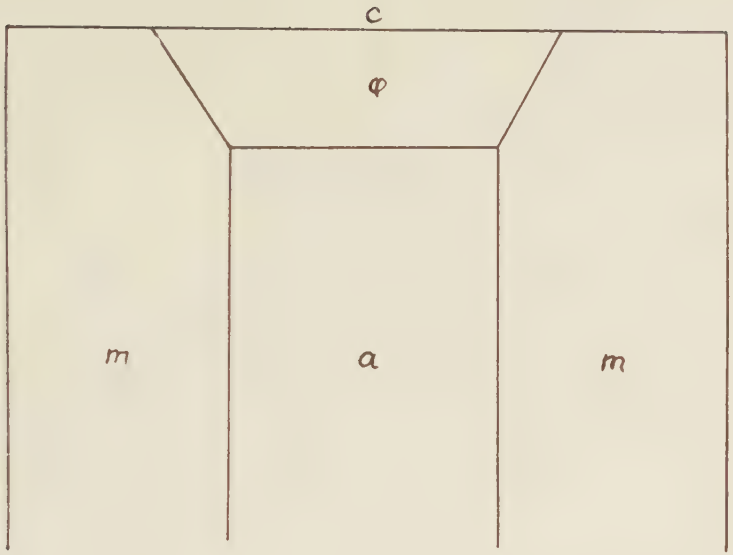

Large Pseudomorph of Malachite after Azurite.

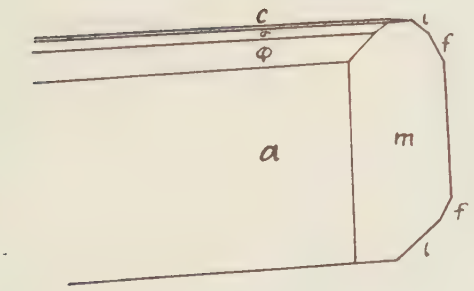

FIG. 36

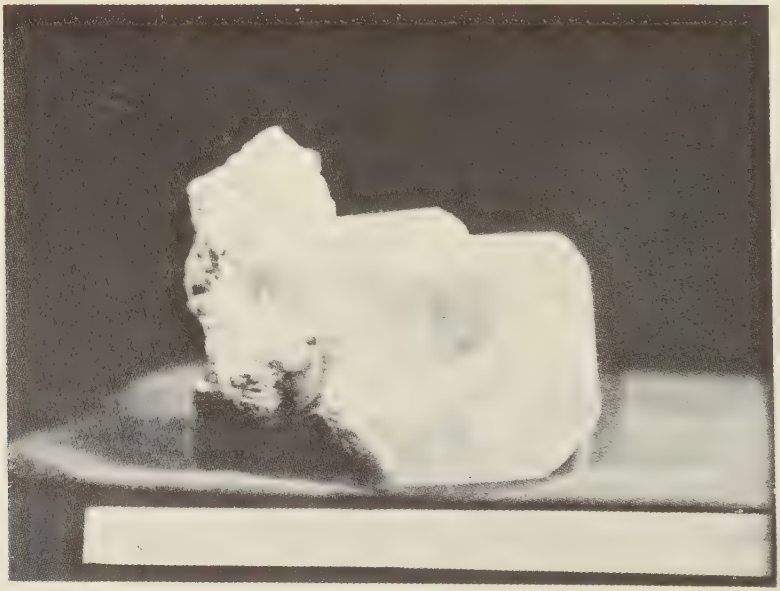

FIG. 37

Form	Number of crystal				
	1	2	3	4	5
c (001)	x	x	x	x	x
a (100)	x	x	x	x	x
σ (101)	x				x
v (201)	x	x	x	x	x
θ ($\bar{1}$01)	x	x	x	x	x
n ($\bar{1}$02)			x	x	x
D ($\bar{1}$04)				x	
($\bar{7}$.0.15)		x		x	
ψ (301)				x	x
($\bar{1}\bar{1}$.0.13)		x			
($\bar{4}$.0.11)	x			x	
A ($\bar{1}$03)		x			
($\bar{4}$.0.13)			x		
m (110)	x	x	x	x	x
h (221)	x	x	x	x	x
k ($\bar{2}$21)	x	x			x
x ($\bar{1}$11)		x	x	x	x
d ($\bar{2}$43)	x	x	x	x	x
e ($\bar{2}$45)	x	x	x	x	x
ρ ($\bar{1}$34)		x	x		x
R ($\bar{2}$41)	x		x	x	x
P (223)			x	x	x
s (111)	x		x	x	x
l (023)	x	x	x	x	x
f (011)	x	x	x	x	x
p (021)	x	x	x	x	x
ω (124)					x
*ƒ (6.10.1)				x	x
*r ($\bar{3}$.5.7) ($\bar{5}$73)				x	x
*ℜ (564)					x
*𝔇(453)					x
*π (123) (231)					x
*u ($\bar{1}$35) ($\bar{3}$51)				x	
*t (315) (153)				x	
*ȝ (728) (287)				x	
*Ω (301)					x

* New forms

The table on page 116 gives the average measured angles. New forms:

ƒ (6.10.1) was observed on two crystal . It forms a triangular face between *m* (110) and *p* (021), and gives a sharp signal. It is also found on Kelly crystals.

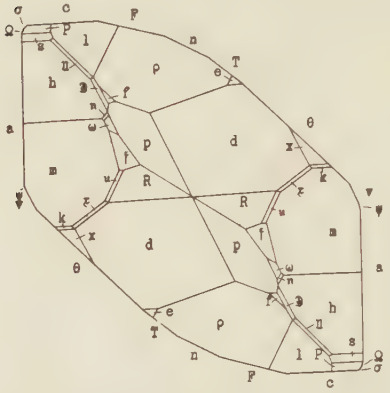

Fig. 38. Orthographic Projection, on the Side Pinacoid, of an Azurite Crystal from Laurium, Greece.

		ϕ	ρ
f (6.10.1)	Measured	9°03′	36°11′
		9 04	35 56
	Average	9 04	36 03
	Calculated	9 06	35 34
	Δ	0 02	0 29

r ($\bar{5}73$) is present on two crystals as a narrow line face between, and in zone with, *m* (110) and *d* ($\bar{2}43$). The signal was faint and difficult to center accurately.

		ϕ	ρ
r ($\bar{5}73$)	Measured	$\bar{3}2°$—′	43°20′
		$\bar{3}1$	43 10
	Average	$\bar{3}1$ 30	43 15
	Calculated	$\bar{3}0$ 46	43 27
	Δ	0 44	0 12

$\mathfrak{N}$ (564) occurs as a line face between *l* (023) and *h* (221) and is in zone with them.

		ϕ	ρ
7 (564)	Measured	36°56′	51°48′
		37 —	51 18
	Average	37 —	51 33
	Calculated	36 51	51 29
	Δ	0 09	0 04

$\mathfrak{D}$ (453) is also a line face and is in zone with *h* (221) and *f* (011).

		ϕ	ρ
$\mathfrak{D}$ (453)	Measured	37°—′	49°30′
		36 —	49 24
	Average	36 30	49 27
	Calculated	35 07	49 41
	Δ	1 23	0 14

$\mathfrak{n}$ (231) was observed as a narrow face between h (221) and ω (241), and it is definitely in zone with these two.

		ϕ	ρ
$\mathfrak{n}$ (231)	Measured	24°48′	41°00′
		25 10	41 30
	Average	24 55	41 15
	Calculated	25 22	41 20
	Δ	0 27	0 05

$\mathfrak{u}$ ($\bar{3}\bar{5}1$) was observed only once as a line face between R ($\bar{2}41$) and m (110).

	φ	ρ
Measured	17°39′	36°15′
Calculated	$\bar{1}8$ 06	36 03
Δ	0 27	0 12

$\mathfrak{t}$ (153) was only observed once.

	ϕ	ρ
Measured	68°06′	37°05′
Calculated	68 51	36 02
Δ	0 45	1 03

$\mathfrak{z}$ (287). A line face between h (221) and f (011) gave a dim signal.

	ϕ	ρ
Measured	72°16′	46°40′
Calculated	72 21	46 14
Δ	0 55	0 26

Ω (301) was observed twice as a line face on crystal 5.

		ϕ	ρ
	Measured	18°32′	90°00′
		19 00	90 00
	Average	18 44	90 00
	Calculated	17 39	90 00
	Δ	1 05	0 00

Azurite from Kelly, New Mexico

The crystals studied from this locality are of four distinct types. The numbering will follow the scheme employed for the Tsumeb crystals to avoid confusion.

Habit I. Elongated parallel to the *c* axis.

Type 2. Prismatic.
Dominant—*m* (110).
Prominent—*a* (100), *c* (001), *σ* (101).

Type 3. Elongated pyramidal.
Dominant—*m* (110), *h* (221).
Prominent—*c* (001), *σ* (110).

Habit III. Elongated parallel to the *b* axis.

Type 9. Tabular parallel to the negative orthodome zone.
Prominent in orthodome zone—*v* ($\bar{2}01$), *η* ($\bar{3}02$), *θ* ($\bar{1}01$), *n* ($\bar{1}02$), *a*(100), *c*(001).
Dominant truncation—*m* (110), *ρ* ($\bar{1}34$).
Prominent truncation—*h* (221), *d* ($\bar{2}43$).

Type 10. Plan of orthodome zone essentially equant.
Prominent in orthodome zone—*a* (100), *c* (001), *σ* (101).
Prominent truncations—*m* (110), *d* ($\bar{2}43$), clinodome zone.

The table on page 117 gives the average angles for the forms measured. The following combination table shows the forms observed on the different types.

COMBINATION TABLE OF FORMS ON AZURITE FROM KELLY, N. M.

Letter	Miller Symbol (001)	Habit I			Habit III		
		Type 2	Type 3		Type 9		Type 10
		Crystal 1	2	3	4	5	6
c	(001)	x	x	x	x	x	x
a	(100)	x	x	x	x	x	x
b	(010)	x					x
σ	(101)	x	x	x	x		x
θ	($\bar{1}$01)	x	x	x	x	x	x
η	(3̄02)		x		x		x
v	(2̄01)		x	x	x	x	x
n	($\bar{1}$02)			x	x		
α	(2̄05)	x				x	
A	($\bar{1}$03)						x
ψ	(3̄01)		x				
F	(2̄07)		x				
T	(4̄05)				x		
	(5̄03)	x			x		
	(4̄.0.13)						x
	($\bar{1}\bar{1}$.0.13)					x	x
	(3̄.0.10)					x	
m	(110)	x		x	x	x	x
w	(210)	x		x		x	
l	(023)	x		x	x	x	x
f	(011)	x		x	x	x	x
p	(021)	x	x	x	x	x	x
h	(221)	x	x	x	x	x	x
s	(111)	x	x	x	x	x	x
P	(223)	x	x	x	x	x	x
γ	(121)		x	x	x	x	x
ω	(241)			x	x	x	x
k	(2̄21)			x	x	x	
ρ	($\bar{1}$34)	x	x		x	x	x
R	(2̄41)		x	x	x	x	x
d	(2̄43)	x	x	x	x	x	x
e	(2̄45)	x	x	x	x	x	x
u	(2̄23)			x		x	
p	(112)		x				
f	(6.10.1)			x			
j	(4̄76)			x			
h	(2̄73)			x			
l	(743)				x	x	
m	(5̄25)				x	x	
c	(4̄.10.1)					x	
q	(212)						x
δ	(243)		x		x	x	

New forms:

$\mathfrak{p}$ (112). This form was observed as a line face in zone between c (001) and P (223). The signal was not sharp but could be read to the nearest degree.

	ϕ	ρ
Measured	61° —′	69° —′
Calculated	60 48	68 54
Δ	0 12	0 06

$\mathfrak{f}$ (6.10.1) occurred on crystal 3 giving a poor but definite signal. This form was first observed on Laurium crystals.

Measured	9° 18′	35° 57′
Calculated	9 06	35 34
Δ	0 12	0 23

$\mathfrak{j}$ ($\bar{4}76$) also a line face giving a fair signal.

	ϕ	ρ
Measured	$\overline{57}$° 08′	49° 34′
Calculated	$\overline{57}$ 06	49 06
Δ	0 02	0 28

$\mathfrak{h}$ ($\bar{2}73$) was observed as a small face on crystal 3.

	ϕ	ρ
Measured	$\overline{\overline{57}}$° 08′	30° 20′
Calculated	$\overline{57}$ 06	29 20
Δ	0 02	1 00

I (743) is present as a large etch face on crystal 4. The signal was blurred but the second reading below was centered on a discernible signal.

	ϕ	ρ
Measured	23° 30′	65° —′
	23 09	65 26
	21 52	65 —
Average	22 50	65 08
Calculated	22 53	65 22
Δ	0 03	0 14

$\mathfrak{w}$ ($\bar{5}25$) forms well developed faces between d ($2\bar{4}3$) and θ ($\bar{1}01$) on crystals 4 and 5. The signals were good.

	ϕ	ρ
Measured	$\overline{45}$° 12′	75° 53′
	$\overline{45}$ 14	76 00
	$\overline{45}$ 07	75 54
Average	$\overline{45}$ 12	75 56
Calculated	$\overline{45}$ 15	75 55
Δ	0 03	0 01

c ($\bar{4}$.10.1) was present on crystal 5 as a good face giving a fair signal. It was also observed on Bisbee crystals.

	ϕ	ρ
Measured	$\bar{1}3°$ 36′	25° 33′
Calculated	$\bar{1}3$ 44	25 08
Δ	0 08	0 05

q (212) This form was present as two good faces on crystal 6, lying in zone between σ (101) and s (111). It is also present on Bisbee crystals.

	ϕ	ρ
Measured	42° 41′	78° 20′
	42 55	73 24
Average	42 48	73 22
Calculated	42 55	73 15
Δ	0 07	0 07

Azurite from Bisbee, Arizona

The crystals observed on six hand specimens studied belong to two types:

Habit III. Elongated parallel to the *b* axis.

Type 9. Flattened parallel to negative orthodome zone.

Prominent in orthodome zone—v ($\bar{2}01$), η ($\bar{3}02$), θ ($\bar{1}01$).

These crystals were taken from the deeper workings of the Copper Queen Mine in 1909 and reach a length of 5 cm. with greatest diameter of 2 cm. They are implanted as a secondary growth in parallel position upon well formed pseudomorphs of malachite after azurite of even larger dimensions, the largest pseudomorph having a length parallel to the *b* axis of 7 cm. These characteristics are illustrated in the specimen shown on the colored plate. The azurite crystals are of magnificent blue color on the exterior but for the most part, when broken through, a green malachite center is visible which indicates that the second generation of azurite is also in process of alteration to malachite. Some of the crystals present both terminations with reference to the *b* axis and the quality of the faces except in the orthodome zone, which is somewhat striated, is of the best.

Three crystals were measured and the presence of the following forms shown in figure 39 in average development, was established.

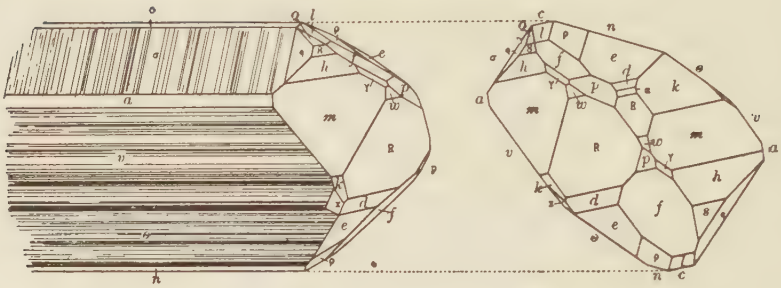

Fig. 39. Clinographic and Orthographic Projections, on the Side Pinacoid, of Azurite from Bisbee, Arizona.

c (001), *a* (100), *m* (110), *w* (120), *l* (023), *f* (011), *p* (021), *σ* (101), *μ* (105), *A* (103), *n* (102), *θ* (101), *h* (221), *s* (111), *P* (223), *k* (221), q (212), *R* (241), *ρ* (134), *d* (243), *e* (245), *γ* (121), *α* (121).

Habit V. Tabular parallel to *σ* (101).

Dominant—*σ* (101)

Prominent—*m* (110), *h* (221), *l* (023), *f* (010), p (021).

Crystals of this habit occur as reticulated plates on a specimen from the Czar mine. The following forms were identified: *c* (001), *a* (100), *σ* (101), *v* (201), *θ* (101), *m* (110), *l* (023), *f* (011), *p* (021), *h* (221), *P* (223), *k* (221), *R* (241), *e* (245).

New forms:

q (212). This form, which was also identified on the Kelly crystals, occurs as a large face between *σ* (101) and *f* (011).

	φ	*ρ*
Measured	43° 23′	73° 28′
	43 06	73 16
	42 53	73 31
	42 51	73 09
Average	42 33	73 23
Calculated	42 55	73 15
Δ	0 22	0 08

i (681) occurs as a line face between *R* (241) and *m* (110) and is in zone with them.

	φ	*ρ*
Measured	9° 37′	41° 20′
	10 44	40 —
	10 44	40 30
Average	10 22	40 37
Calculated	9 13	41 25
Δ	1 09	0 48

c (4.10.1) was identified on one crystal as a small face. It was first observed on Kelly specimens.

	ϕ	ρ
Measured	$\bar{1}3°$ 07′	24° 10′
Calculated	$\bar{1}3$ 44	25 24
Δ	0 37	1 14

Azurite from Barnaul, Siberia

Etched azurite crystals associated with malachite coatings are found in cavities of a quartz vein. The crystals are elongated parallel to the orthodome zone and tabular parallel to θ $(\bar{1}01)$.

Habit III. Elongated parallel to the *b* axis.

Type 9. Tabular parallel to θ $(\bar{1}01)$.

Dominant in orthodome zone—θ $(\bar{1}01)$.

Prominent in orthodome zone—a (100) and σ (101).

Prominent truncations—m (110), h (221), p (021).

The faces of the orthodome zone are only slightly etched but the truncating forms are badly pitted and it was often necessary to use alcohol to obtain a signal. The side pinacoid is always present as a rather large rectangular face.

Azurite from Copiapó, Chile

One hand specimen had small needle-like crystals of azurite forming a drusy coating. They are elongated parallel to the *b* axis and tabular parallel to the negative striated orthodome zone. The following forms were observed:

c (001), a (100), σ (101), v $(\bar{2}01)$, θ $(\bar{1}01)$, m (110), l (023), p (021), h (221), s (111), R $(\bar{2}\bar{4}1)$, and e $(\bar{2}45)$.

Azurite from Chessy, France

The crystals from this locality that were quite perfect and used to check the axial ratio are elongated parallel to the *b* axis and tabular parallel to the base.

Habit III. Elongated parallel to the *b* axis.

Type 8. Tabular parallel to c (001).

Dominant in the orthodome zone—c (001).

Prominent in the orthodome zone—v (201), θ $(\bar{1}01)$.

Prominent truncations—m (110), x (111).

The front pinacoid is absent and the sharp angle between negative orthodomes and the base gives a thin wedge-like appearance. The following forms were also observed: f (011), p (021), h (221), R $(\bar{2}41)$, e $(\bar{2}45)$.

HOLDENITE, A NEW ARSENATE OF MANGANESE AND ZINC, FROM FRANKLIN, NEW JERSEY

CHARLES PALACHE AND E. V. SHANNON[1].

The single specimen on which the mineral here described has been seen was found in the collection of A. F. Holden, fifteen years ago, mistakenly labelled leucophoenicite. Crystals were then measured by the senior author and practical certainty was reached that they represented a new arsenate of manganese. To determine its chemical nature, however, it would have been necessary to remove most of the material from the only specimen. In the many ensuing years, continued search for more examples of the mineral proved fruitless. The resolution was finally reached that the sole specimen must be sacrificed and this was done, all but two or three crystals being detached. The material so obtained has been analyzed by the junior author, the result confirming the conclusion that the mineral is a distinct species.

Holdenite is orthorhombic with the axial ratio:

$$a:b:c = .3802:1:.2755. \quad p_0 = .7230. \quad q_0 = .2755.$$

Seven crystals were measured giving concordant results in angular values from a complex form series as shown in Table 1. The crystals are tabular parallel to the face taken as the macropinacoid, the largest one on the specimen measuring 8 mm. in greatest diameter.

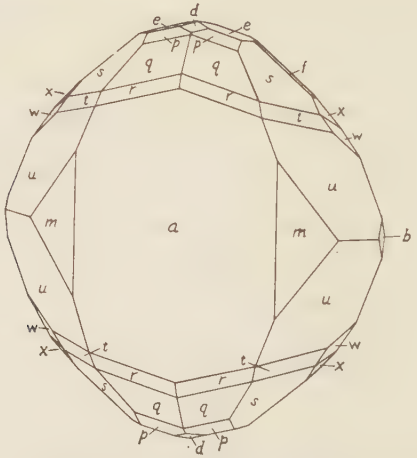

Figure 1. Crystal of Holdenite

[1] Published by permission of the acting Secretary of the Smithsonian Institution.

TABLE I. FORMS AND ANGLES OF HOLDENTE.

Symbol	Number of faces	Number of crysts	Calculated Angles ϕ	Calculated Angles ρ	Measured (average) Angles ϕ	Limits ϕ	Measured (average) Angles ρ	Limits ρ
c (001) ρ	1	1	00°00′	00°00′	00°00′		00°00′	
a (100) ρ	7	1	90 00	90 00	90 00		90 00	
b (010) °	7	7	00 00	"	00 00		"	
m (110) ρ	20	7	69 08	"	69 12	+6′ −4	"	
l (120) ρ	2	2	52 41	"	52 46	+1	"	
n (130) ρ	4	4	41 10	"	41 12	+12 −4	"	
e (011)	7	6	00 00	15 24	00 00		05 41	+16 −10
f (031)	2	1	"	39 34	00 10	+10	39 33	+2 −2
d (102)	2	2	90 00	20 03	90 00		20 02	+1 −1
p (111)	23	7	69 08	37 44	69 11	+12 −9	37 47	+8 −4
q (211)	23	7	79 13	55 49	79 11	+9 −4	55 48	+12 −2
r (311)	9	6	82 46	65 26	82 44	+6 −14	65 24	+3 −1
s (131)	15	6	41 10	47 41	41 08	+7 −4	47 41	+7 −13
w (151)	3	1	27 41	57 16	27 28	+4 −5	57 18	+7 −8
t (251)	5	5	46 23	63 24	46 20	+5 −10	63 32	+15 −9
x (182)	2	1	18 10	49 14	18 12	+14 −14	48 55	+15 −16
u (7.16.2)	2	1	48 57	73 24	49 23	+12 −12	73 35	+5 −5

The crystals vary little in habit and most of the forms occur on all of them as shown in Table 1. The base, *c* was seen but once and *n* and *e* were found on but two crystals. The forms *f*, *w* and *x* were also found but once, all on the most complex crystal measured which is shown in the figure. There was, however, a form present on all the crystals with relatively large faces which varied widely in its angular position. This is the pyramid *u* to which has been assigned the symbol (7. 16. 2). As shown in the figure this form is in a zone with *t* and *s*; and the angles as found on this one crystal agree well with the calculated values. On other crystals, however, the value of ϕ varied from 47° 14′ to 54° 36′ and that of ρ from 72° 10′ to 76° 06′. The symbol (491) is simpler in form and also lies in the zone with *t* and *s*; but while the value of ϕ for it, 49° 23′, agrees exactly with the best measured angle, the ρ angle is two degrees too large and the preference was therefore given to the more complex symbol.

Holdenite has a poor cleavage parallel to the brachypinacoid. Its hardness is 4 and the specific gravity, determined by floating in Clerici solution, is 4.07. The color varies from clear pink to deep red and yellowish red. Biaxial (+). The plane of the optic axes is parallel to (010) with the acute bisectrix emerging normal to (100). $2V = 30°\ 20'$ (measured), 28° 58′ (calculated). Dispersion easily perceptible, $\rho > \nu$.

α || to *c*	$\alpha = 1.769$
β || to *b*	$\beta = 1.770$
γ || to *a*	$\gamma = 1.785$

We are indebted to Professor Larsen for the index values, determined by the immersion method.

About 0.42 gr. of fairly pure material was prepared by Mr. Berman for the analysis. It contained willemite and calcite as impurities.

1. Analysis of Holdenite by E. V. Shannon.
2. Molecular ratio of 1.
3. Molecular ratio after eliminating willemite and calcite.

	1.	2.	3.	
	Per cent			
SiO_2	2.01	.033		
As_2O_5	17.40	.076	.076	.076 = 1 × .076
MnO	37.75	.532	.532	
FeO	1.80	.025	.025	
ZnO	28.08	.345	.279	.914 = 02 × .076
CaO	3.80	.067	.042	
MgO	1.45	.036	.036	
H_2O	6.62	.367	.367	.367 = 5 × .073
PbO	trace			
Mn_2O_3	trace			
Al_2O_3	trace			
	98.91			

The presence of calcite in the sample was proved optically and by effervescence of grains on solution in acid. The sample, however, was not sufficiently large to permit determination of CO_2. We assume the deficiency of the analysis, 1.09%, to be CO_2 and take enough of the CaO to satisfy this as $CaCO_3$. We regard the SiO_2 as due to willemite and take sufficient ZnO to satisfy this compound. On this basis there was 7.38% of willemite and 2.49% of calcite in the sample. Deducting these from the analysis we obtain the ratios of column 3 above which leads to the formula for holdenite

$$12R''O \cdot As_2O_5 \cdot 5H_2O.$$

Manganese and zinc are present in the proportion of approximately 2:1. The formula may then be expanded to the form

$$8MnO \cdot 4ZnO \cdot As_2O_5 \cdot 5H_2O$$

which requires the following composition:

As_2O_5	18.96
MnO	46.78
ZnO	26.83
H_2O	7.43
	100.00

Holdenite is thus a very basic arsenate of manganese and zinc. The only mineral at all resembling it in composition is the recently described mineral chlorophoenicite, also from Franklin, to which was assigned the formula $10R''O \cdot As_2O_5 \cdot 7H_2O$ with R'' chiefly manganese and zinc in the proportion of 3:2.

Holdenite is named in honor of A. F. Holden in whose splendid collection now at Harvard University the unique specimen of this mineral was discovered. This was a slab of massive franklinite ore with a slickensided surface 10 by 7 cm. in dimensions, clearly one wall of a narrow veinlet. The crystals of holdenite were attached for the most part directly to the vein wall or to a thin coating of manganiferous calcite. With it was associated barite, galena, pyrochroite and fibrous willemite, all in minute amount.

CAHNITE, A NEW BORO-ARSENATE OF CALCIUM FROM FRANKLIN, NEW JERSEY

C. PALACHE AND L. H. BAUER.

The mineral here to be described was first observed and sketched by Mr. Lazard Cahn about 14 years ago in the form of a few minute implanted crystals. The specimens containing them were placed in the hands of the senior author for study and became part of the Holden Collection at Harvard University. The tiny white glassy crystals were very characteristically twinned and their form and angles suggested strongly a relation to the barium zeolite edingtonite but material for analysis or for any but the simplest chemical tests was lacking. However, the writer believed that he could show that barium was lacking and that in its stead there was calcium. It was therefore regarded as a calcium edingtonite and the name cahnite was proposed for it as a recognition of Mr. Lazard Cahn's indefatigable efforts to preserve and to make known to science the rarer Franklin minerals. This name appeared in the *American Mineralogist* for 1921 in the title of a paper[1] which was neither read nor printed.

Thus the matter stood until the spring of 1926 when Mr. George Stanton of Franklin rediscovered this mineral in moderate abundance in veins in massive ore, in the northern part of the mine.

Its identity remained at first concealed as the newly found material was poorly crystallized. The junior author had established its peculiar chemical nature before the characteristic twinned crystals were again found. Spectroscopic examination of one of the original crystals was then made at the Palmerton laboratory of the New Jersey Zinc Company by Mr. Nitchie which established the complete chemical identity of the two finds.

Cahnite crystallizes in the tetragonal system with sphenoidal symmetry. Measurements were made both on the first-found crystals and on the later ones, the quality of both lots being poor. While the measurements of different crystals agree fairly closely in value, all are unsatisfactory by reason of the etching of practically all crystal faces. The crystals are generally small, rarely exceeding 2 or 3 mm. in diameter and are always characteristically

[1] Holdenite and Cahnite, two new minerals from Franklin Furnace, New Jersey, *Am. Mineral.* **6**, 39, 1921.

twinned with the appearance, essentially, of interpenetrating tetrahedrons twinned with parallel axes as in sodalite. This mode of twinning causes the positive and negative sphenoids to be brought to parallel position in the two individuals and they therefore reflect simultaneously. The larger, more brilliant sphenoid has been taken as the positive form $p(111)$: the smaller faces as the negative form $o(1\bar{1}1)$. The better developed prism is truncated by the perfect prismatic cleavage, m, (110). The angular values given by the two best measured crystals follow.

Crystal 1. Forms $a(100)$, $p(111)$, $o(1\bar{1}1)$

	Observed Angles					Calculated Angles			
	ϕ		ρ			ϕ		ρ	
a	00°	02′	90°	00′		00°	00′	90°	00′
	90	02	90	00					
	180	02	90	00					
p	44	39	41	02		45	00	41	02
	−44	31	41	02					
o	−135	15	41	02		135	00	41	02
	+135	16	41	02					

Crystal 2. Forms $a(100)$, Cleav. (110), $p(111)$, $o(1\bar{1}1)$

	ϕ		ρ			ϕ		ρ	
a	00°	00′	90°	00′		00°	00′	90°	00′
	90	00	90	00					
cleav.	135	00	90	00		135	00	90	00
	−135	00	90	00					
(110)									
p	44	52	41	03		45	00	41	02
o	135	52	41	01		135	00	41	0

The average value of the sphenoid angles, ϕ 45°, ρ 41° 42′ yields the axial ratio $a:c=1:0.615$. $p_0=0:615$

Other signals were obtained from some of the crystals but they were variable in position and were undoubtedly from rounded etched faces, yielding no simple indices.

The figure shows an idealized twin crystal. One group approximated to this development but generally the twins are far less regularly formed. Characteristic for all however are the reentrant angles appearing on the prism face a, which is common to the two parts of the twin; and the rectangular crossing of the two sphenoid edges of p. The sharpness of the form is commonly lost by the rounding and facetting due to etching. In the latest find

of cahnite the etching is so extensive that the twin crystals are reduced to plates parallel to the basal plane, still however, showing reentrants on the bright prism faces.

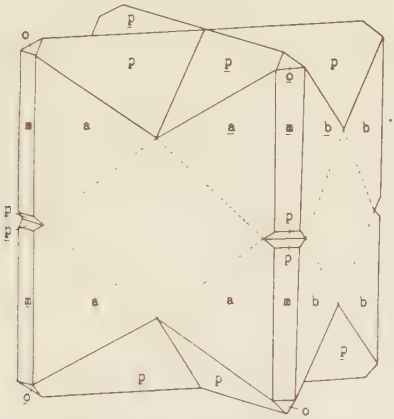

Cahnite. Idealized Twin Crystal.

Cahnite is white and transparent with a notable glassy lustre. The optical characters, determined by Mr. Berman, are as follows:

Uniaxial, positive. Dispersion strong,

Refractive indices, $\omega = 1.662$; $\epsilon = 1.663$

The double refraction is therefore very low.

Due to the low birefringence and considerable dispersion of cahnite it exhibits abnormal interference colors somewhat similar to the same phenomena shown in torbernite as described by Bowen.[2] This striking effect makes the mineral easily recognizable under the microscope.

The hardness of cahnite is about 3 and the specific gravity 3.156. The very perfect cleavage parallel to the first order prism (110) is noteworthy. The appearance of the mineral is very much like that of the barite with which it is sometimes associated.

Material for the analyses was purified by hand picking, and for the largest sample, by the use of heavy solutions.

[2] Abnormal Birefringence of Torbernite, *Am. Jour. Sci.*, Vol. **48**, p. 195, 1919.

1. Analysis of a sample of cahnite of .1 gr. with slight impurities of hedyphane and calcite by L. H. Bauer.

2. Analysis of a sample of cahnite of .26 grams with slight impurity by L. H. Bauer.

3. Analysis of a very pure sample of .5 gram by L. H. Bauer.

4. Molecular ratio of 3.

5. Calculated composition of $4CaO.B_2O_3.As_2O_5.4H_2O$.

	1.	2.	3.	4.	5.
CaO	38.27	37.13	37.62	.671=4×.168	37.64
B_2O_3	10.14	11.64	11.86	.169=1×.167	11.74
As_2O_5	36.79	37.47	38.05	.166=1×.167	38.54
H_2O	11.75	11.78	12.42	.689=4×.172	12.08
PbO	1.15	trace			
MgO	0.24				
ZnO	trace	1.58			
CO_2	trace				
	99.99	99.60	99.95		100.00

The determination of boron was made by Chapin's modified distillation method on a separate portion in each case.

The close agreement of the three analyses made on different samples of cahnite is striking. The molecular ratio leads to the simple formula $4CaO \cdot B_2O_3 \cdot As_2O_5 \cdot 4H_2O$ or $Ca_4B_2As_2O_{12} \cdot 4H_2O$. Cahnite is thus an entirely new type of chemical compound among minerals.

Cahnite fuses quietly at about 3 yielding the green flame of boron. It is easily and completely soluble in dilute hydrochloric acid. In the closed tube, heated alone it yields water and becomes opaque but does not fuse; heated with potassium carbonate and carbon it yields an arsenic mirror.

Cahnite has been found only at Franklin. The first crystals occurred on specimens which probably came from the Parker Shaft. They present two distinct types of paragenesis. In one cahnite is implanted on the walls of cavities in beautifully crystallized axinite together with barite and pyrochroite. In the second type cahnite, calcite, and olive green willemite crystals are implanted on massive friedelite and barite or on garnet. One crystal on such a specimen, exceptional in being untwinned, is also the largest crystal of cahnite yet seen, measuring 6 mm. in diameter.

Plate VIII

Cahnite. Twin Crystals, Deeply Etched, Implanted on Rhodonite.

The specimens found by Mr. Stanton in 1926 came from pillar No. 229 north, 36 feet above the 700′ level of the Franklin Mine. The specimens are always associated with axinite which constitutes veins with narrow open cavities. Resting on this are rhodonite crystals, barite, hedyphane, sometimes in crystals, and willemite of either the usual prismatic habit or in thin plates with the base dominant. The cahnite is later than and implanted upon all these associated minerals. The only mineral to form after cahnite is datolite in the form of a coating of fibrous nature like what has been called botryolite at Arendal, Norway. This coats all other minerals in the veins although the cahnite crystals are generally free from it and clearly belong to the same period of deposition. Cahnite has also been found in a neighboring part of the mine associated only with rhodonite, on crystals of which it is implanted.

Still another association of the new mineral has come to light as this article is being written. Specimens from the picking table show small drusy cavities in franklinite lined with dodecahedral crystals of garnet. The garnet is pink on the free surfaces, and shows successively white and yellow bands towards the walls of the cavities. Tiny glass-clear crystals of cahnite are implanted on the garnet and show to the minutest detail the complete symmetry of the twin figured above. The only associated mineral is a brown to light yellow biotite mica in slender, long prismatic crystals projecting into the cavities.

The authors are indebted to Mr. Stanton for both gifts and oans of cahnite specimens for analysis and study.

A SAW ATTACHMENT ADAPTING GOLDSCHMIDT'S MODEL CUTTING MACHINE TO THE SAWING OF WOODEN MODELS

CHARLES PALACHE AND LYMAN W. LEWIS.

The instrument[1] devised by Professor Goldschmidt for cutting crystal models from plaster has attained wide usefulness in many mineralogical laboratories. The writers' experience with this instrument made it seem desirable so to modify its construction as to permit the cutting of wooden models. This has been accomplished without destroying its usefulness for its original purpose. Three attachments have been devised consisting of a circular saw to replace the plane, a new model holder and a vise to enable the model to be reversed for cutting the second termination. Since the results attained with these attachments are satisfactory and the cutting of wooden models accurately and rapidly is made possible, the present description is offered.[2] The instrument with the first two attachments is shown in figure 1.

A. CIRCULAR SAW ATTACHMENT.

This consists of a small electric motor, *m*, mounted on a movable carriage, *c*, adjusted to the runners, *r*, (carrying the plane of the original machine) and balanced by a counter-weight, *cw*. A smooth-cutting saw, *s*, is connected to the motor shaft by means of a steel spindle, and is protected by a light guard, *g*. The axis of the saw is adjusted to give clearance for a model $2'' \times 2'' \times 6''$. A motor switch, *ms*, is conveniently located on the carriage.

[1] Constructed by F. Rheinheimer successor to P. Stoe, Heidelberg. Described by Goldschmidt, *Zeits. f. Kryst.* 45, p. 573, 1898, and by Tutton, CRYSTALLOGRAPHY AND PRACTICAL CRYSTAL MEASUREMENT, Vol. 1, p. 489.

[2] Complete working drawings of saw, screw chuck, and centering vise may be obtained from the Department of Mineralogy, Harvard University for $1.50, the cost of the photostat prints. All the plans have been sent to Rheinheimer who may in the future modify his design to include the saw attachment. Meanwhile, the attachments may be procured from Mr. D. E. Littlefield, Preparator in the Department of Mineralogy, Harvard University, complete for the sum of $100, or the two parts, saw and model holder, necessary for cutting models with a single termination, for $60.

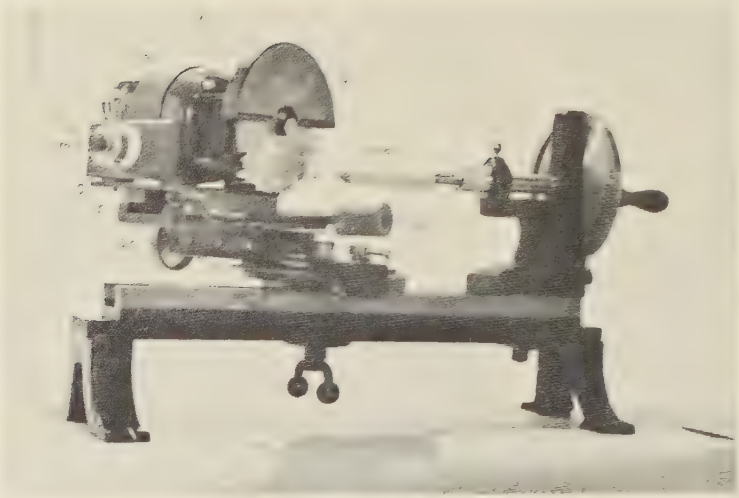

Figure 1. The Goldschmidt Model-making Machine Showing the Saw Attachments Adapting it to Wooden Model Cutting.

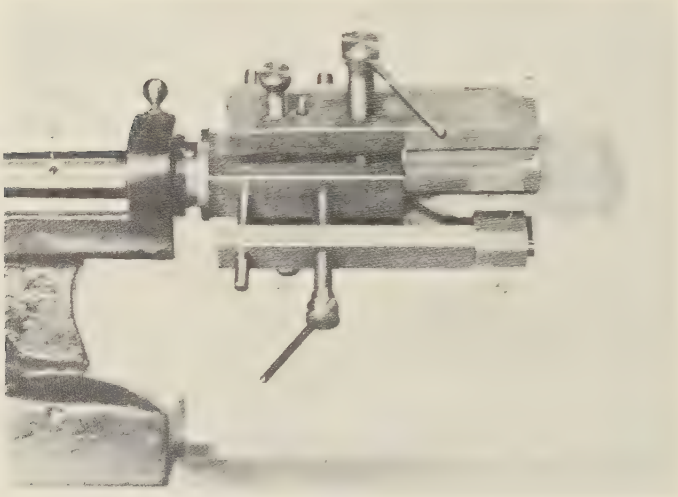

Figure 2. Centering Vise for Cutting Doubly Terminated Wooden Models.

B. MODEL HOLDER

The block is held on a stout screw fixed in a brass holder threaded to the spindle of the vertical circle in the same manner as is the socket for plaster blocks. The diameter of the front of the brass holder is reduced to allow sufficient clearance to complete the prismatic cuts the entire length of the block. The prism zone and truncations of one end of the model are cut on this holder.

C. CENTERING VISE

If the crystal has a prism zone and it is desired to cut the opposite termination, the crystal is removed from the screw holder and by means of the centering vise is clamped and centered in reverse position. This device is shown in figure 2. A pair of wide jaws *j*, close or open by means of the screw, *s*, bearing right and left threads at its opposite ends. These clamp the model by the two most prominently developed prismatic faces and center it in one plane. Perfect centering and rigidity is effected by the two set screws, *ss*. Auxiliary jaws, *aj*, at right angles to the first pair and similarly operated, center the model in the perpendicular plane. This adjustment is effected before the main jaws, *j*, are clamped tight. The auxiliary jaws, the faces of which rotate on pivots, not only center the model but by clamping another pair of faces, also add rigidity to the grip of the vise. The entire vise, with the centered model, is itself centered with respect to the axis, *a*, of the vertical circle, a condition necessary in order to cut the second termination symmetrically to the first.

The plans were drawn by Mr. D. E. Littlefield, and the attachments were constructed under his direction. The photographs illustrating the machine were made by Mr. E. B. Dane, Jr., who also contributed valuable suggestions on the designs.

The saw operates at 1700 revolutions per minute and leaves a surface so smooth that no further finishing is necessary. Any wood that takes a smooth cut without regard to direction of the grain is suitable. Pear wood is probably best but was not available. Maple is easily obtained and gives entirely satisfactory results. A stock of blocks $2''\times2''\times6''$ and $2''\times1''\times6''$ will serve as blanks for most models. The blanks are squared at one end and bored to fit the model holders. (See Fig. 1, B., plate 9.)

The operation of cutting wooden models is essentially the same as the procedure followed in using plaster: the most notable

difference being that with the saw a single cut develops the face to any desired depth, while in using plaster, repeated shavings must be removed, which introduces a slight uncertainty in making ideal models. This same difference makes it possible to cut a complete wooden model in the time required to make one in plaster with the single termination. The model illustrated in Fig. 3, plate 10, was made from published data in an hour. Simple forms in all the systems may be cut without removing the block from the screw holder. Doubly terminated models of any crystal can be cut provided there is sufficient prismatic development to provide clearance when gripped in the vise.

PLATE X

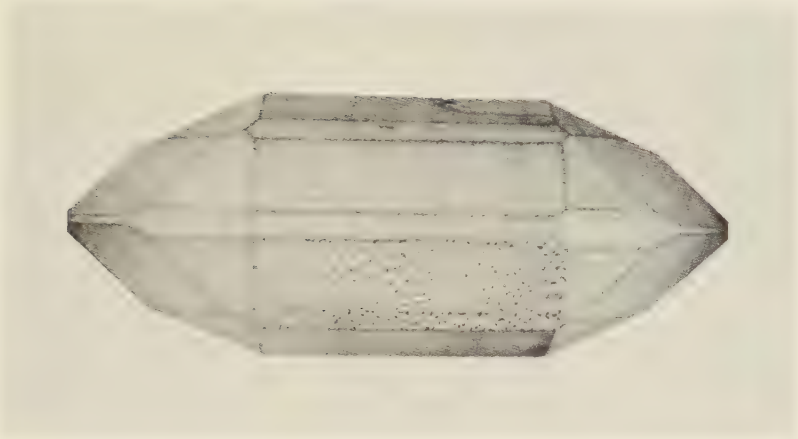

Figure 3. Wooden Model of Phosgenite Cut from Published Angles and Drawing.

ALPINE MINERAL DEPOSITS

IAN CAMPBELL, *Louisiana State University.*

For many years past a considerable literature has been developing about the Swiss "Alpine Mineral Deposits." Recently a paper[1] by Parker has appeared giving an excellent general summary of the present state of knowledge of these interesting deposits, and it has seemed worth while to make a rather extended review of this work.

From the historical standpoint alone the deposits are interesting since they were among the first to be studied and have been among the most important in the development of the science of mineralogy. From these deposits came the "super-frozen" ice, which the ancients called "*Krystallos*," giving our science the name crystallography. But it is more than a name that crystallography owes to this "ice stone," for it has been from similar specimens of this quartz that many of the laws, the complexities and the simplifications of the modern science have been developed. And it is not only the quartz of these deposits that has made them famous; superbly crystallized specimens of many other species, adularia, hematite, epidote, titanite, etc., from these occurrences are known in collections all over the world.

If the contribution of these deposits to the science has been great in the past, even greater things are promised for the future. In this further development, crystallography will be by no means the only gainer, for some years ago the Swiss mineralogists led by Koenigsberger recognized the wider geological and mineralogical significance of the deposits; and now, under the leadership of Niggli, a group has been organized to study these deposits from various points of view: crystallographic, paragenetic, chemical and physico-chemical. Altogether it should prove a fruitful field of research.

The title "Alpine Mineral Deposits" may properly be applied to the unique occurrences with which this paper is concerned, since no other of the infrequent and unimportant mineral deposits of the Alps is deserving of it. The "Alpine Minerals" are not only the most interesting and the most characteristic but

[1] Alpine Minerallagerstätten, Robert L. Parker. *Schweizer Mineralogische und Petrographische Mitteilungen*, No. **3**, 1923, 298.

are also actually the most important deposits of the region from an economic standpoint, as many are being actively prospected by collectors today.

The deposits of these "Alpine Minerals" are widely distributed throughout the Tyrol, the French and the Swiss Alps. Perhaps the most important general feature of the deposits is their relation to structure. In shape they tend to be lens-like, usually a very much flattened lens. This lens is always in cross-cutting (perpendicular) relationship to the rock structure in which it occurs. The country rock is generally schist or gneiss. Chemical composition of the country rock may vary widely, from the equivalent of granite to that of olivine gabbro, though the salic types are by far the more common. In these rocks the plane of schistosity is very often vertical, or nearly so, and the plane of the deposit then is roughly horizontal, following the transverse tensional cracks produced by the tectonic forces responsible for most of the Alpine structure. (See figure.)

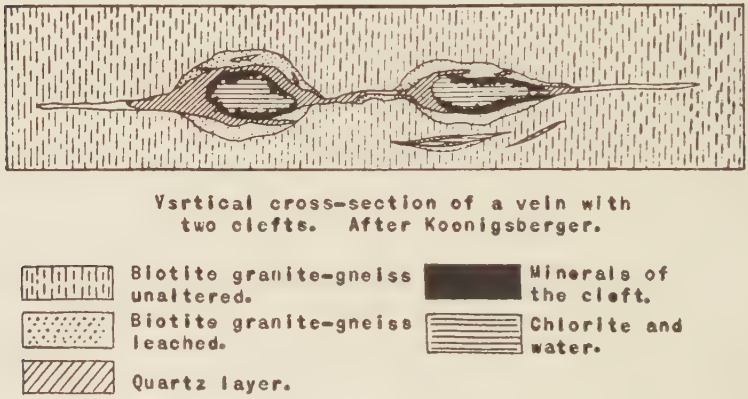

Vertical cross-section of a vein with two clefts. After Koenigsberger.

In size they vary from the merest cracks to open crevices 6 to 8 feet in their shortest dimension, and 50 to 100 feet in their two longer horizontal dimensions.

Now, while individual occurrences vary widely, there is, nevertheless, a notable similarity between all deposits in the general outline of their structure and mineralogy. They all show a zoning, concentric to the "lens," and in most of the deposits, three such zones can be recongnized.

The outermost zone, that farthest from the center of the crevice, consists simply of leached country rock, and naturally grades outward into unaltered gneiss or schist as the case may be.

Leaching is always most severe in the direction of the open space, and in many cases so much of the rock material has been removed that the remainder has become an exceedingly porous and even friable mass.

In width, the leached zone never exceeds double the width of the adjoining open cavity. The most interesting feature about this leached zone is that its width is always proportional to the size of the crevice. The larger the crevice, the greater the width of the leached zone. This noteworthy relationship is true not only in respect to the size (i.e. width) of the two succeeding zones, but also holds good for the size of individual crystals formed in the innermost zone. All of these factors, the width of the three concentric zones, the size of individual crystals and even the relative power of the leaching solutions seem to be directly dependent on the size of the crevice itself.

The zone lying immediately within the leached zone (in the direction of the open cavity) is called the quartz zone or quartz layer. By this is meant the large mass of quartz found deposited in part upon the rock or its decomposition product and in part even within it. This mass of quartz is the preponderant part of the "vein" filling, in some cases making up the entire crystallization within the crevice. Indeed, the only case where it is absent is where the crevice has formed in relatively basic rocks.

This quartz zone consists of a mass of rather loosely interlocking, tiny, idiomorphic quartz crystals. While they have not been studied as carefully as the larger crystallizations of the inner zone, it is believed that these, too, are all of the alpha variety of quartz, having formed below 575° C.

The third and last zone, the one, therefore, that forms the innermost filling of the crevice, and the one usually referred to when speaking of Alpine "Veins," immediately adjoins the quartz layer. It is the one characterized by the superb crystallizations which have made Alpine minerals the standards for crystallographers. Evidently these minerals must have been deposited from a very slowly cooling solution. The crystals are attached in rather irregular and haphazard fashion to the quartz layer, and project into the free open space of the crevice. They are found

growing from both the roof and the floor of the crevice, and gravity seems to have played no part in influencing crystallization or location. An exception is the case of such a mineral as chlorite, the fine flakes of which evidently remained floating in suspension for some time after crystallization, eventually to settle more abundantly on the crystals growing from the floor of the crevice. A remarkable feature of the attachment of these large crystals is that many are so delicately suspended that the least touch or tremor dislodges them. Now, since there is no indication that crystals have fallen, either during their period of growth or later, it would seem evident that this entire formation must have postdated all of the tectonic movements of the Alpine region.

The assemblage of minerals formed in this zone is unique. (See appended table for complete list). It may perhaps be compared to the suite from some pegmatites and certain hydrothermal veins—and yet the points of difference are many. The order of succession of the minerals has been well established from studies on many of these crevice deposits. In general, it is the same in all, and so far as now known the phenomenon of recurrence of crystallization is entirely lacking. Whenever the deposition of a mineral started, it continued uninterruptedly until the supply was exhausted. This feature, even without the remarkable crystallizations, would set these deposits apart from most hydrothermal veins.

Space does not permit a detailed discussion of the various mineral species. Because, however, of its abundance and importance, certain features of the quartz crystals found in this zone will be mentioned.

On these crystals the positive and negative rhombohedrons are usually very unequally developed and the faces of the trigonal pyramid and trigonal trapezohedron can nearly always be discerned. These features are usually taken to indicate the low temperature, alpha, variety of quartz. Inclusions of liquid and gas bubbles, and of various minerals, notably chlorite and golden brown rutile needles are very common.

Quartz of the smoky variety is common too, and Koenigsberger has made the interesting observation that the degree of coloring or smokiness is dependent upon elevation above sea level. Thus, up to 1400 meters, the quartz remains colorless; at about 1500 meters a brownish color is perceptible; at 1860 it has become dis-

tinctly brown; at 2300 it is really smoky quartz; and at 2900 meters it is the deep blue-black variety known as morion. Now x-rays or the gamma rays of radium emanations are known to produce this coloring effect; and the variation in color with altitude is thought to be due in part to the changing effect of the radioactive material in the rocks and in part to the much greater seasonal changes in temperature at the higher altitudes.

In looking over the appended list of minerals, it can be seen that the chemical elements present are the same as those that make up the preponderant constituents of the rocks themselves; Al, Fe, Ti, Na, K, Ca, and Al combined with SiO_2. Quantitatively as well, there has been found to be a close agreement between the proportions of elements present in the country rock and in the crevice filling. Such a rare element as fluorine, for instance, was found to be present in the unaltered country rock to an amount of 0.06%. In the crevice filling the percentage was 0.05.

This remarkable qualitative and quantitative agreement leads naturally to the assumption that the rocks in which the crevices have been found have themselves furnished the material for the filling.

Considering that there has been little if any change in qualitative and quantitative chemical composition it will be interesting to note what mineralogical changes have taken place. Obviously, the material obtained from the rock has undergone a complete rearrangement before the deposition of the new minerals, since they are in the main so different. The outstanding difference is in the almost complete absence in the crevice filling of the feldspars (except the two alkali feldspars, and even these show a striking change in habit) and of all the common femic rock-forming silicates. What, then, becomes of these minerals?

One group is made up of minerals which are soluble, but have stable molecules. As might be expected, they appear in chemically similar form in both rock and crevice filling. A small proportion of the quartz probably belongs to this group, as does orthoclase feldspar in part. Muscovite, apatite, fluorite, and titanite may also be included here. It is significant that this group is not the one of major importance as regards the crystallizations of the inner zone.

Another group are those rock minerals which are also soluble, but possess less stable molecules. It is this group which has

furnished most of the material for the crevice filling. The calcic plagioclases, for instance, undergo a rather complete disintegration with subsequent formation of muscovite, zoisite, zeolites, quartz and, in extreme cases, carbonates. The original plagioclase contains some $KAlSi_3O_8$, and when decomposed this goes to form adularia. The formation of zeolites appears to be particularly dependent upon the presence of calcic plagioclase in the rock, as might be expected, since Ca is an essential part of the molecule of nearly all of these zeolites. The presence of K and Na in the depositing solution also seems necessary for the formation of zeolites. It is significant that it is in the crevices formed in dominantly alkaline rocks that the zeolites are most abundant.

The biotite of the rocks varies greatly in its composition, and consequently gives rise to a variety of products. The principal crystallization resulting from its decomposition is chlorite. Probably hematite, additional quartz, and some carbonates may be formed. Most of the titanium of the rocks is probably in the biotite and pyroxenes, and to them then, is to be attributed the rutile, anatase, and brookite appearing in the vein. Much of the formation of fluorite too is undoubtedly dependent on the decomposition of the biotite, since its fluorine content is known to be relatively high in these rocks.

Hornblende and pyroxene have much the same story as biotite. They may form some of the epidote, and part of the hornblende passes over to actinolite and amianthus (an exceedingly fine silky variety of asbestos).

A third group consists of insoluble minerals. Strictly speaking, of course, there is none actually so. But such minerals as quartz and the purer varieties of orthoclase may be grouped here since they remain in large part in the leached rock and form the insoluble residuals, the porous friable mass of the outermost zone.

With this survey of the features of the Alpine deposits we are ready to sum up the points in the theory of origin proposed for them.

First of all, of course, came the formation of these transverse rifts in the rocks, to be explained perhaps partly by thrust faulting and partly by tensional stresses.

Then came the filling of these cavities by waters soaking in from the surrounding rocks or along the extensions of the rifts. The

origin of these waters is doubtful. Parker suggests that they may have been largely of magmatic origin, citing the propinquity of metalliferous veins and the presence of porphyry dikes in the region as proof that the magmatic zone once reached near or to the surface and could therefore have been capable of furnishing the water.

It is admitted that ground water percolating downward may have been in part responsible, though it is not apparent why to ground water should not have been assigned the entire part. However, it matters not so much from whence the waters came. The important fact is that they brought nothing with them but CO_2 and heat, both easily explainable whatever their origin. CO_2 is a common constituent of both ground water and igneous emanations With the crevice filled with hot carbonated water, solution of the adjoining rock material began immediately. Leaching continued until a maximum concentration in the water solution had been reached for the prevailing temperature. Any cooling from this stage would cause precipitation, and the beginning of the formation of the "vein," but it would naturally mean an end of leaching.

The solution thus formed can be treated just as a complex mixture of salts dissolved in water. Deposition is controlled entirely by falling temperature. The succession of minerals is strictly a salt sequence, comparable in every way to the salt deposits of evaporating sea water and, indeed, they have been studied in much the same way as the Stassfurt deposits. Doelter and Koenigsberger have performed experiments on natural minerals of the rocks which tend to show as well as could be expected, that hot carbonated waters do dissolve these rock minerals, and that the resultant solution will deposit its material in just such fashion as these Alpine minerals have been deposited.

Because of the limitation of the time factor, these experiments have never been quite as conclusive or satisfactory as might be desired. More important is the fact that the deposits, or rather the behavior of such a theoretical solution as they are assumed to have come from, has been studied by aid of the phase rule and equilibrium diagrams, with the result that the sequence has been accurately predicted. It is true that in the theoretical sequence, certain compounds occurred not known in the Alpine deposits

or even in nature. Yet the fact that these are not known, or rather, perhaps, have not been found, does not reflect on the importance of this study in confirming the "salt sequence" theory of deposition for these deposits. Indeed some of these synthetic "minerals" with no known natural counterparts have been proved to be meta-stable forms and therefore not likely to occur in nature.

Last there remains to be considered the temperature range over which deposition occurred. (See appended table). For this only the upper and lower limits can be fixed at all definitely. Other points in the series have been determined largely by interpolation.

Quartz and adularia are the oldest formations. Much of this quartz is later than the adularia, it is true, but a part is definitely earlier. Mention has already been made of the fact that all of the Alpine quartz is the alpha, or low temperature variety. It must, then, have formed below 575° C. For adularia, the lowest temperature of formation is known to be 340°C. plus or minus 20°C.

The first deposition must therefore have taken place between 500° and 350°C. Now, toward the close of the adularia period, a much larger deposition of other minerals begins to appear, so that evidently the larger part of the deposits was formed from 350°C, downward. Experiments made on the disappearance of the smoky color of quartz and of the "bubble line" in the quartz with inclusions when subjected to heating confirm these temperatures.

The lower temperature limits are determined principally by the zeolites. In connection with the synthetic work on these complex hydrous silicates, it seems proved that zeolites can form only from solutions whose chemical composition is very similar to the solid phase which separates. Considering this, it is interesting to note in the natural sequence that zeolites do not begin to appear until most of what might have been interfering compounds have been exhausted. They appear just about the time that calcite, fluorite, and hematite are finishing their crystallization, a further proof of the correctness of the general theory.

Generalized Diagram Showing Order of Crystallization of the Alpine Minerals for Different Types of Rocks.

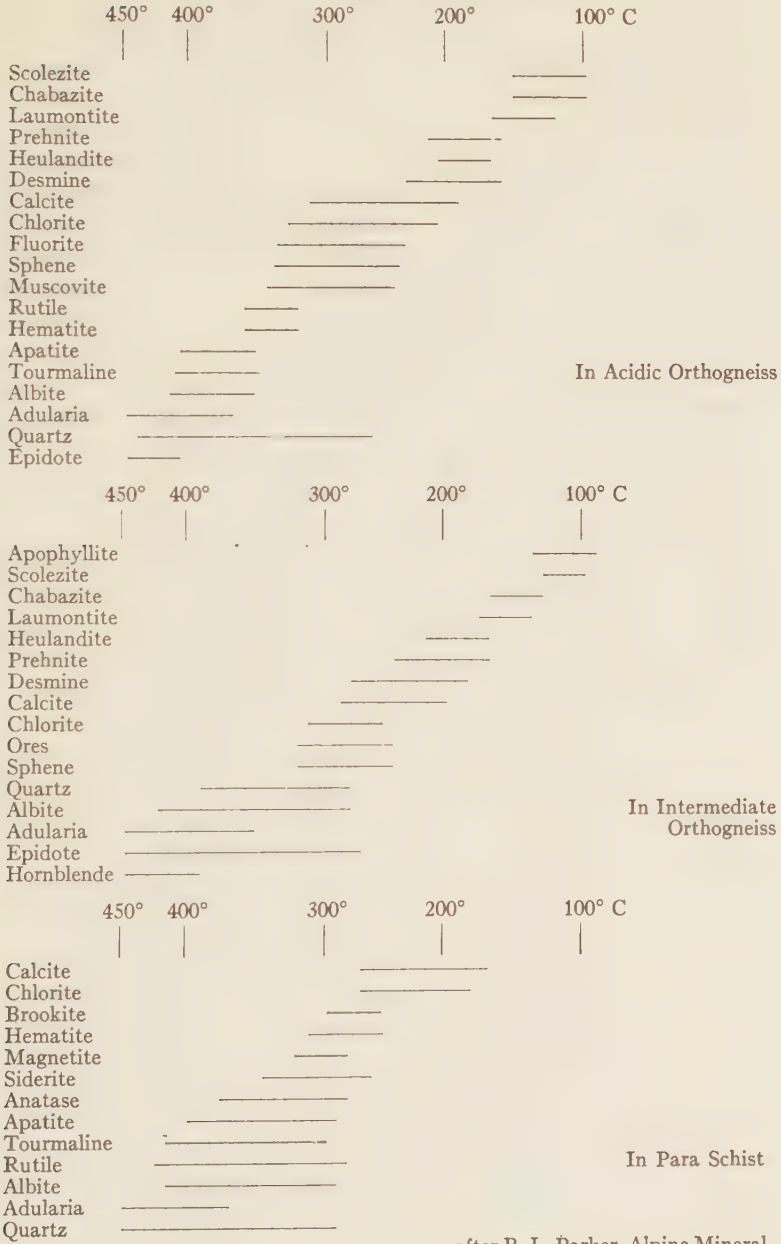

after R. L. Parker, Alpine Mineral-lagerstätten.

Synthetically, zeolites have been formed at temperatures as low as 90°C. Their upper limit is just about 300°C. In general the zeolites develop most abundantly at the lower temperatures, their typical range is 100° to 200°C. In these deposits it seems unlikely that the lower limit was ever quite reached, so the lower limit is set at 130°C.

Two other points on the temperature range are accurately known. The red color frequently found in the fluorite disappears on heating to 175°C. The formation of fluorite must therefore lie below this. And, finally, hematite is known to be deposited from water solution at about 200°C.

The temperature limits, then, between which deposition has taken place, may be set between 500° and 130°C., with most of the deposition occurring in the interval between 350° and 150°C.

Finally, to sum up the remarkable features of these deposits, all of which point toward the "lateral secretion" theory, we have:

First; the dependence in size both of the leached zones, of the "vein" filling and of individual crystals upon the size of the crevice.

Second; the remarkable dependence of the chemical character of the "vein" filling on the chemical character of the country rock.

Third; the mineralogical changes, molecular simplification and hydration, indicative of hydrothermal action.

Fourth; the evidence of a "salt sequence" type of deposition controlled by progressively declining temperatures.

This article of Parker's is to be regarded as particularly timely, since in these days when the pendulum of popular opinion is swinging toward the direct igneous explanation for all sorts of deposits, it affords a very clear cut and unequivocal example of lateral secretion—lateral secretion in the strictest sense. And, too, because it presents a detailed picture of the conditions of that deposition, a deposition which, while differing in structure and sequence and individual crystallizations, yet is comparable in mineral assemblage to many hydro-thermal veins or "vein dikes," and which indeed, in point of variety of species present, rivals even some of the pegmatites.

The pioneer in the foregoing theory of the origin of the Alpine mineral "crevices" is Koenigsberger, who has also collected most carefully the data upon which it rests. Among other papers by him may be mentioned: Die Minerallagerstätten im Biotit-

protogin des Aarmassivs, *Jahrb. für Min.*, B.B. **14**, p. 43; and Die Paragenesis der Kieselsaure-mineralien in Doelter's HANDBUCH DER MINERALCHEMIE, Vol. **II**, 1, p. 27.

Further papers on this subject from Niggli's group of investigators should be looked forward to by all who are interested in these classic deposits—deposits which bid fair to become a Rosetta stone of Geology.

In conclusion the writer wishes to express his thanks and appreciation to Dr. Palache for first calling his attention to this interesting field; for help at many stages in the preparation of this review; and for the privilege of studying the Alpine suite of minerals in the Harvard collection.

LIST OF MINERALS APPEARING IN THE "ALPINE VEINS"

SULPHIDES
- Sphalerite
- Pyrrhotite
- Galena
- Chalcopyrite

OXIDES
- Quartz
- Brookite
- Anatase
- Rutile
- Magnetite
- Hematite
- Ilmenite
- Limonite

CARBONATES
- Calcite
- Dolomite
- Magnesite
- Siderite
- Aragonite
- Strontianite
- Cerussite
- Malachite
- Azurite

SULPHATES
- Leadhillite
- Anhydrite
- Barite

PHOSPHATES
- Xenotime
- Monazite
- Apatite

SILICATES
- Tourmaline
- Cyanite
- Epidote
- Phenacite
- Danburite
- Prehnite
- Axinite
- Muscovite
- Penninite
- Talc
- Kaolinite
- Diopside
- Hornblende
- Amianth
- Beryl
- Adularia
- Albite
- Milarite
- Faujasite
- Scolezite
- Laumontite
- Chabazite
- Stilbite
- Heulandite
- Apophyllite

MISCELLANEOUS
- Fluorite
- Wulfenite
- Scheelite
- Titanite

THE OPTICAL PROPERTIES OF ZINCITE FROM FRANKLIN, NEW JERSEY

HARRY BERMAN.

A specimen of especially pure zincite was recently obtained by this laboratory through the kindness of Mr. D. Jenkins, chief chemist of the New Jersey Zinc Company. The following analysis was made by Mr. L. H. Bauer, also of the New Jersey Zinc Company.

ZnO	= 99.63
MnO	= 0.27
FeO	= 0.01
SiO_2	= 0.08
	99.99

A study of the optical properties of the analyzed zincite was made on a prism cut with its edge parallel to the *c*-axis so that the indices of refraction, ω and ϵ, were measured at one setting. The source of light was a calibrated monochromatic illuminator. The following graph and table give the values obtained for the various wave lengths of light employed.

The "specific refractive energy"[1] constant of the oxides has been found to be very useful in this laboratory in the detection of errors, and in the approximation of the index of refraction and the density of minerals. It may be obtained, according to the law of Gladstone and Dale by the use of the formula

$$\frac{n-1}{d} = K$$

where

n = mean index of refraction.
d = density
K = specific refractive energy constant

E. S. Larsen[2] has determined the value of K for most of the oxides occurring in minerals so that the above formula may be effectively used in checking data.

[1] Gladstone and Dale; Refraction, Dispersion and Sensitiveness of Liquids. *Phil. Trans.*, Vol. **153**, p. 317, 1863.

[2] Larsen, E. S.; Microscopic Determination of Nonopaque Minerals. *U. S. Geol. Surv. Bull.* **679**, 1921.

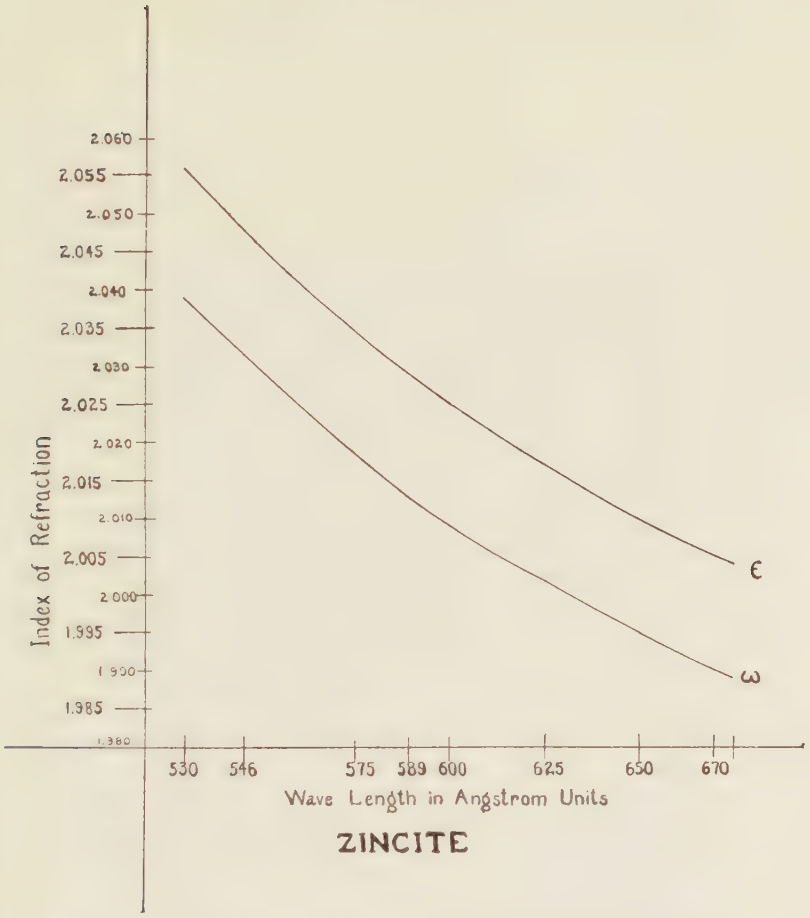

The data in this paper, using sodium light (589Å units) gives $K = 1.80$ which is close to the value obtained by Larsen.

INDEX OF REFRACTION OF ZINCITE, FRANKLIN, N. J.

Wave length-A°	530	546 mercury green	575	589 sodium yellow	600	625	650	670 lithia red	675
Extraordinary ray ϵ	2.056	2.048	2.035	2.029	2.025	2.017	2.010	2.005	2.004
Ordinary ray-ω	2.039	2.032	2.019	2.013	2.009	2.002	1.995	1.990	1.989
Birefringence	.017	.016	.016	.016	.016	.015	.015	.015	.015

GRAFTONITE FROM A NEW LOCALITY IN NEW HAMPSHIRE

HARRY BERMAN.

Graftonite, one of the most interesting of the iron-manganese phosphates, has hitherto been found only at one locality.[1] A new occurrence of this mineral in superior specimens and comparative abundance seems, therefore, worthy of record.

The specimens described in this paper were collected at the Palermo Mica Mine on Bald Face Mountain, a mile and a half southwest of North Groton, New Hampshire. The granite pegmatite[2] from which mica was mined for many years is intruded in Montalban schist in a direction parallel to the schistosity.

None of the graftonite specimens examined were found in place but were all picked from one portion of the dump at the southeast corner of the pegmatite, near the wall rock. Several of the specimens weighed over five pounds, and one mass, partly crumbled, weighed over nine pounds, indicating that the pocket in which the material was found was large. It seems to have been similar in size to a triphylite pocket seen in place in the immediate vicinity of the dump where the graftonite was found, which measured four feet in greatest diameter, two feet across, and extended into the pegmatite for some distance. The specimens present a striking appearance due to the large number of bands of clear brown graftonite alternating with deep purple heterosite,[3] an alteration product of triphylite. The graftonite bands, which do not exceed 4 mm. in width are, as a rule, wider than the bands of heterosite. Figure 1. shows the relation of the two minerals in a

[1] Penfield, S. L.; On Graftonite, a new mineral from Grafton, New Hampshire, and its Intergrowth with Triphylite. *Am. J. Sci.*, Vol. 9, p. 20, Jan. 1900.

[2] A more detailed description is given by Sterrett, *Bull. U. S. Geol. Surv.* **580F**, p. 72, 1914.

[3] The optical properties, by means of which heterosite has been identified in this paper, are close to those given by Larsen in *Bull.* **679**, *U. S. Geol. Surv.* for purpurite. Schaller, in *Bull.* **490**, *U. S. Geol. Surv.* proposes to restrict the name heterosite to the ferric phosphate and the name purpurite to them anganic phosphate. Neither of the end members have as yet been reported as occurring in nature so that the distinction seems somewhat arbitrary. Heterosite and purpurite vary in their optical properties to a marked degree, even within the same specimen so that it is difficult to differentiate the two minerals optically. Lacking a chemical analysis of the material the author, therefore, uses the older name heterosite for the occurrence at Palermo Mine.

PLATE XI

Figure 1. Thin section Enlargement 36 times. Intergrowth of Graftonite (white) and Heterosite(black).

thin section. The same banded structure and association with altered triphylite characterizes the type material from Grafton, New Hampshire.

It is interesting to note that while the triphylite found in association with the graftonite is completely altered to heterosite, in which the iron and manganese are in a higher state of oxidation, the graftonite is unaltered, although the manganese and iron in it are present as MnO and FeO. A study of the optical properties of the graftonite from Palermo indicates that it is similar in composition to the original material from Grafton.

The minerals found in association with graftonite were, muscovite, biotite, almandite garnet coated with a uranium mineral probably uranochalcite, and a few small zircon crystals. The pocket in which the graftonite occurred seems to have been lined with muscovite and biotite in which zircon and almandite crystals are embedded. Most of the specimens also contain considerable amounts of triphylite without graftonite so that a portion of the pocket probably had a considerable amount of this mineral.

A specimen picked up on the dump some distance from the place where the graftonite was found consisted of an intimate mixture of apatite and quartz spotted with a blue mineral which has not been identified. Another specimen presented by the

Mineral	Optical Character	2V	Indices			Pleochroism			Dispersion
			α	β	γ	α	β	γ	
Graftonite	+	50° ±	1.704	1.706	1.725				$\rho > \nu$ fairly strong
Heterosite[3]	+	very small	1.85	1.86	1.91	green grey	blood red	deep purple red	fairly strong
Vivianite	+	medium	1.584	1.600	1.634	deep blue	almost color-less	color-less	
Blue mineral	−	medium	1.620	1.635	1.643	color-less	light blue	deep blue	
Almandite*			$n = 1.830$						

* This value for the index of refraction corresponds to the data given by Larsen in *Bull. 679, U. S. Geol. Survey,* for the pure mineral.

superintendent of the mine, and probably from the same deposit, was essentially triphylite with narrow bands of vivianite throughout the mass. There are also pyrite cubes, pyrrhotite and some chalcopyrite distributed in the triphylite, all of which are somewhat oxidized.

The table on page 171 presents the optical properties of some of the minerals occurring at the Palermo mine.

On the dump of the Valencia Mine, about two miles from the Palermo Mine, a crystal was found embedded in quartz, which proved to be a pseudomorph of heterosite after triphylite. The crystal is 4 cm. long with a diameter of about 2 cm. It is somewhat similar in habit to the triphylite from Bodenmais, as figured in Dana p. 756. The following forms are present: *c*(001), *b*(010), *e*(101), (021), *m*(110), *l*(120).

TOPAZ AND PHENACITE FROM BALDFACE MOUNTAIN, CHATHAM, NEW HAMPSHIRE

MARLAND P. BILLINGS.

INTRODUCTION

In the mineralogical collections at Harvard University there are approximately two hundred crystals of topaz and forty crystals of phenacite from South Baldface Mountain, Chatham, New Hampshire. The specimens were collected by E. C. Andrews of Chatham about thirty or forty years ago and purchased from him about 1910. Kunz[1] called attention to this occurrence of topaz and phenacite in 1890 and Eakle[2] published a brief paper on the topaz in 1898. The phenacite has been studied crystallographically by Farrington and Tillotson[3] and also by Schaller.[4]

GEOLOGICAL RELATIONS

The present writer has visited the pocket from which some of the topaz and phenacite are reputed to have come. It is a very irregular ellipsoid in shape, being about five feet along its greatest axis. A detailed study of the mineralogy has not yet been made, but the pegmatite is composed essentially of perthitic feldspar, smoky quartz, and biotite. Apparently many of the topaz and phenacite crystals found by Andrews were detached, lying on the floor of the pocket, or more commonly in the talus of the mountain slopes. The phenacite was implanted on smoky quartz, topaz, or feldspar. The pocket mentioned is located on the east slope of South Baldface Mountain, at about 2900 feet elevation; a number of other pockets are found in the vicinity. The country rock is a medium textured somewhat miarolitic alkaline biotite granite exposed as an oval-shaped stock, the north-south axis of which is a mile and a half long. This stock is satellitic to the late Paleozoic alkaline batholith of the White Mountains.

[1] Kunz, G. F. GEMS AND PRECIOUS STONES OF NORTH AMERICA, p. 100, **1890.**

[2] Eakle, A. S. Topaz Crystals in the Mineralogical Collection of the United States National Museum. *Proc. U. S. National Museum*, pp. 361–369, **1898.**

[3] Farrington, O. C. and Tillotson, E. W., Jr. Notes on Various Minerals in the Museum Collection. *Field Columbian Museum Publications, Geological Series*, Volume **3**, pp. 131–163, 1908.

[4] Schaller, W. T. Phenacite from New Hampshire. *Bulletin* **490**, *U. S. G. S.*, pp. 53–54., 1911. *Zeit. Kryst.*, **48**, p. 554, 1910.

TOPAZ

DESCRIPTION OF THE FORMS. The topaz crystals vary in size from the largest whose dimensions are nine by six centimeters to those less than a centimeter in diameter. They are in general of short or moderate prismatic development, and bounded at one end by a cleavage plane. A number are however doubly terminated, often with extreme distortion of the terminal faces. They are clear and either colorless or faintly pink, sometimes with a bluish border. The ten crystals measured completely yielded the forms of the following table. The letters and axes of Dana's System are used. The angles agreed on the whole very well with those given in Goldschmidt's Winkeltabellen.

TABLE I. FORMS ON TOPAZ FROM SOUTH BALDFACE MOUNTAIN.

c (001)	Often present, either as a narrow facet or occasionally as a broad face.
b (010)	Not rare, but inconspicuous.
m (110), *l* (120)	Always present and one or both dominant in the prism zone.
M (230)	Rare and narrow face.
π (250), *g* (130)	Observed, as narrow facets, but once.
G (065)	Rare and narrow face.
X (043)	Common and sometimes dominant brachydome.
K (085), *J* (053)	Rare and narrow forms.
f (021)	Usually the dominant brachydome and a center of interesting zones.
y (041)	Common, sometimes large.
h (203), *d* (201)	Common faces, often well developed.
δ (405)	Seen but once.
i (223), *u* (111), *o* (221)	All of these pyramids are generally present with variable development.
r (241)	Seen but once.

NEW AND RARE FORMS. The unique feature of the topaz from Baldface Mountain is a series of narrow pyramid faces grouped about the brachydome *f*(021). Their zonal relations are well shown in the gnomonic projection, fig. 1, which contains also the forms of Table 1. The form $\mathfrak{A}$ (1•11•6) lies at the intersection of the zone [11$\bar{2}$], which contains *f* and *u*, and the zone [9$\bar{3}$4], which contains *X* and *g*. $\mathfrak{D}$ (2•18•9), $\mathfrak{F}$ (2•24•11), and $\mathfrak{H}$ (2•30•13) all lie in the zone [92$\bar{6}$] containing *h* and (031) and at the intersections with it of the three zones [01$\bar{2}$], [1$\bar{1}$2], and [2$\bar{1}$2] containing

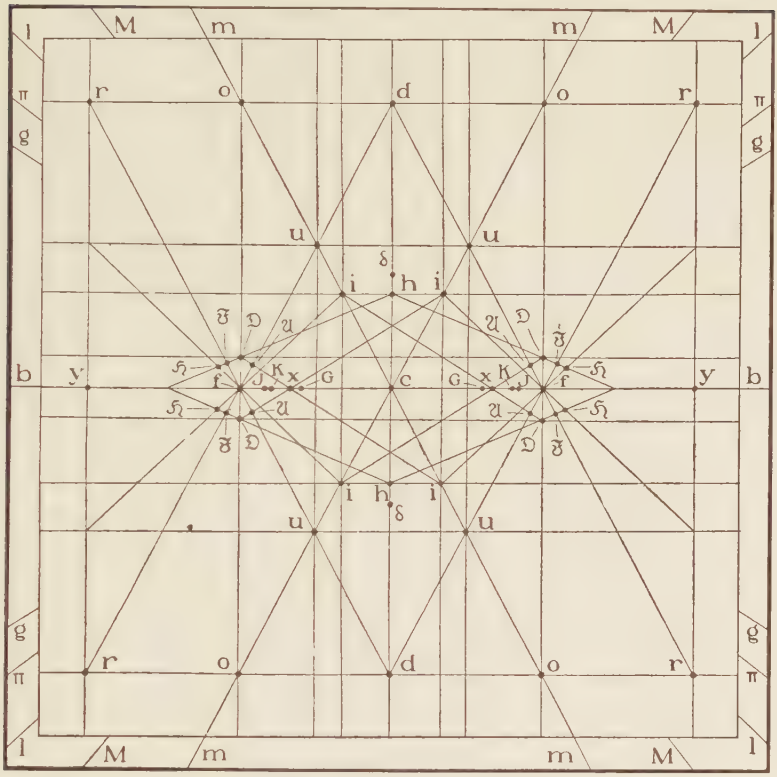

Figure 1. Gnomonic Projection of Topaz from Baldface Mtn.

respectively the forms *f* and *o*, *f* and *m*, and *f* and *l*. Although these forms have complex indices, the fact that they are true forms is demonstrated not only by the definite zonal relations but also by the number of times they were observed and the constancy of the angles. The form $\mathfrak{D}(2\cdot18\cdot9)$ was noted sixteen times; in ten of these cases the edges were so rounded that a blurred and continuous signal resulted, but in six cases the signal was sufficiently good for accurate measurement and the readings are noted in the accompanying table. The close agreement of the measured and calculated values emphasizes the legitimacy of the form. The form $\mathfrak{A}$ $(1\cdot11\cdot6)$ is nearly as well developed; in four of the ten occurrences the signal was sufficiently sharp for purposes of calculation. The forms $\mathfrak{F}(2\cdot24\cdot11)$ and $\mathfrak{H}(2\cdot30\cdot13)$ are not so

definite; both were found six times, but in only one case for each form was the face free from rounding. Nevertheless, the observed and calculated angles are close. The appearance of these narrow faces grouped about $f(021)$ is shown in figure 4. The form $\mathfrak{A}(1 \cdot 11 \cdot 6)$ has been reported as uncertain by Bücking[5] from the Fichtelgebirges and also by Rosicky;[6] the other three forms have not been reported.

Table 2. Angles of New and Rare Forms on Topaz from Baldface Mtn.

Letter	Miller Indices	Calculated		Measured	
		ϕ	ρ	ϕ	ρ
$\mathfrak{A}$	(1.11.6)	9° 45′	41° 26′	9° 09′ $^{+8}_{-9}$	41° 35′ $^{+5'}_{-11}$
$\mathfrak{D}$	(2.18.9)	11 52	44 17	12 01 $^{+22}_{-27}$	44 24 $^{+8}_{-13}$
$\mathfrak{F}$	(2.24.11)	8 58	46 29	9 30	46 45
$\mathfrak{H}$	(2.30.13)	7 11	48 00	7 36	48 10

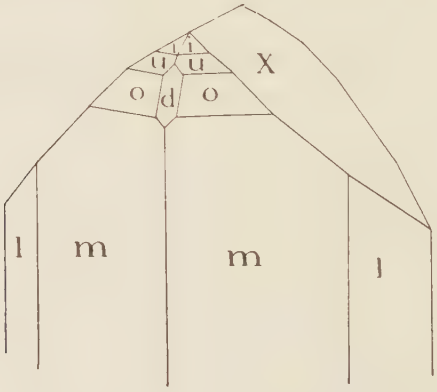

Figure 2. Topaz. Typical Baldface Habit.

[5] Bücking, H. Neues Vorkommen von Kalfeldspat, Turmalin, Apatit, und Topas im Granit des Fichtelgebirges. *Ber. Sneckenbergische Naturfor. Gesel. Frankfort*, p. 148, **1890.**

[6] Rosický, *Abh. Böhm. Ak.*, p. 23, **1916.**

HABIT. The topaz crystals fall generally into two types of habit. The most common, illustrated by figure 2, is of rhombic section, rather short prismatic, with the base very subordinate, *m* dominant in the prism zone, and *f* the dominant brachydome. Frequently *l* rather than *m* is dominant in the prism zone. Sometimes *X* is the most prominent brachydome, as in the doubly terminated crystal in figure 3. The second habit, which has an equant section with a broad basal plane, is seen on but few crystals. Figure 4 is of this habit, but more modified than usual.

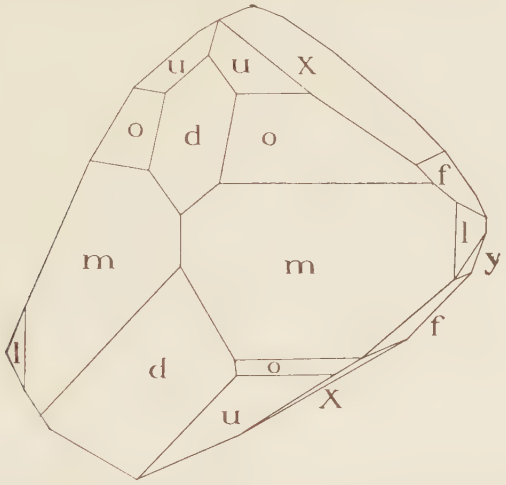

Figure 3. Doubly Terminated Topaz from Baldface Mountain.

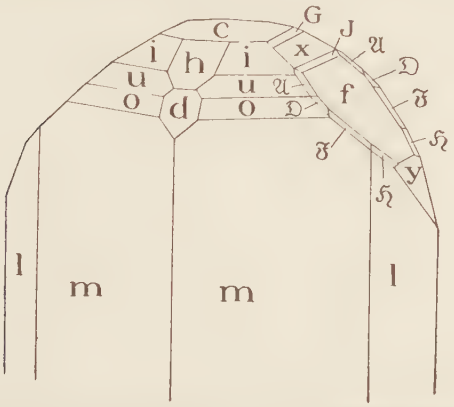

Figure 4 Baldface Topaz Showing Strong Development of the Base and the Rare Pyramids around the Brachydome *f*.

Etching. The prisms are often striated parallel to the c-axis. Etching of all common forms is noted. In some forms the brachydomes are more affected, in other crystals the pyramids are most strongly attacked. In general the etch figures on the orthodomes and pyramids are more closely spaced and smaller than those on the brachydomes, the resulting surface in the former case simulating ground glass.

PHENACITE

The Baldface phenacite is always lenticular due to the dominance of the positive unit rhombohedron and the slight development of the prisms. Six of the forty phenacite crystals were measured on the two-circle goniometer; on two of these crystals both terminations were measured. Five other crystals were set up for partial study. The prisms $a(11\bar{2}0)$ and $m(10\bar{1}0)$ when present occur as narrow faces; the prism $k(41\bar{5}0)$ is very rare. The positive unit rhombohedron $r(10\bar{1}1)$ is always conspicuous and usually the dominant form; the negative rhombohedron $d(01\bar{1}2)$ is usually prominent, occasionally surpassing in development the positive unit rhombohedron. The negative rhombohedron $\mu(02\bar{2}1)$ is often present as a narrow face between d and m.

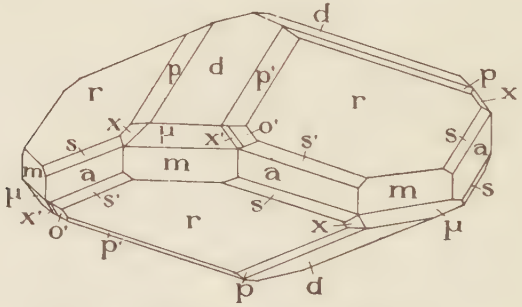

Figure 5. Phenacite from Baldface Mountain.

The complementary second order rhombohedrons p $(11\bar{2}3\ r)$ and $p_1(2\bar{1}\bar{1}3\ l)$ are often prominent, occurring as rectangular faces between r and d. The second order rhombohedron o_1 $(4\bar{2}\bar{2}3\ l)$ occurs as a small face and has been found only four times, twice on each of two crystals. The crystals are arbitrarily set up so as to throw this form onto the left hand boundary of the positive quadrant. The complementary form $o(22\bar{4}3\ r)$ has not been found. The

third order rhombohedrons are always inconspicuous. The complementary forms $s(21\bar{3}1\ r)$ and $s_1\ (3\bar{1}\bar{2}1\ l)$ are found as narrow faces in the positive quadrant between r and a. $x(\bar{1}3\bar{2}2\ r)$ and $x_1\ (12\bar{3}2\ l)$ are in the negative quadrant and inconspicuous. The third order rhombohedron $\nu_1\ (3\bar{1}\bar{2}4\ l)$, which occurs in the left hand portion of the positive quadrant, was found but once, on one of the crystals showing $o_1\ (4\bar{2}\bar{2}3\ l)$. The complementary from $\nu(21\bar{3}4\ r)$ has not been observed by the present writer, but Schaller[4] has reported it, and also one other form, $\delta(14\bar{5}6\ l)$, not found on these crystals. The typical lenticular habit and the tetartohedral rhombohedral symmetry are shown in the accompanying figure 5. Etching of the Baldface phenacite is common.

CRYSTALLOGRAPHIC NOTES
1. PHOSPHOPHYLLITE; 2. HEMATITE; 3. WILLEMITE; 4. HEDYPHANE

CHARLES PALACHE AND HARRY BERMAN

1. PHOSPHOPHYLLITE FROM HAGENDORF, BAVARIA.

CRYSTALLOGRAPHY. The mineral phosphophyllite was described by Laubmann and Steinmetz[1] in 1920. It is a complex hydrous phosphate and sulphate of iron, magnesium and potassium showing no clear chemical relationship to the previously known groups of such compounds.[2]

Good crystals of this mineral were found in the Holden Collection on specimens from the type locality, Hagendorf, Bavaria. Through their study attention was drawn to the somewhat unusual form series described in the original paper. The observations obtained from two-circle measurements of several crystals are here presented together with a new orientation which seems to yield more satisfactory indices for the forms present.

Phosphophyllite is monoclinic with prominent tabular development parallel to a form taken by Laubmann and Steinmetz as $a(100)$ and with perfect cleavage and twinning parallel to a form taken as $c(001)$. With this position there are no prism forms and it was therefore simpler to measure the crystals on the two-circle instrument with the clinopinacoid (not present) as pole and the orthodome zone as prism zone. When these measurements were plotted in gnomonic projection, discussion showed that a different choice of axes was preferable.

[1] *Zeit. f. Kryst.*, **55**, p. 566, 1920.

[2] During the publication of this paper a second article on phosphophyllite has appeared by Steinmetz in *Zeit. für Kryst.*, **64**, 405, 1926. A new analysis establishes its composition according to the following simpler formula: $3RO.P_2O_5.4H_2O$ in which RO consists of (FeO+MnO):(ZnO) in the proportion 1:1.75.

One new form is recorded as p (125) which in the new position would correspond to the form p ($\bar{3}11$).

New optical data are also given which agree closely with those given below in this paper except for β which is 1.606 instead of Larsen's value of 1.614. This low value of β is inconsistent with the observed axial angle given by Steinmetz in his previous article. That angle, $2E = 70° - 80°$, would give by calculation the index 1.614 as given by Larsen.

The best results were obtained by taking the base of Laubmann and Steinmetz as orthopinacoid and their negative orthodome as base. The symbols for the forms in the two positions are shown in table 1.

TABLE I

	Symbol (L. and S.)	Symbol (P. and B.)		Symbol (L. and S.)	Symbol (P. and B.)
c	(001)	(100)	τ	($\bar{1}$03)	(101)
ρ	($\bar{1}$01)	(001)	a	(100)	($\bar{1}$02)
q	(011)	(110)	s	(102)	($\bar{3}$02)
k	(012)	(210)	ω	($\bar{1}$23)	(111)
g	(021)	(120)	λ	($\bar{1}$25)	(211)
π	($\bar{1}$21)	(011)	o	(123)	($\bar{2}$11)

The symbols in this position become simpler and the dominant forms on the crystal a, π, ω and q all become, except the first, fundamental forms. Figure 1 shows the crystal measured in the new position. The axial ratios in the two positions are as follows:

	Position of L. and S.	Position of this paper
$a:b:c$	= 1.0381:1:1.7437	2.079:1:2.026
β	= 90° 28′	120° 25′
$p_0\ q_0$	=1.680 1.744	1.026 1.793
μ	= 89° 32′	59° 35′

Coordinate angles have been calculated from the axes given above and are shown together with the measured angles of the forms found by us in Table 2.

TABLE II.

	Calculated		Measured	
	ϕ	ρ	ϕ	ρ
c (100)	90° 00′	90° 00′	90° 00′	90° 00′
ρ (001)	90 00	30 25	90 00	30 28
q (110)	29 47	90 00	29 49	90 00
k (210)	48 51	90 00	48 50	90 00
g (120)	15 58	90 00	.....	
q (011)	15 46	65 10	15 45	65 08
x (013)	40 16	42 15	40 55	42 00
τ (101)	90 00	60 38	.....	
a ($\bar{1}$02)	−90 00	0 27	−90 00	−0 19
s ($\bar{3}$02)	−90 00	50 08	.....	
ω (111)	40 31	69 55	40 32	69 52
λ (211)	54 58	74 34	54 51	74 35
o ($\bar{2}$11)	−40 46	69 59	.....	

Since in the original article on phosphophyllite, the measured angles are all interfacial, they cannot be compared directly with our calculated coördinate angles. In Table 3 are given a few of the angles of Laubmann and Steinmetz with their calculated values and similar values calculated from our axes.

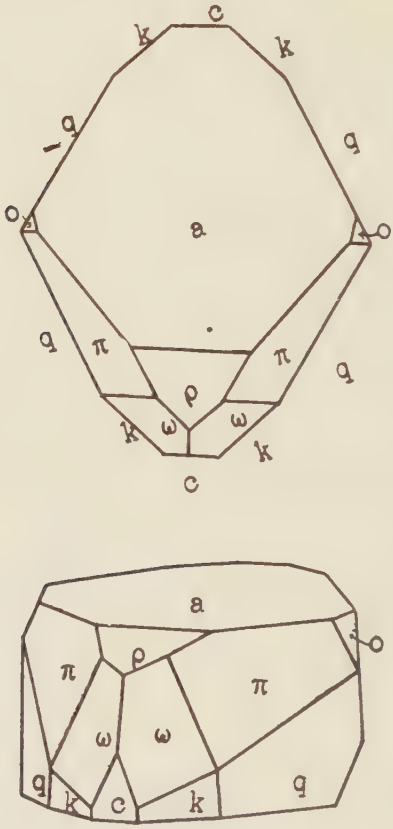

Figure 1. Phosphophyllite, Hagendorf, Bavaria

The figure shows a crystal of phosphophyllite in the new position with the commonest forms. In this position the twin plane becomes $a(100)$. The best cleavage is parallel to the same form with secondary cleavages parallel to $a(\bar{1}02)$ and $b(010)$.

TABLE III.

INTERFACIAL ANGLES OF PHOSPHOPHYLLITE

	L. and S. measured	L. and S. calculated	P. and B. calculated
$a \wedge c$	89° 32′	89° 32′	89° 33′
$\rho \wedge c$	59 24	59 39	59 35
$s \wedge c$	39 50	39 50	39 52
$q \wedge c$	60 06	60 10	60 13
$k \wedge c$	41 05	41 05	41 09
$\pi \wedge c$	75 46	75 42	75 44
$\pi \wedge \pi$	52 25	52 21	52 24
$\omega \wedge c$	121 34	121 38	121 40
$\omega \wedge \omega$	91 07	91 00	91 08
$\lambda \wedge c$	37 40	37 49	37 52
$\lambda \wedge \lambda$	67 10	67 3	67 10

OPTICAL PROPERTIES. In the original description the optical data are incomplete. The following observations by Dr. Larsen, referred to the new position of the crystals, are in part new; Biaxial (−). $2V$ about 50°. $Z = b$ $Y \wedge a = 50° \pm$ Bx_a about normal to $c(100)$. $\alpha = 1.594$, $\beta = 1.614$, $\gamma = 1.616$.

2. HEMATITE FROM FRANKLIN, NEW JERSEY.

A small specimen of Franklin ore with a surface dotted with tiny black cube-like crystals was sent to the Harvard Mineralogical Laboratory for determination by Mr. Jenkins, chief chemist of the New Jersey Zinc Company in 1926. The best crystals were covered with a film of red substance (Fe_2O_3?) which easily scaled off revealing the splendent metallic lustre. Measurement showed the crystals to be hematite with a habit and a group of forms rare for this mineral. Although a common mineral at Franklin, measurable crystals of hematite have hitherto been unknown there and the observations seem worthy of record.

The dominant form is the unit rhombohedron which determines the cuboid habit as shown in figure 2. The single modifying form there shown is really one of a group shown in figure 3, the enlarged detail of one coign of the crystal. Although so minute, these faces are clean cut and brilliant, giving excellent goniometer readings. Figure 4 shows a twin crystal, twinning on the ordinary law parallel to $c(0001)$, the composition plane parallel to a face of the first order prism. The faces are the same as on the simple crystals but symmetrical distortion parallel to the composition plane gives the oblong or in some cases hexagonal habit to the twin groups.

The forms found are as follows:

Letter	Symbol		Letter	Symbol	
Dana	G_2	Bravais	Dana	G_2	Bravais
c	0	(0001)	*z*	60	$(22\bar{4}1)$
r	-1	$(10\bar{1}1)$	*x*	$-2\frac{1}{2}$	$(12\bar{3}2)$
e	$-\frac{1}{2}$	$(01\bar{1}2)$	*ψ*	$-\frac{4}{5}\ \frac{1}{5}$	$(12\bar{3}5)$
n	20	$(22\bar{4}3)$	*P*	$-\frac{8}{7}\ \frac{2}{7}$	$(24\bar{6}7)$

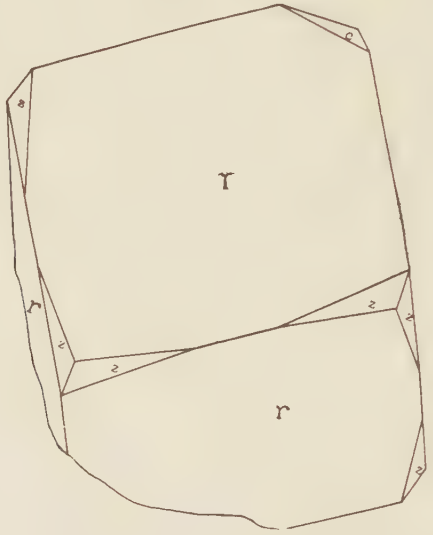

Figure 2. Hematite, Franklin, N. J.

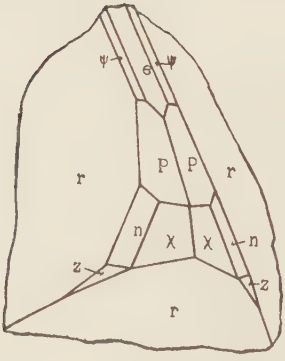

Figure 3. Hematite, Enlargement Detail of one Coign of Figure 2.

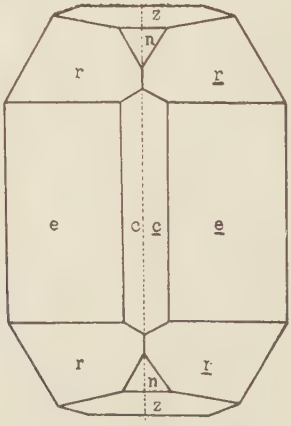

Figure 4. Hematite Twin.

The last three forms are scalenohedrons, none of them of frequent occurrence on hematite, constituting a radial zone.

The hematite is associated with a rhombohedral carbonate probably calcite, and with perfectly white sphalerite ("Cleiophane") in flattened twin crystals.

3. WILLEMITE FROM FRANKLIN, NEW JERSEY.

Beautifully crystallized willemite has been found at Franklin in recent years more frequently than for a long time. Among the many specimens of this mineral for which the Harvard Collection is indebted to Messrs. Jenkins and Bauer, Chemists of the New Jersey Zinc Company, two stand out by reason of their novel habit. One illustrated in figure 5 is noteworthy for its exceedingly thin tabular habit, the prism being present only in traces. These tiny white scale-like crystals accompany cahnite with axinite, rhodonite

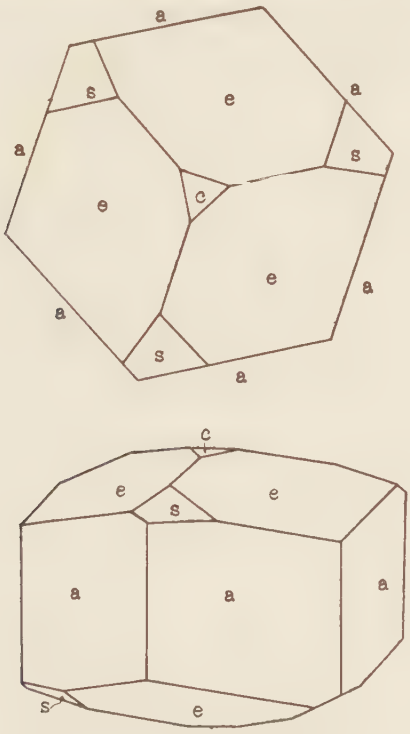

Figure 5. Willemite, Franklin, N. J.

and the hedyphane crystals to be described below. The second novel habit is shown in figure 6, a and b. It is a stout prism, 1.3 cm. diameter by 1 cm. high, of snow white color inplanted in parallel growth upon a much more slender prism of glassy willemite and in such a way that both terminations are complete. It is unusual in showing the negative rhombohedron *e* as the chief terminal form. And the distribution of the faces of the second order rhombohedron *s* reveals well the peculiar symmetry of willemite.

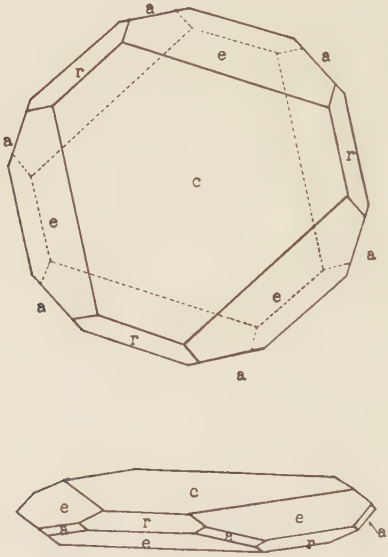

Figure 6. Willemite, Franklin, N. J.

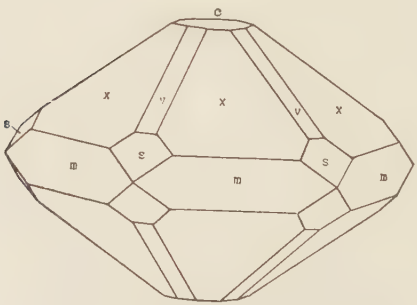

Figure 7. Hedyphane, Franklin, N, J.

Specimens of crystallized willemite which were quite colorless and of almost perfect purity have been analyzed by Mr. Bauer and the optical indices determined by Mr. Berman.

	Per cent	Molecular Ratio	
SiO_2	26.55	.440	.440=1×.440
ZnO	72.11	.886	
FeO	0.075	.001	
MnO	0.12	.002	.902=2×.451
MgO	0.13	.003	
Al_2O_3	1.00	.010	

The optical indices of these crystals which are by far the purest zinc silicate ever analyzed from Franklin, are as follows: $\omega=1.691$, $\epsilon=1.719$ for white light by the immersion method.

4. HEDYPHANE FROM FRANKLIN, NEW JERSEY.

The hedyphane crystals associated with cahnite and the tabular willemite described above are shown in figure 7. A prism of this hedyphane was cut parallel to the vertical axis and yielded the following optical data:

Uniaxial (+), $\epsilon=1.958$, $\omega=1.948$ for sodium light

Examination of part of the collection of Franklin minerals left by the late F. A. Canfield reveals the fact that hedyphane is more widely distributed there than has been recognized. Several specimens from the Parker Shaft taken out at least twenty years ago show bluish hedyphane associated with axinite, caswellite and hancockite. It was there and in such specimens that the first native lead was found at Franklin. Hedyphane was first identified at Franklin by Foshag and Gage in 1925.

THE OCCURRENCE OF CINNABAR IN DUTCH GUIANA

CHARLES PALACHE.

For some years past mineral collections have been supplied by dealers with unusual and very striking specimens of cinnabar in well rounded pebbles accompanied by the vague locality, Surinam River, Dutch Guiana. The writer has been supplied with accurate information concerning this occurrence of cinnabar and deems its peculiar character a sufficient reason for placing the known facts on record. He is indebted to Mr. D. V. Keedy of Melrose Highlands Massachusetts, for this information and for permission to publish it as well as for interesting specimens of the cinnabar.

The cinnabar occurs in the Nassau Mountains in the interior of Dutch Guiana, about seventy-five miles in an air line south and east of Paramaribo, the capital of the colony, but distant four days travel by boat and trail. The area where it is found, now known as the Keedy Concession, is in the Marowyne District near the headwaters of the Tempati River. It is reached either by ascending that river through its lower course, the Commewyne, or by a longer route up the larger Marowyne river, depending upon the season and the corresponding depth of water in the rivers.

The cinnabar pebbles were first found some twenty years ago in the gold placers of the region and the concession where they were most abundant had passed through many hands before the present owners took it over. The search for the primary deposits from which the cinnabar pebbles were derived has yielded interesting information as to their geological nature.

The cinnabar occurs in specks, grains and pebbles up to a pound in weight in the river gravels and surface soil. The pebbles are well rounded and are of a dull vermillion color. On breaking them open they show either a granular texture or almost as often a brilliant cleavage, the whole pebble consisting of a single crystal. Occasional crystals of pyrite and specks of chalcopyrite are imbedded in the cinnabar and in many pebbles brown ochreous limonite is interspersed through it.

With cinnabar in the placer concentrates is found gold in scales and small nuggets, magnetite and ilmenite constituting a black sand, and in one creek monazite. Free mercury was seen in some pebbles but may have been introduced by the gold washers who use it in their work.

In trenching the hillsides drained by the cinnabar-bearing creeks, Mr. Keedy's prospecting operations brought to light some large boulders of cellular lateritic iron ore in which were definite veins of cinnabar up to an inch in width and extending through the boulders. This cinnabar is identical in character with that of the pebbles and it is evident that such veins are the source of the alluvial material. Extensive search, however, failed to reveal the laterite anywhere in place. It is widely distributed throughout the region, often in very large masses, but is devoid of cinnabar except where the veins were seen. It is believed by the geologists who have studied the deposits that, prior to the development of the present topography, this iron laterite constituted a blanket deposit overlying the mica schist which composes the bedrock. Two considerable faults were observed in the trenches along which were small gold-bearing quartz veins carrying, however, no cinnabar. The formation of the cinnabar veins must have been later than the formation of the iron laterite but earlier than the recent erosion. It seems certain that the veins were deposited from hot spring waters and that somewhere in the region they must have intersected the bedrock. What seems most strange in these specimens is that the cinnabar is so closely confined to the narrow veins and is not disseminated in the porous limonite which seems a material peculiarly well suited to permit the type of impregnation so common in deposits of cinnabar.

Among the specimens collected was a single boulder of peculiar mineralogical interest. It consists of quartz and a bluish green granular mineral thought at first to be pyroxene. It proved on microscopic examination, however, to be serendibite, a borosilicate of aluminum, first found in placers in Ceylon, and later found in abundance in a contact deposit in the Adirondack Mountains in New York, which has not yet been described. The boulder contained no cinnabar and the presence of this contact mineral probably has no bearing on its origin.